

INVESTIGATING PHARMACEUTICAL CO-CRYSTALS AS A MEANS TO
IMPROVE THE SOLUBILITY OF A DRUG

BY

Rebecca Brown

Submitted to the graduate degree program in
Pharmaceutical Chemistry and the Graduate Faculty
of the University of Kansas in partial fulfillment of the
requirements for the degree of Master's of Science

Chairperson

Committee Members*

*

*

*

*

*

Date defended:

May 11, 2012

The Thesis Committee for Rebecca Brown certifies
that this is the approved version of the following thesis:

**INVESTIGATING PHARMACEUTICAL CO-CRYSTALS AS A MEANS TO
IMPROVE THE SOLUBILITY OF A DRUG**

Committee:

Chairperson

Date approved:

May 11, 2012

Abstract

Recently co-crystals have emerged as a potential approach to improve the solubility, dissolution, and bioavailability of active pharmaceutical ingredients (API). Often co-crystal formation is studied in the development stage in order to solve an issue (with solid form or formulation) or to expand intellectual property. However, co-crystals may have the potential of enhancing the developability of a poorly soluble lead candidate in the discovery stage. In this study, piroxicam, a BCS (Biopharmaceutical Classification System) Class II compound with low solubility, was chosen as a model drug to explore this possibility. The solution phase reaction crystallization method was chosen over slow evaporation as a way to make co-crystals because it can produce pure co-crystals that can be scaled by simply using the solubility data of the parent and coformer. A screen of carboxylic acid cofomers yielded six piroxicam co-crystals which were characterized. Co-crystal aqueous solubility was measured and models were used to calculate co-crystal pH dependent solubility. Intrinsic dissolution rates of the co-crystals were measured in biorelevant media. Co-crystals were found to be more soluble and the dissolution rates were lower than the parent. Piroxicam oral exposure in rat from the co-crystals was determined and was similar to free piroxicam.

Acknowledgements

I would like to thank my on site research advisor, Dr. Deborah Galinis, for her guidance and encouragement throughout this research project. I am very grateful for the support and flexibility afforded to me from Cephalon and Teva Pharmaceuticals to pursue this masters program as well as the enthusiasm from my directors Dr. Mehran Yazdanian and Dr. Rob McKean, and vice president Dr. Craig Heacock. I am appreciative of the University of Kansas Pharmaceutical Chemistry Department for offering this distance masters program and am especially thankful for my KU advisor, Dr. Valentino Stella, for his guidance and scientific discussions. I am extremely grateful to Dr. Nair Rodríguez-Hornedo for personally sharing her expertise with me on solution phase reaction crystallization and co-crystal solubility. Much of this work would not have been possible without the help from several of my colleagues including Dr. Laurent Courvoisier, Steve Bierlmaier, and Curtis Haltiwanger for their help with solid state analysis techniques, Dr. Lisa Aimone for sharing her *in-vivo* knowledge and suggestions, and Damaris Rolon-Steele and Kelli Zeigler for performing *in-vivo* pharmacokinetic studies. Lastly, I would like to thank my husband and family for their love, support, and patience while I pursued this degree.

Table of Contents

Chapter 1. Introduction

Pharmaceutical Interest in Co-crystals	1
Co-crystal Synthesis Methods	3
Piroxicam as a Model Compound	4
References	6

Chapter 2. Piroxicam Co-crystals by Slow Evaporation

Introduction	8
Experimental	9
Results and Discussion	14
Conclusions	19
References	20

Chapter 3. Piroxicam Co-crystals by Reaction Crystallization

Introduction	21
Experimental	23
Results and Discussion	26
Conclusions	33
References	34

Chapter 4. Co-crystal Solubility

Introduction	35
Experimental	36
Results and Discussion	38
Conclusions	45
References	46

Chapter 5. Intrinsic Dissolution and Pharmacokinetics

Introduction	47
Experimental	48
Results and Discussion	50
Conclusions	60
References	61

Chapter 6. Final Conclusions and Future Considerations

Chapter 7. Appendix

Slow Evaporation Solid State Data	65
Reaction Crystallization Solid State Data	83
Co-crystal Solubility	93
Intrinsic Dissolution	99
Pharmacokinetic Data	119

CHAPTER 1. Introduction

Purpose of the Research Performed

The purpose of the research covered in this thesis was to explore the use of co-crystal formation to alter the physical/chemical properties of the non-steroidal drug, piroxicam, in order to improve drug solubility, dissolution, and bioavailability.

Pharmaceutical Interest in Co-crystals

In the past decade, drug candidates have evolved toward compounds with increasing molecular weight and lipophilicity often resulting in poorly water soluble drugs.¹ This has remained a key issue for pharmaceutical candidates with drugs often failing in development due to their low aqueous solubility.² Limited solubility often causes poor and variable oral absorption because the dissolution rate or solubility is insufficient to completely dissolve the drug in the gastrointestinal tract.³

Recently pharmaceutical co-crystals have emerged as a promising solid state technique to improve API (active pharmaceutical ingredient) properties such as solubility, dissolution rate, bioavailability, and stability.⁴⁻⁸ A review by Schultheiss and Newman on pharmaceutical co-crystals and their physiochemical properties lists several definitions of a co-crystal such as a solid molecular complex at room temperature containing a neutral, ionic, or zwitterionic molecule of the API and one or more complementary molecules (coformers) including excipients (non-toxic ingredients) or other APIs.⁸ However, the FDA guidance that was recently released on pharmaceutical co-crystals specifies that the co-crystal components exist in their neutral states

and interact via non-ionic interactions, as opposed to ionic interactions, which would classify this crystalline solid as a salt form.⁹ The API and coformer can interact through hydrogen bonding, π -stacking, or van der Waals forces.¹⁰ In theory, all types of drug molecules have the capability to form co-crystals; therefore, co-crystals have advantages over traditional solid-state modification techniques (e.g., salts, solvates, hydrates, and polymorphs). For example, co-crystals provide an alternative for APIs that are unable to form salts due to lack of ionization moieties.

Pharmaceutical co-crystals provide a means to increase API solubility, dissolution rate, and bioavailability. For example, the aqueous solubility of seven carbamazepine co-crystals measured by Good and Rodriguez-Hornedo was approximately 2 to 152 times greater than the solubility of the stable carbamazepine dihydrate form.¹¹ In a study by Stanton et. al., AMG 517 co-crystals paired with cinnamic acid, benzoic acid, cinnamamide, and benzamide gave significant increases in dissolution rate and oral exposure compared to the free base form.¹² Jung et. al. created indomethacin-saccharin co-crystals that produced higher *in vitro* dissolution rates at pH 1.2 and 7.4 as well as higher bioavailability in dogs than indomethacin.¹³ However, this improvement was not significantly different from the marketed product, Indomee[®]. In another study, an increase in bioavailability in dogs was also demonstrated using glutaric acid co-crystals.¹⁴

Co-crystals have also been used to overcome API stability issues such as polymorphism and hygroscopicity.⁷⁻⁸ An example where co-crystals were used to reduce hygroscopicity was with caffeine. It is well known that caffeine is subject to hydrate formation.¹ Caffeine-dicarboxylic acid co-crystals resisted hydrate formation, even when prepared from the hydrated

drug form.¹⁵ Furthermore, caffeine co-crystals with oxalic acid were non-hygroscopic and stable over several weeks when maintained at 43-98% relative humidity.¹⁵ In a similar case, Trask et. al. found that theophylline co-crystals with oxalic, malonic, maleic, and glutaric acid did not hydrate at high relative humidity.¹⁶ A carbamazepine/saccharin co-crystal created by Hickey et. al. is a case where co-crystallization reduced the incidence of polymorphism compared to pure carbamazepine, which has four known polymorphs and several solvates.¹⁷ The physical and chemical stability as well as the oral bioavailability of the carbamazepine co-crystal was proven to be quantitatively similar to the pure drug in the marketed product, Tegretol[®].

Co-crystal Synthesis Methods

It is relatively straight forward for the medicinal chemist to create a salt form based on the pK_a value(s) of a lead molecule and that of the intended acid or base used to form the salt.⁷ However, several different methods have been reported to screen and make co-crystals including wet cogrinding, sonic slurry, and slow evaporation.^{2, 5, 18} These studies are generally carried out in ternary systems (API, coformer, and solvent) and phase diagrams are generated that describe the conditions for thermodynamic stability and provide insight into the experimental conditions that may lead to co-crystal formation.¹⁸ With these methods, solvent or solvent mixtures with similar solubilities for reactants are chosen and stoichiometric amounts of the reactants are used. Often times, slow evaporation experiments are performed in a high throughput screening mode in which small quantities of co-crystals are identified in a 96 well plate.¹⁹ Slow evaporation accounts for approximately 40% of the co-crystallization techniques appearing in the literature.²⁰

Reaction crystallization is another strategy used to identify and generate co-crystals. This method is also based on the solubilities of the reactants; however, nonstoichiometric reactant solution concentrations are used.¹⁸ Co-crystals are generated via supersaturation with respect to the co-crystal in a liquid phase that is ideally saturated or undersaturated with respect to the reactants.^{21, 22} In other words, a saturated solution of the reactants is made with the intention of creating an environment where the co-crystal form is supersaturated and precipitates out of solution.

These methods afford a variety of options but also make it difficult to decide which approach will be the most successful. Ideally the method used will identify and produce co-crystals relatively quickly so that the co-crystals can be tested to determine if they have an advantage over the API itself. It is also important that the co-crystal synthesis method chosen is reproducible and scalable in order to produce the significant amount of material required for solubility, intrinsic dissolution, and *in vivo* studies. Finally and most importantly, the method has to yield pure co-crystal material so that accurate conclusions can be made when the co-crystals are tested.

Piroxicam as a Model Compound

Piroxicam was chosen as a model compound to explore co-crystal formation in this research because it is a Biopharmaceutics Classification System (BCS) Class II compound, which by definition has low solubility and high permeability. It is a nonsteroidal anti-inflammatory drug used in the symptomatic treatment of rheumatoid arthritis and osteoarthritis.²³ Solubility and permeability are the fundamental properties determining the bioavailability of an

orally active drug; therefore, poor oral absorption is often an issue for BCS Class II drug.²⁴ Co-crystals of Class II compounds have been shown to increase bioavailability in some cases.¹⁰ When dosed orally, it takes more than two hours for piroxicam to reach maximum concentration which indicates the oral exposure is limited by solubility.²⁵⁻²⁷ Piroxicam (Figure 1.1) is a zwitterionic molecule with two pK_a values (pK_{a1} = 1.8, pK_{a2} = 5.1).²⁸

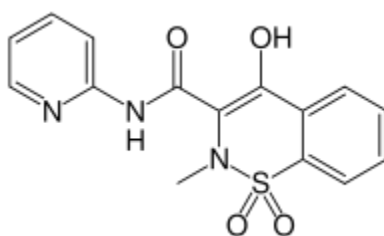


Figure 1.1: Structure of piroxicam.

Co-crystals of piroxicam have been previously reported.^{29, 30} In a small scale screening experiment, fifty co-crystals containing piroxicam and a carboxylic acid coformer were identified.²⁹ A study of saccharin as a salt former also yielded a piroxicam-saccharin co-crystal.³⁰ Based on these reports of piroxicam co-crystals, several coformers were chosen for this research in order to explore different co-crystal synthesis strategies and to improve solubility and potential oral bioavailability in an early drug development setting. Piroxicam co-crystal solubility, dissolution rate, and oral bioavailability were also investigated.

References

1. Meanwell NA. 2008. The emerging utility of co-crystals in drug discovery and development. *Annual Reports in Med Chem* 43(8):373-404.
2. Qiao N, Li M, Schlindwein W, Malek N, Davies A, Trappitt G. 2011. Pharmaceutical co-crystals: An overview. *Int J Pharm* 419(1-2):1-11.
3. Varma MVS, Khandavilli S, Ashokraj Y, Jain A, Dhanikula A, Sood A, Thomas NS, Pillai O, Sharma P, Gandhi R, Agrawal S, Nair V, Panchagnula R. 2004. Biopharmaceutic classification system: A scientific framework for pharmacokinetic optimization in drug research. *Current Drug Metabolism* 5(5):375-388.
4. Blagden N, de Matas M, Gavan PT, York P. 2007. Crystal engineering of active pharmaceutical ingredients to improve solubility and dissolution rates. *Adv Drug Deliv Rev* 59(7):617-630.
5. Miroshnyk I, Mirza S, Sandler N. 2009. Pharmaceutical co-crystals: An opportunity for drug product enhancement. *Expert Opin Drug Deliv* 6(4):333-341.
6. Rodríguez-Hornedo N, Nehm SJ, Jayasankar A. 2007. Cocrystals: Design, Properties and Formation Mechanisms. *Encyclopedia of Pharm Technology* 615-635.
7. Peterson ML, Hickey M.B, Zaworotko MJ, Almarsson O. 2006. Expanding the scope of crystal form evaluation in pharmaceutical science. *J Pharm Sci* 9(3):317-326.
8. Schultheiss N, Newman A. 2009. Pharmaceutical co-crystals and their physiochemical properties. *Cryst Growth Des* 9(6):2950-2967.
9. Draft Guidance for Industry 2011. Regulatory Classification of Pharmaceutical Co-crystals. <http://www.fda.gov/Drugs/GuidanceComplianceRegulatoryInformation.htm>.
10. Sekhon BS. 2009. Pharmaceutical co-crystals – a review. *Ars Pharm* 50(3):99-117.
11. Good DJ, Rodríguez-Hornedo N 2009. Solubility advantage of pharmaceutical cocrystals. *Cryst Growth Des* 9(5):2252-2264.
12. Stanton MK, Kelly RC, Colletti A, Kiang YH, Langley M, Munson EJ, Peterson ML, Roberts J, Wells M. 2010. Improved pharmacokinetics of AMG 517 through co-crystallization part 1: Comparison of two acids with corresponding amide co-crystals. *J Pharm Sci* 99(9):3769-3778.
13. Jung MS, Kim JS, Kim MS, Alhalaweh A, Cho W, Hwang SJ, Velaga SP. 2010. Bioavailability of indomethacin-saccharin co-crystals. *J Pharmacy and Pharmacology* 62(11):1560-1568.
14. McNamara DP, Childs SL, Giordano J, Iarriccio A, Cassidy J, Shet MS, Mannion R, O'Donnell E, Park A. 2006. Use of a Glutaric acid co-crystal to improve oral bioavailability of a low solubility API. *Pharm Res* 23(8):1888-1897.
15. Trask AV, Motherwell WDS, Jones W. 2005. Pharmaceutical co-crystallization: Engineering a remedy for caffeine hydration. *Crys Growth Des* 5(3):1013-1021.
16. Trask AV, Motherwell WDS, Jones W. 2006. Physical stability enhancement of theophylline via co-crystallization. *Int J Pharm* 320(1-2):114-123.
17. Hickey MB, Peterson ML, Scoppettuolo LA, Morrisette SL, Vetter A, Guzmán H, Remenar JF, Zhang Z, Tawa MD, Haley S, Zaworotko MJ, Almarsson Ö. 2007. Performance comparison of a co-crystal of carbamazepine with marketed product. *Euro J Pharm Biopharm* 67:112-119.

18. Childs SL, Rodríguez-Hornedo N, Reddy LS, Jayasankar A, Maheshwari C, McCausland L, Shipplett R, Stahly BC. 2008. Screening strategies based on solubility and solution composition generate pharmaceutically acceptable cocrystals of carbamazepine. *Cryst Eng Comm* 7(10):856-864.
19. Morissette SL, Almarsson Ö, Peterson ML, Remenar JF, Read MJ, Lemmo AV, Ellis S, Cima MJ, Gardner CR. 2004. High-throughput crystallization: polymorphs, salts, co-crystals and solvates of pharmaceutical solids. *Adv Drug Deliv Rev* 56(3):275-300.
20. Sheikh AY, Rahim SA, Hammond RB, Roberts KJ. 2008. Scalable solution co-crystallization: case of carbamazepine-nicotinamide I. *Cryst Eng Comm* 11:501-509.
21. Rodríguez-Hornedo N, Nehm SJ, Seefeldt KF, Pagán-Torres Y, Falkiewicz CJ. 2005. Reaction crystallization of pharmaceutical molecular complexes. *Molecular Pharm* 3(3):362-367.
22. Nehm SJ, Rodríguez-Spong B, Rodríguez-Hornedo N. 2006. Phase solubility diagrams of cocrystals are explained by solubility product and solution complexation. *Cryst Growth Des* 6(2):592-600.
23. Gwak H, Choi J, Choi H. 2005. Enhanced bioavailability of piroxicam via salt formation with ethanolamines. *Int J Pharm* 297(1-2):156-161.
24. Varma MVS, Khandavilli S, Ashokraj Y, Jain A, Dhanikula A, Sood A, Thomas NS, Pillai O, Sharma P, Gandhi R, Agrawal S, Nair V, Panchagnula R. 2004. Biopharmaceutic classification system: A scientific framework for pharmacokinetic optimization in drug research. *Current Drug Metabolism* 5(5):375-388.
25. Fernandez S, Chevrier S, Ritter N, Mahler B, Demarne F, Carrière F, Jannin V. 2009. In Vitro gastrointestinal lipolysis of four formulations of piroxicam and cinnarizine with the self emulsifying excipients labrasol® and gelucire® 44/14. *Pharm Res* 26(8):1901-1910.
26. Kimura E, Bersani-Amado CA, Sudo LS, Santos SR, Oga S. 1997. Pharmacokinetic profile of piroxicam β -cyclodextrin in rat plasma and lymph. *Gen Pharmac* 28(5):695-698.
27. Tagliati CA, Kimura E, Nothenberg MS, Santos SR, Oga S. 1999. Pharmacokinetic profile and adverse gastric effect of zinc-piroxicam in rats. *Gen Pharm* 33(1):67-71.
28. Cheong HA, Choi HK. 2002. Enhanced percutaneous absorption of piroxicam via salt formation with ethanolamines. *Pharm Res* 19(9):1375-1380.
29. Childs SL, Hardcastle KI. 2007. Cocrystals of Piroxicam with Carboxylic Acids. *Cryst Growth Des* 7(7):1291-1304.
30. Bhatt PM, Ravindra NV, Banerjee R, Desiraju GR. 2005. Saccharin as a salt former. Enhanced solubilities of saccharinates of active pharmaceutical ingredients. *Chem Commun* 1073-1075.

CHAPTER 2. Piroxicam Co-crystals by Slow Evaporation

Purpose of the Research Performed

The purpose of the research performed in this chapter was to explore the feasibility of creating scale-up batches of co-crystals by slow evaporation.

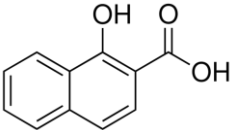
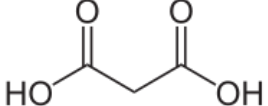
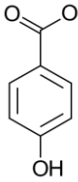
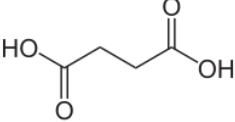
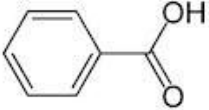
Introduction

Childs and Hardcastle performed an extensive small scale co-crystal screen with piroxicam and 23 carboxylic acids using solution based and solid-state grinding methods.¹ The solution based screen was done in a 96-well format with stoichiometric amounts of piroxicam and the carboxylic acids and various solvent mixtures. These solutions were allowed to slowly evaporate to dryness at room temperature. Solid-state grinding screening methods were also utilized to study physical mixtures of piroxicam and 20 carboxylic acids in 1:1 and 1:2 API/coformer combinations. Raman spectroscopy and X-ray powder diffraction (XRPD) were used to characterize the solids. Single piroxicam co-crystals were also grown by slow evaporation with 10 carboxylic guest compounds and four different solvent combinations. From these experiments, single crystal data was reported for nine piroxicam/carboxylic acid co-crystals.

Five of these acid/solvent combinations were used in this thesis in order to determine the feasibility of growing co-crystals by slow evaporation on a larger scale (50 mg – 2 g). The structures of the cofomers used as well as the ratio of piroxicam to coformer are listed in Table 2.1. The solids were characterized by XRPD, differential scanning calorimetry (DSC), and

thermal gravimetric analysis (TGA). XRPD patterns were compared to the single crystal data reported by Childs and Hardcastle¹ to determine whether or not the solid was in fact a co-crystal. XRPD and DSC data were also obtained for piroxicam, each acid, and physical mixtures of piroxicam and each acid. The solid XRPD patterns were also compared to other known forms of piroxicam.²

Table 2.1: Coformer structures and co-crystal ratio.

Coformer	Structure	Piroxicam / Coformer Ratio
1-hydroxy, 2-Naphthoic acid		1:1
Malonic acid		1:1 and 2:1
4-hydroxy Benzoic Acid		1:1
Succinic Acid		1:1 and 2:1
Benzoic Acid		1:1

Experimental

The materials listed in this chapter as well as the XRPD, DSC, and thermogravimetric analysis methods were used throughout the entirety of this research.

Materials

Piroxicam was obtained from 3B Pharmachem International Co. Ltd. (China). Gentisic acid was obtained from MP Biomedicals (Solon, OH). Saccharin was purchased from Spectrum Chemicals (New Brunswick, NJ). Benzoic acid, fumaric acid, maleic acid, malonic acid, tetrahydrofuran, and 2,2,2, trifluoroethanol were purchased from Alfa Aesar (Lancashire, UK). 4-hydroxy benzoic acid was obtained from TCI America (Portland, OR). Salicylic acid and monobasic potassium phosphate were purchased from J.T. Baker (Phillipsburg, NJ). Sodium chloride, 1-hydroxy 2-naphthoic acid, alprenolol, and mandelic acid was obtained from Sigma-Aldrich (St. Louis, MO). Succinic acid and tetrahydrofuran were purchased from EMD Chemicals (Cincinnati, OH). Water, 0.1% trifluoroacetic acid in water, acetonitrile, isopropanol, and methanol were all HPLC grade and purchased from J.T. Baker (Phillipsburg, NJ).

X-ray Powder Diffraction (XRPD)

Powder XRD patterns were recorded on a PANalytical X'Pert Pro diffractometer equipped with an X'celerator detector using Cu K α radiation at 45 kV and 40 mA. K α 1 radiation is obtained with a highly oriented crystal (Ge111) incident beam monochromator. A 10 mm beam mask, and fixed (1/4 $^\circ$) divergence and anti-scatter (1/8 $^\circ$) slits were inserted on the incident beam side. A fixed 5 mm receiving slit was inserted on the diffracted beam side. The X-ray powder pattern scan was collected from *ca.* 2 to 40 $^\circ$ 2 θ with a 0.0080 $^\circ$ step size and 96.06 sec counting time which resulted in a scan rate of approximately 0.5 $^\circ$ /min. The sample was spread on a silicon zero background (ZBG) plate for the measurement. The sample was rotated at 15 revolutions/min on a PANalytical PW3065/12 Spinner.

Differential Scanning Calorimetry (DSC)

Thermal curves were acquired using a Perkin-Elmer Sapphire DSC unit equipped with an autosampler running Pyris software version 6.0 calibrated with Indium prior to analysis. Solid samples of 1-10 mg were weighed into 20 μL aluminum sample pans with pin hole lids. The DSC cell was then purged with nitrogen and the temperature heated from 0 to 375°C at 10°C / min. Indium ($T_m = 156.6^\circ\text{C}$; $\Delta H_{\text{FUS}} = 28.45 \text{ J g}^{-1}$) was used for calibration.

Thermogravimetric Analysis (TGA)

Thermal curves were acquired using a Perkin-Elmer Pyris 1 TGA unit running Pyris software version 6.0 calibrated with alumel (95% nickel, 2% manganese, 2% aluminum and 1% silicon), nickel and calcium oxalate monohydrate. TGA samples between 1-5 mg were monitored for percent weight loss as heated from 25 to 250°C at 10°C/min in a furnace purged with Helium at ca. 50 mL/min.

High Performance Liquid Chromatography (HPLC)

The purity of the co-crystal components was assessed by HPLC. The HPLC-UV instrument used was an Agilent 1200 series (Palo Alto, CA) equipped with a UV diode array detector (Agilent Technologies, Palo Alto, CA) and contained an Agilent Zorbax Bonus RP 4.6 x 150mm, 3.5 micron column. Concentrations were determined using a gradient method from 5% solvent B (acetonitrile containing 0.1% trifluoroacetic acid) in solvent A (water containing 0.1% trifluoroacetic acid) to 95% solvent B in solvent A in 25 minutes, isocratic at 100% solvent B for 1.5 minutes, then equilibrate for 5 minutes at 5% solvent B in solvent A. The flow rate was 1 mL/min. Calibration curve standards were prepared in methanol at 1, 10, 100, and 250 $\mu\text{g/mL}$.

The wavelengths of absorbance monitored for piroxicam and 4-hydroxy benzoic acid were 325 and 254 nm respectively. All other acids were monitored at 210 or 220 nm.

Co-crystal Slow Evaporation Method

Crystals were grown by slow evaporation at room temperature using the methods and solvents described by Childs and Hardcastle.¹ The amount of piroxicam and coformer required for the desired co-crystal yield (e.g. 50 mg, 100 mg, etc.) was calculated based on the molecular weight of the co-crystal. Piroxicam and cofomers were weighed into a glass vial and solvent was then added until all the solid was dissolved. The vials were sealed with paraffin wax paper and a small hole was punched in the paper and then set to evaporate. Table 2.2 lists the experimental details for each co-crystal.

Table 2.2: Experimental parameters for co-crystal slow evaporation.

Co-Crystal	MW (g/mole)	Batch Scale (mg)	Amount Piroxicam Used (mg)	Amount Coformer Used (mg)	Total Solvent Volume (mL)	Evaporation Time (weeks)	Solvent
1:1 Piroxicam/ 1-hydroxy 2-Naphthoic Acid	519.52	50	31.44	18.74	15	6	2:1 Tetrahydrofuran/ Isopropanol
		500	323.1	177.27	30	3	
		1000	639.61	363.39	75	5	
1:1 Piroxicam/ Malonic Acid	662.69	50	25.14	7.91	16	7	1:1 Trifluoroethanol/ Acetonitrile
		500	259.5	78.5	50	6	
		2000	1007	314.22	140	5	
2:1 Piroxicam/ Malonic Acid	766.77	500	500.49	78.71	80	6	1:1 Trifluoroethanol/ Acetonitrile
		1000	1000	158.28	160	6	
		2000	1999	313.9	300	6	
1:1 Piroxicam/ 4-hydroxy Benzoic Acid	469.46	50	35.5	14.8	16	6	1:1 Methanol/ Acetonitrile
		500	359	150	90	3	
1:1 Piroxicam/ Succinic Acid	449.43	100	84.12	30.43	30	4	2:1 Tetrahydrofuran/ Isopropanol
		500	424.65	151.25	105	4	
		1000	849.27	302.62	180	5	
2:1 Piroxicam/ Succinic Acid	780.786	200	84.75	15.27	15	6	2:1 Tetrahydrofuran/ Isopropanol
		1000	422.84	147.63	45	3	
		2000	1697.3	301.17	120	5	
1:1 Piroxicam/ Benzoic Acid	453.46	50	36.4	13.4	16	6	1:1 Methanol/ Acetonitrile
		500	366	135.69	90	3	
		2000	1451	543.31	250	4	

Results and Discussion

In the piroxicam co-crystal study by Childs¹, more detailed experimental synthesis methods were given for the nine single crystal co-crystals reported. Out of these nine, the five piroxicam/acid/solvent sets used in this thesis were chosen because they did not require heating/cooling or produce a mixture of co-crystal forms. Co-crystal XRPD results for the batches of co-crystals made in this research could then be directly compared to the single crystal data reported by Childs.

A total of seven slow evaporation experiments with piroxicam and five carboxylic acid cofomers in either 1:1 or 2:1 piroxicam/acid stoichiometric ratios were performed. A summary of the data collected for each batch of co-crystal is listed in Table 2.3. Cofomer melting points are also included in this table as a reference. The melting point of the piroxicam material used was 207°C. The remaining solids after evaporation were analyzed by HPLC to assess the purity of piroxicam and the cofomers. No chemical degradation was observed. A stability study of piroxicam in all the solvent combinations proved piroxicam to be stable at room temperature for at least 42 days. XRPD patterns and DSC thermograms not shown in this chapter can be found in the appendix.

Table 2.3: Summary of co-crystal recovery and characterization.

Co-Crystal	Batch Scale (mg)	Pure Co-crystal?	Weight Loss by TGA (%)	Co-crystal MP by DSC (°C)	Cofomer MP by DSC (°C)
1:1 Piroxicam/ 1-hydroxy 2- Naphthoic Acid	50	Maybe	<1	195	200.8
	500	Maybe	1.6	195	
	1000	Maybe	<1	188, 196	
1:1 Piroxicam/ Malonic Acid	50	No	7.2	145, 162, 191	95.5, 139.6
	500	No	11.0	85, 140, 143, 160, 199	
	2000	No	15.8	88, 139, 142	
2:1 Piroxicam/ Malonic Acid	500	No	16.9	110, 160, 204	95.5, 139.6
	1000	No	8.6	157, 203	
	2000	No	10.4	87, 160, 205	
1:1 Piroxicam/ 4-hydroxy Benzoic Acid	50	No	<1	186, 197	217.9
	500	No	1.4	188, 197	
1:1 Piroxicam/ Succinic Acid	100	No	<1	156, 170, 180	193.3
	500	No	1.3	155, 170, 180	
	1000	No	1.3	155, 170, 177	
2:1 Piroxicam/ Succinic Acid	200	No	<1	170, 180	193.3
	1000	No	<1	47, 81, 170, 188	
	2000	No	<1	155, 170, 204, 234, 245	
1:1 Piroxicam/ Benzoic Acid	50	No	13.1	122, 141, 168, 198	124.7
	500	No	18.3	135, 168, 198	
	2000	No	10.2	118, 169	

1:1 Piroxicam/1-hydroxy 2-Naphthoic Acid. XRPD results (Figure 2.1) were reproducible for the 50 mg, 500 mg and 1 g scales made. The XRPD data mostly matched the single crystal data in the literature with the exception of a few peaks, which could be small

impurities or other crystalline forms. The co-crystals had very little weight loss (< 1 %) when heated up to 250°C and DSC (Figure 2.2) gave one endotherm at 195°C for the 50 and 500 mg batches suggesting that the material was mostly pure. A small endotherm at 188°C was observed for the 1 g batch. Based on these results, it is possible that the material is a co-crystal.

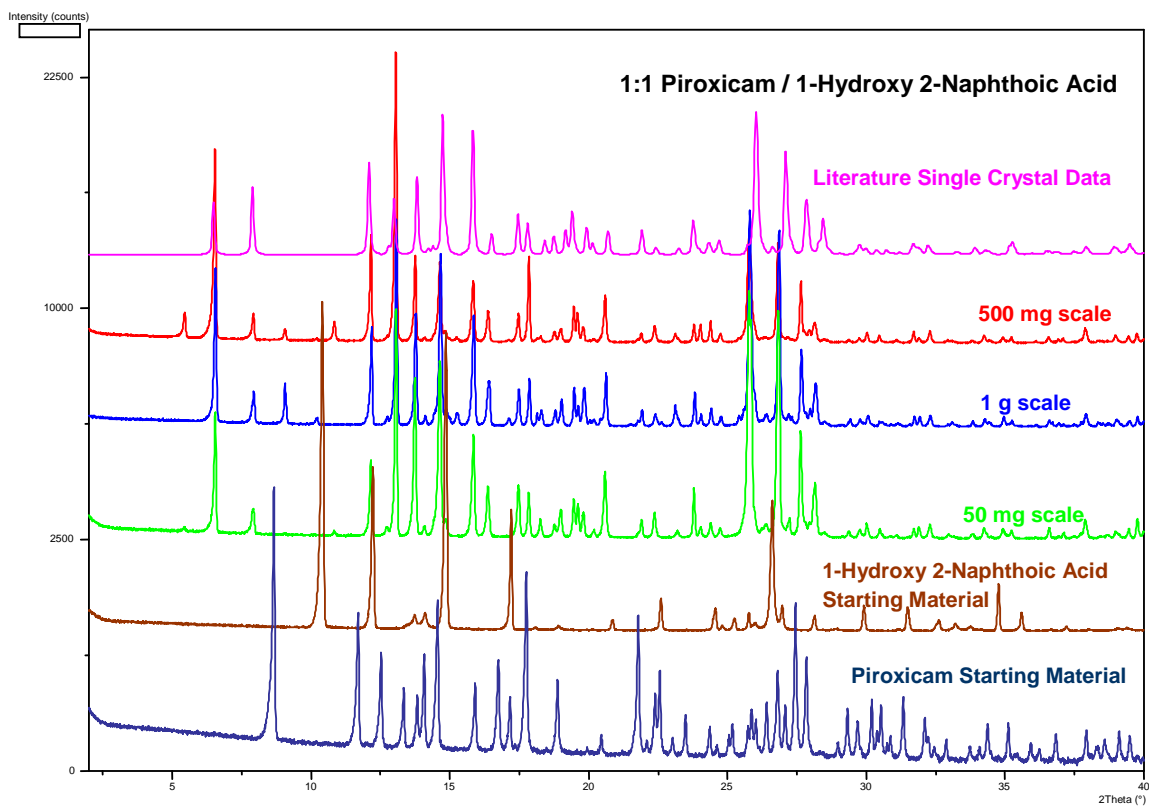


Figure 2.1: XRPD patterns for 1:1 piroxicam/1-hydroxy 2-naphthoic acid and starting materials.

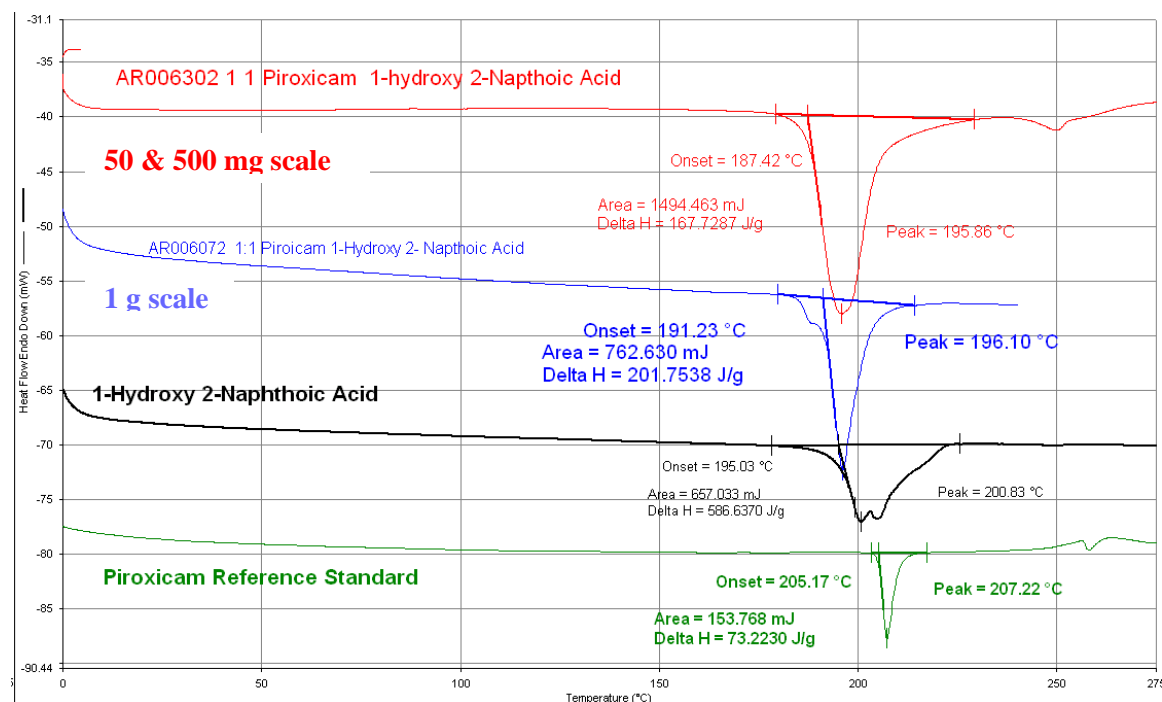


Figure 2.2: DSC thermograms for 1:1 piroxicam/1-hydroxy 2-naphthoic acid and starting materials.

1:1 and 2:1 Piroxicam/Malonic Acid. The 1:1 crystals had a few peaks that matched the literature single crystal data as well as peaks that matched the malonic acid starting material. Water and excess malonic acid were observed in the DSC data. A broad endotherm at 160°C matched the DSC results for the physical mixture. This endotherm could also represent a solvate, which would correlate with the large weight loss by TGA (7-15%). Due to the excess malonic acid observed in the DSC data, an attempt was made to make a 2:1 co-crystal. XRPD patterns of 1:1 and 2:1 piroxicam/malonic acid crystals did not compare. The 1 g and 2 g scales for the 2:1 crystals produced large crystals so a crystal was submitted for single crystal analysis. Single crystal data proved the crystal to be piroxicam monohydrate and not a co-crystal. The XRPD pattern also correlated with the malonic acid starting materials. DSC data had multiple

endotherms suggesting water and piroxicam. Like the 1:1 crystals, the 2:1 also had a broad endotherm at 160°C. About 10-17% weight loss was observed. From this data it was concluded that the 2:1 crystals were not co-crystals and most likely a mixture of piroxicam monohydrate, piroxicam, and malonic acid. The 1:1 crystals appear to be a mixture of co-crystal and malonic acid.

1:1 Piroxicam/4-hydroxy Benzoic Acid: XRPD results for the 50 mg and 500 mg 1:1 piroxicam/4-hydroxy benzoic acid crystals were reproducible. Only a few peaks matched the literature single crystal data. Some of the peaks matched the physical mixture pattern. DSC results had one split endotherm with peaks at 187 and 197°C. There was very little weight loss by TGA. It is possible that the crystals could be a mixture of co-crystals along with the starting materials.

1:1 and 2:1 Piroxicam/Succinic Acid: Results for the 1:1 and 2:1 piroxicam/succinic acid crystals were confusing. The 2:1 XRPD patterns did not correlate with the literature single crystal data. The 1:1 and 2:1 patterns were very similar with the exception of a few peaks. Both patterns also had a few peaks that compared with the starting materials. There were multiple endotherms in the DSC data for the crystals. The DSC data for the 1:1 crystals were reproducible for all the batches made. However, the 2:1 DSC results were not reproducible, with the number of endotherms increasing as the scale increased. The largest endotherm, which was present in all of the 1:1 and 2:1 crystals, was at 170°C. In all of the DSC data, the endotherms were sharp peaks which suggests, along with the small weight loss by TGA, that no solvates were present. Overall, there appeared to be multiple substances in the crystals which may or may not include co-crystals.

1:1 Piroxicam/Benzoic Acid: The XRPD patterns for all three scales were not consistent. Some of the peaks from each batch matched the literature single crystal data; however, many also compared with the physical mixture patterns as well. The 50 and 500 mg DSC data was similar with endotherms at 168 and 198°C. The 2 gram scale had an endotherm at 168°C but not at 198°C. All three scales had endotherms within the 118-140°C region which could correspond to the melt of benzoic acid (melting point at 124°C). This theory was also supported by the weight loss (10-18%) observed within this temperature region. It is possible that the endotherm at 168°C could correspond to a co-crystal. Based on these results, the crystals were most likely a mixture of the reactants and possibly some co-crystal material.

Conclusions

Out of seven slow evaporation experiments with five carboxylic acid cofomers, only the 1:1 piroxicam/1-hydroxy, 2-napthoic acid crystals appeared to be co-crystals. All of the other crystals produced were physical mixtures of the reactants that may or may not have also contained co-crystals. The Childs reference did not report the concentrations of piroxicam and cofomer used as well the solution volume and the exact rate of evaporation.¹ It is possible that the scale-up batches did not contain the ideal ternary system of API, cofomer, and solvent to make the co-crystal form.³

While the slow evaporation method works well for identifying co-crystals on a small scale, it does not appear to be ideal for scale-up without further method development. The long evaporation time required for large batches of co-crystals is not practical to identify and test new API forms. Obtaining a pure batch of co-crystals was also a major issue for most, if not all, of

the slow evaporation experiments conducted. Without a significant amount of pure material, co-crystal performance cannot be accurately tested in dissolution, solubility, and *in vivo* studies.

References

1. Childs SL, Hardcastle KI. 2007. Cocrystals of Piroxicam with Carboxylic Acids. *Cryst Growth Des* 7(7):1291-1304.
2. Vrečer F, Vrbinc M, Meden A. 2003. Characterization of piroxicam crystal modifications. *International J Pharm* 256:3-15.
3. Childs SL, Rodríguez-Hornedo N, Reddy LS, Jayasankar A, Maheshwari C, McCausland L, Shipplett R, Stahly BC. 2008. Screening strategies based on solubility and solution composition generate pharmaceutically acceptable cocrystals of carbamazepine. *Cryst Eng Comm* 7(10):856-864.

CHAPTER 3. Piroxicam Co-crystals by Reaction Crystallization

Purpose of the Research Performed

The purpose of the research performed in this chapter was to investigate co-crystal formation by reaction crystallization and to determine if this method was applicable for making small and large scale batches of co-crystals.

Introduction

Preliminary attempts to create large scale batches of co-crystals by slow evaporation proved unsuccessful. The reactions were difficult to control and produced a mixture of products containing little, if any, co-crystal. Therefore, this method was abandoned in favor of a less time consuming and more controlled technique to create co-crystals.

The mechanisms of the reaction co-crystallization method have been extensively studied by Rodríguez-Hornedo and Nehm et. al. using carbamazepine/nicotinamide co-crystals as a model.^{1,2} These experiments are performed by adding reactant B to a saturated or close to saturated solution of reactant A, thus supersaturating the solution with respect to co-crystal AB.³ The idea being that once the solution is supersaturated with co-crystal, pure co-crystal will precipitate out of solution. The solubilities of the reactants are used to determine the concentration regions required to potentially form a co-crystal, rather than the stoichiometry of the co-crystal.⁴ It should be noted that these techniques were explored as early as the 1950's by Higuchi and coworkers.⁵⁻⁷ However, his work was more focused on improving the aqueous

solubility of poorly soluble compounds via solution complexation and less on the insoluble complexes that formed.

The advantages of the reaction crystallization method are that it can be used in a high throughput mode to screen for co-crystals, it is transferable to larger scale co-crystallization processes, it affords co-crystal formation at ambient temperature, and can produce pure co-crystals.¹ Childs et. al. used reaction crystallization as a screening strategy to identify 11 carbamazepine co-crystal forms with nine carboxylic acid cofomers.⁸ In a study by Li et. al., reaction crystallization was used to scale up glutaric acid co-crystals that were originally identified in a small scale screen using co-grinding methods.⁹ Co-crystals formed via reaction crystallization are often visibly observed quickly. Reddy et. al. observed co-crystallization of gabapentin with several carboxylic acids within minutes.¹⁰ Carbamazepine co-crystals with malonic acid, glutaric acid, saccharin, oxalic acid, succinic acid, and salicylic acid have also been reported using this technique.¹¹

Piroxicam carboxylic acid cofomers explored by Childs et. al.¹² including benzoic acid, salicylic acid, 4-hydroxy benzoic acid, malonic acid, mandelic acid, succinic acid, gentisic acid, fumaric acid, and maleic acid were used in this research to study the reaction crystallization method. Saccharin was also chosen as a cofomer to try with this method because a piroxicam co-crystal with saccharin has also been reported in the literature.¹³ Piroxicam and cofomer solubilities in several solvents were measured to determine co-crystal experimental parameters. Co-crystals were characterized by XRPD, DSC, TGA, and HPLC.

Experimental

Solubility of Piroxicam and Coformers in Organic Solvents

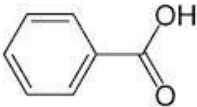
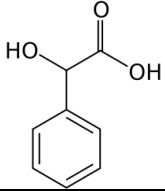
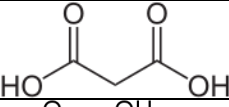
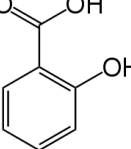
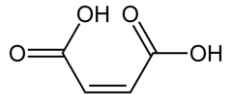
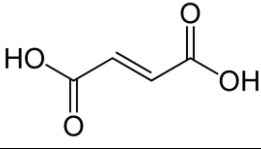
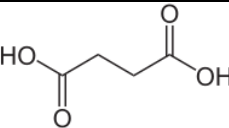
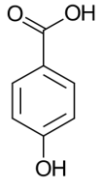
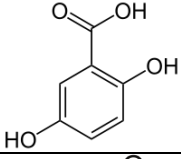
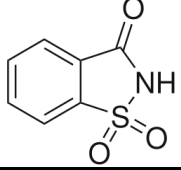
Equilibrium solubility of piroxicam and acid coformers in various organic solvents (Table 3.2) was determined at room temperature by shaking samples with excess solid overnight on an orbital shaker (Lab-Line Instruments, Melrose Park, IL). Samples were then filtered using a 0.45 μm polyvinylidene fluoride membrane (Whatman, Piscataway, NJ). If necessary, samples were diluted in methanol prior to analysis. Saturated solution concentrations were determined by high performance liquid chromatography (HPLC). The HPLC-UV instrument used was an Agilent 1200 series (Palo Alto, CA) equipped with a UV diode array detector (Agilent Technologies, Palo Alto, CA) and contained an Agilent Zorbax Bonus RP 4.6 x 150mm 3.5 micron column. Concentrations were determined using a gradient method from 5% solvent B (acetonitrile containing 0.1% trifluoroacetic acid) to 95% solvent B in 25 minutes, isocratic at 100% solvent B for 1.5 minutes, then equilibrate for 5 minutes at 5% solvent B. Solvent A was water containing 0.1% trifluoroacetic acid. The flow rate was 1 mL/min. Calibration curve standards were prepared in methanol at 1, 10, 100, and 250 $\mu\text{g/mL}$. The wavelengths of absorbance monitored for piroxicam and 4-hydroxy benzoic acid were 325 and 254 nm respectively. All other acids were monitored at 210 or 220 nm.

Piroxicam Co-crystal Synthesis

Table 3.1 lists the coformers and solvents tried using the reaction crystallization method. For co-crystals that were successful, the experimental parameters (also summarized in Table 3.4) are as follows: Benzoic acid, gentisic acid, salicylic acid, 4-hydroxy benzoic acid, and saccharin

co-crystals were made in 2,2,2 trifluoroethanol. Approximately 80 – 500 mg of piroxicam was added to 1 – 8 mL of presaturated solutions of benzoic acid, salicylic acid, and 4-hydroxy benzoic acid cofomers. The amount of piroxicam added was based on its solubility limit in 2,2,2 trifluoroethanol (Table 3.2). Solutions were shaken on an orbital shaker. Benzoic acid and salicylic acid co-crystals were observed within minutes. 4-hydroxy benzoic acid co-crystals were apparent after three days. Gentisic acid and saccharin co-crystals were made by suspending 200 – 450 mg of the acids in 6 – 12 mL of presaturated piroxicam solutions and shaken over night. Succinic acid co-crystals were made by adding approximately 90 mg of piroxicam to 3 mL of a saturated succinic acid solution in 2:1 tetrahydrofuran (THF) / 2-propanol (IPA). The solution was shaken overnight. Succinic acid co-crystals were observed after 2 – 3 hours. Co-crystals were collected by vacuum filtration to remove excess solvent and dried in a hood. Co-crystals were characterized by XRPD, DSC, and TGA. The piroxicam/acid co-crystal ratio was determined by HPLC. Approximately the same ratios of piroxicam and cofomer concentrations were used for scale up batches.

Table 3.1: Coformers and solvents tried using reaction crystallization.

Carboxylic Acid	Structure	Solvent	Co-Crystal Apparent?
Benzoic Acid		Trifluoroethanol	Yes
Mandelic Acid		Trifluoroethanol	No
Malonic Acid		Trifluoroethanol 1:1 THF/IPA 2:1 THF/IPA	No No No
Salicylic Acid		Trifluoroethanol	Yes
Maleic Acid		Trifluoroethanol	No
Fumaric Acid		Trifluoroethanol 1:1 TFE/MeOH 2:1 TFE/MeOH 1:1 THF/IPA 2:1 THF/IPA	No No No No No
Succinic Acid		Trifluoroethanol 1:1 THF/IPA 2:1 THF/IPA	No Yes Yes
4-hydroxy Benzoic Acid		Trifluoroethanol	Yes
Gentisic Acid		Trifluoroethanol	Yes
Saccharin		Trifluoroethanol	Yes

Results and Discussion

Based on a small library of solubility data generated for piroxicam in organic solvents (Table 3.2), trifluoroethanol was chosen as the preferred solvent to screen for co-crystals because it had the highest piroxicam solubility (100 mg/mL). High piroxicam solubility was thought to be desirable because the aim was to produce a high yield of co-crystal using a minimal amount of solvent (1-10 mL). The solubilities of the co-crystal cofomers in the solvents used are listed in Table 3.3.

Table 3.2: Piroxicam solubility in organic solvents.

Solvent	Piroxicam Solubility (mg/mL)
Trifluoroethanol (TFE)	100
Tetrahydrofuran (THF)	51
Methanol (MeOH)	2.3
Acetonitrile (ACN)	8.3
Isopropanol (IPA)	1
1:1 TFE/MeOH	6.1
1:1 TFE/ACN	11.8
2:1 TFE/MeOH	9.1
1:1 THF/IPA	17.5
2:1 THF/IPA	29.3

Table 3.3: Cofomer solubilities in solvents used to screen and make co-crystals.

Cofomer	TFE	1:1 TFE/MeOH	2:1 TFE/MeOH	1:1 THF/IPA	2:1 THF/IPA
Benzoic Acid	35	-	-	-	-
Mandelic Acid	84	-	-	-	-
Salicylic Acid	11	-	-	-	-
Malonic Acid	38	-	-	460	490
Maleic Acid	43	-	-	-	-
Fumaric Acid	0.2	4.7	2.3	74	80
Succinic Acid	6.3	-	-	121	112
4-hydroxy Benzoic Acid	3.0	-	-	-	-
Gentisic Acid	3.3	-	-	-	-

*ND = Not Determined

In the screening experiments, saturated solutions of the least soluble component (coformer) were made, filtered, and then the more soluble component (piroxicam) was added in an amount just under its solubility limit. The goal was to not have any excess piroxicam or acid in the starting solutions that could be confused as a co-crystal in the initial screening experiments. Furthermore, by not exceeding the solubility limits of the components, the co-crystal that precipitated out of solution was pure. Solution concentrations were monitored by HPLC throughout the crystallization process to evaluate whether the solid observed appeared to be a complex of the reactants (co-crystal). The solid precipitate was also collected and analyzed by HPLC to determine the stoichiometry of the complex. If the solid appeared to be a co-crystal (i.e. had a 1:1 or 2:1 stoichiometry) based the HPLC results, it was further characterized by XRPD, DSC, and TGA.

A summary of the piroxicam and coformer concentrations used to make the co-crystals as well as the solution scale, yield, and stoichiometry of the co-crystals are listed in Table 3.4. Co-crystal molecular weight and thermal properties are in Table 3.5. Co-crystal formation was successful in trifluoroethanol with all of the aromatic acids. Succinic acid was the only aliphatic acid that formed a co-crystal with piroxicam and it only formed in 1:1 and 2:1 THF/IPA. Both the 1:1 and 2:1 THF/IPA solutions gave the same co-crystal form. The 2:1 THF/IPA solution had a higher co-crystal yield because it had greater piroxicam solubility; therefore, this solvent was used to make the scale-up batches. All co-crystals formed a 1:1 complex with the exception of succinic acid, which produced a 2:1 piroxicam/succinic acid co-crystal. XRPD patterns (Figure 3.1) for the co-crystals confirmed unique crystalline forms compared to the starting

materials and other known piroxicam forms.¹⁴ XRPD and thermal data not presented in this chapter can be found in the appendix.

Crystals for the 4-hydroxy benzoic acid co-crystal were large enough to generate single crystal X-ray data (Figure 3.2). It appears as if the co-crystal is comprised of piroxicam in the zwitterionic form. The phenolic hydroxyl group on 4-hydroxy benzoic acid forms a hydrogen bond to the enolate oxygen. The carboxylic acid forms a hydrogen bond to the sulfonyl group on piroxicam as well as accepts a hydrogen bond from a protonated pyridine on a neighboring piroxicam molecule. These results are identical to single crystal data previously generated by Childs et. al.¹² The benzoic acid and succinic acid co-crystal XRPD patterns also compare with single crystal data previously reported.¹²

Table 3.4: Co-crystal experimental parameters, yield, and thermal properties.

Cofomer (Co-crystal Abbreviation)	Solution Scale (mL)	Cofomer^a or Piroxicam^b Solution Concentration (mg/mL)	Cofomer^a or Piroxicam^b Added (mg)	Recovery (mg)	Yield (%)	Piroxicam/ Cofomer Ratio by HPLC
Benzoic Acid (PBA)	1	35 ^a	70 ^b	60	63	1:1
	11	35 ^a	1020 ^b	1064	76	
Salicylic Acid (PSA)	8	11 ^a	500 ^b	155	52	1:1
	45	11 ^a	3200 ^b	1350	80	
4-hydroxy Benzoic Acid (P4hBA)	3	3 ^a	250 ^b	15	49	1:1
	200	3 ^a	15500 ^b	1480	73	
Saccharin (PSacc)	10	73 ^b	447 ^a	741	65	1:1
	12	85 ^b	450 ^a	960	76	
Gentisic Acid (PGA)	6	83 ^b	200 ^a	353	56	1:1
Succinic Acid (PSucA)	5	112 ^a	93 ^b	50	46	2:1
	11	112 ^a	343 ^b	164	41	

Table 3.5: Co-crystal molecular weight and thermal properties.

Co-Crystal	Co-crystal MW (g/mole)	Solution Scale (mL)	Weight Loss by TGA (%)	Co-crystal Melting Point (°C)	Coformer Melting Point (°C)
PBA	453.46	1	25*	170	122
		11	<1	170	
PSA	469.46	8	<1	191	159
		45	<1	190	
P4hBA	469.46	3	<1	200	215
		200	<1	200	
PSacc	514.53	10	<1	225	231
		12	<1	225	
PGA	485.46	6	<1	208	205
PSucA	780.78	5	<1	172	193
		11	1.36	170	

*Melt of benzoic acid

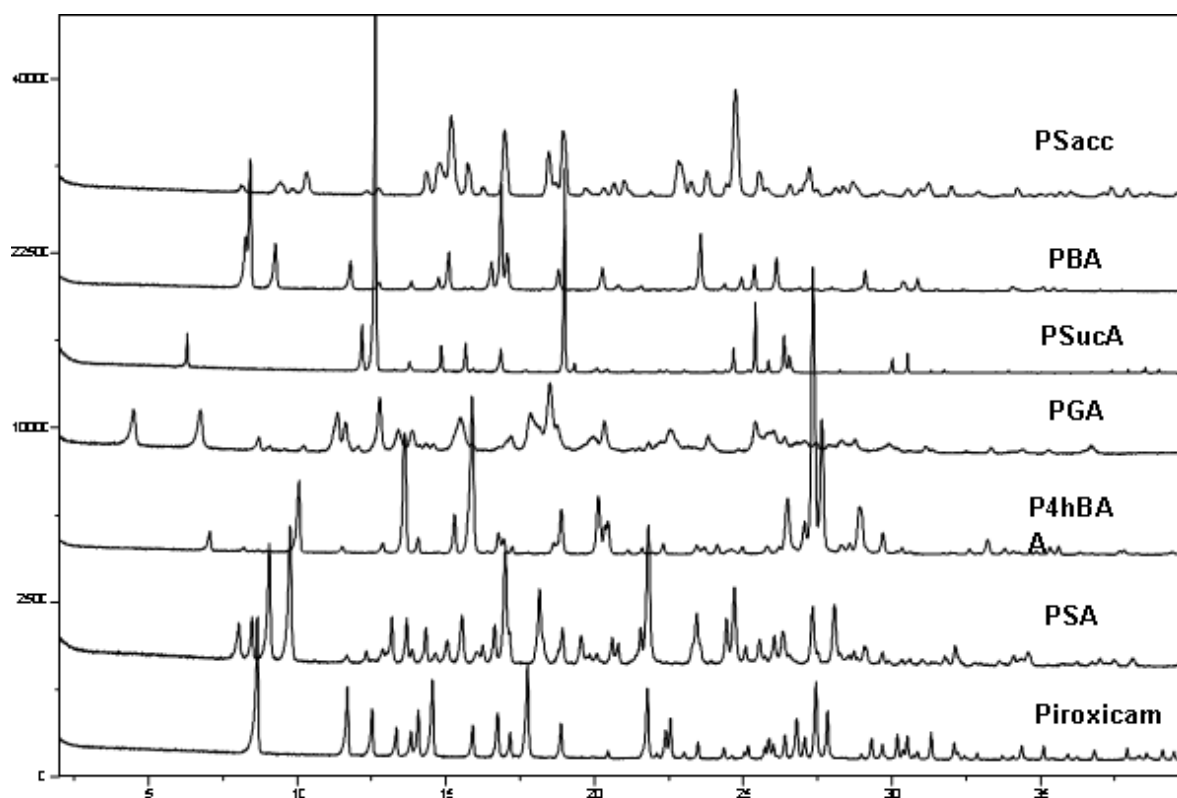


Figure 3.1: Co-crystal XRPD patterns.

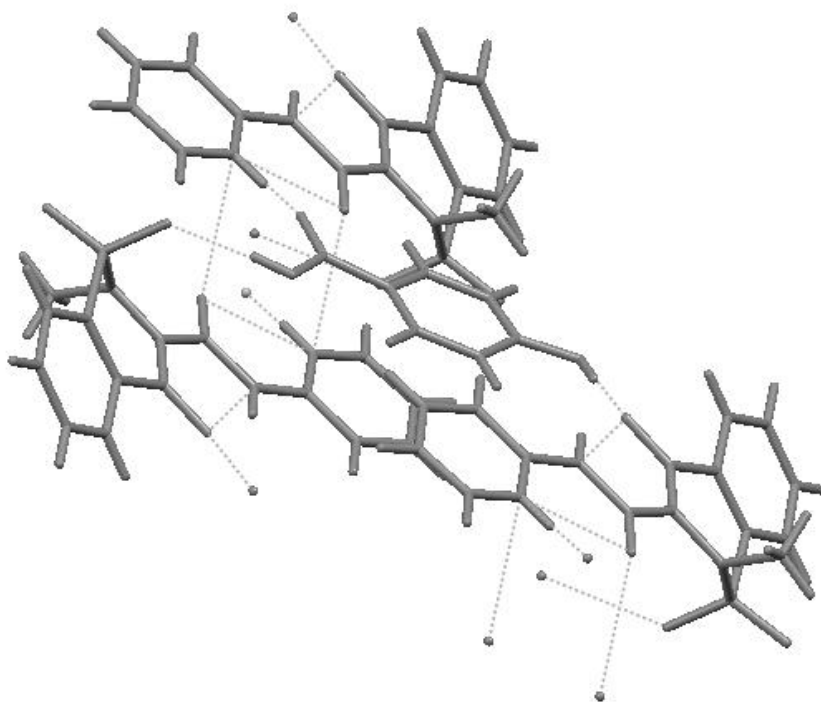


Figure 3.2: 1:1 Piroxicam/4-hydroxy benzoic acid single crystal structure.

Cofomers with low solubility required a higher solution volume to produce the desired amount of co-crystal. This was observed for the P4hBA co-crystal, where the solubility limit of 4-hydroxy benzoic acid in trifluoroethanol was only 3 mg/mL. The scale up batch required 200 mL of saturated 4-hydroxy benzoic acid and 15.5 g of piroxicam to yield only 1.5 g of co-crystal thus leaving a large amount of unreacted piroxicam. This was also an issue in the original screening experiments for the PGA co-crystals, where excess piroxicam left in the solution produced confounding co-crystal stoichiometry when the co-crystals were analyzed by HPLC (Table 3.4). The formation of the piroxicam gentisic acid co-crystals produced a “paste-like”

solution which was difficult to filter off the excess solution. The unreacted piroxicam solution that was not completely removed from the co-crystals by filtration resulted in excess piroxicam in the co-crystals. To overcome this issue, the PGA co-crystal scale-up batch (Table 3.3) was made by suspending the least soluble component (gentisic acid) in a saturated solution of the more soluble component (piroxicam). This was also done for the PSacc co-crystals.

Table 3.4: Piroxicam/gentisic acid co-crystal preliminary screening parameters.

Co-crystal	Acid Concentration	Piroxicam Added (mg)	Solution Scale (mL)	Recovery (mg)	Yield (%)	Piroxicam/Coformer Ratio by HPLC
PGA #1	3.5 mg/mL	270	3	25	76	3:1
PGA #2	3.5 mg/mL	135	2	11	50	2:1
PGA #3	3.5 mg/mL	6600	75	752	91	1.6:1

Optimizing the experimental parameters to give the best co-crystal yield was not the focus of this research and a large amount of unreacted piroxicam was discarded when the co-crystal solutions were filtered. This large amount of API used was not an issue for this research. This would most likely not be acceptable for a pre-development candidate where material may be limited. However, it is possible to adjust the experimental conditions of the reaction crystallization process to optimize co-crystal yield if needed.

For some of the coformers that did not precipitate piroxicam co-crystals, solution complexation was observed. This phenomenon was comprehensively studied in the 1950's by Higuchi et. al. and demonstrated how the solubility of poorly water soluble drugs can increase via solution complexation with a more soluble ligand (or coformer).⁵⁻⁷ Piroxicam solubility doubled in saturated 1:1 and 2:1 THF/IPA solutions of malonic acid. In saturated succinic acid trifluoroethanol solution, piroxicam solubility increased by 20 %. The possibility of solution

complexation reveals the importance of generating solubility data for the API and cofomers in the solvents chosen for co-crystal screening. It also demonstrates the value of monitoring the solution concentration of the reactants during co-crystal screening in order to gain a better understanding of the reaction crystallization process.

Conclusions

Based on the solubility data for piroxicam and nine carboxylic acids in a variety of solvents, experiments were carried out at room temperature using the reaction crystallization method that resulted in piroxicam co-crystals with six of the cofomers. This study was not meant to be an exhaustive co-crystal screen; therefore, it is possible that the three cofomers that did not form piroxicam co-crystals might be successful using this method with other solvents and/or temperatures not explored in this research.

HPLC analysis of the piroxicam and cofomer solution concentrations as well as any solid that precipitated out of the solution was helpful in determining whether the co-crystal synthesis was successful. If the HPLC results suggested that the solid was a co-crystal, it was further characterized by XRPD, DSC, and TGA. Monitoring the solution concentrations of the reactants was also useful because it helped identify any unexpected results such as solution complexation.

The reaction crystallization method proved to have many advantages over co-crystal formation by slow evaporation because it produced pure co-crystals that were easily scalable. Furthermore, co-crystal formation could be visibly observed and the co-crystals often formed quickly in as little as a few minutes to a couple hours.

References

1. Rodríguez-Hornedo N, Nehm SJ, Seefeldt KF, Pagán-Torres Y, Falkiewicz CJ. 2005. Reaction crystallization of pharmaceutical molecular complexes. *Molecular Pharm* 3(3):362-367.
2. Nehm SJ, Rodríguez-Spong B, Rodríguez-Hornedo N. 2006. Phase solubility diagrams of cocrystals are explained by solubility product and solution complexation. *Cryst Growth Des* 6(2):592-600.
3. Qiao N, Li M, Schlindwein W, Malek N, Davies A, Trappitt G. 2011. Pharmaceutical co-crystals: An overview. *Int J Pharm* 419(1-2):1-11.
4. Sekhon BS. 2009. Pharmaceutical co-crystals – a review. *Ars Pharm* 50(3):99-117.
5. Higuchi T, Zuck DA. 1952. Solubilizing action of caffeine on benzoic acid. *J Amer Pharm Assoc* 41(1):10-13.
6. Kostenbauder HB, Higuchi T. 1956. Formation of molecular complexes by some water-soluble amides I 45(8):518-522.
7. Poole JW, Higuchi T. 1959. Complexes formed in aqueous solutions by sarcosine anhydride; interactions with organic acids, phenols, and aromatic alcohols. *J Amer Pharm Assoc* 48(10):592-601.
8. Childs SL, Rodríguez-Hornedo N, Reddy LS, Jayasanka A, Maheshwari C, McCausland L, Shipplett R, Stahly BC. 2008. Screening strategies based on solubility and solution composition generate pharmaceutically acceptable co-crystals of carbamazepine. *Cryst Eng Comm* 10(7):856-864.
9. Zhibin L, Yang BS, Jiang M, Eriksson M, Spinelli E, Yee N, Senanayake C. 2009. A practical solid form screen approach to identify a pharmaceutical glutaric acid cocrystal for development. *Organic Process Res & Dev* 13(9):1307-1314.
10. Reddy SL, Bethune SJ, Kampf JW, Rodríguez-Hornedo N. 2009. Co-crystals and salts of gabapentin: pH dependent co-crystal stability and solubility. *Cryst Growth Des* 9(1):378-385.
11. Good DJ, Rodríguez-Hornedo N. 2009. Solubility advantage of pharmaceutical cocrystals. *Cryst Growth Des* 9(5):2252-2264.
12. Childs SL, Hardcastle KI. 2007. Cocrystals of Piroxicam with Carboxylic Acids. *Cryst Growth Des* 7(7):1291-1304.
13. Bhatt PM, Ravindra NV, Banerjee R, Desiraju GR. 2005. Saccharin as a salt former. Enhanced solubilities of saccharinates of active pharmaceutical ingredients. *Chem Commun* 1073-1075.
14. Vrečer F, Vrbinc M, Meden A. 2003. Characterization of piroxicam crystal modifications. *International J Pharm* 256:3-15.

CHAPTER 4. Co-crystal Solubility

Purpose of the Research Performed

The purpose of the research performed in this chapter was to measure the aqueous equilibrium solubility of the piroxicam co-crystals and predict co-crystal pH – solubility behavior.

Introduction

As a BCS Class II compound, piroxicam oral absorption is solubility limited. Co-crystals have been shown to improve drug solubility;^{1,2} therefore, measuring co-crystal solubility is desirable in order to determine whether the co-crystal form is more soluble than the free form and thus have greater bioavailability. Most co-crystal solubility measurements reported in the literature are kinetic solubility measurements of dissolution and not the true equilibrium solubility of the co-crystal form.^{3,4} Often times during these experiments, the co-crystal will dissociate, in which case what is being measured is really the solubility of the free form of the API. In fact, most relevant pharmaceutical co-crystals are more soluble than pure API and therefore are more prone to transformation when exposed to pure solvent.¹ For co-crystals composed of ionizable compounds, solubility increases seen during kinetic measurements could be due to a pH-solubility effect caused by the acid/base properties of the cofomer and/or API and not the overall solubility of the co-crystal.

Good and Rodríguez-Hornedo have developed methods to determine co-crystal equilibrium solubility that are experimentally accessible and reproducible.¹ The dissociation of a

co-crystal in solution can be described by the solubility product (K_{sp}), which is defined as a product of drug and coformer solution concentrations.^{5,6} For co-crystals that are stable or metastable when exposed to a pure solvent, the equilibrium co-crystal solubility (S_{CC}) can be determined from a single measurement of solution in equilibrium with solid drug and co-crystal.¹ Furthermore, based on the K_{sp} measured in aqueous solution, the pH-solubility behavior of the co-crystal can be predicted.⁷

In this chapter, phase diagram experiments as described by Higuchi et. al.⁸ were conducted in trifluoroethanol to confirm the stoichiometry of the PBA co-crystal. This work led to a better understanding of the theories behind co-crystal formation by reaction crystallization⁶ and equilibrium co-crystal solubility measurements¹. These methods were applied to measure the equilibrium aqueous solubility of the piroxicam co-crystals. The pH-dependent solubility of the co-crystals was also investigated.

Experimental

PBA Phase Diagram Experiments

Individual saturated solutions of benzoic acid in trifluoroethanol were made with the total volume and benzoic acid content the same (0.49 M) for each solution. Increments of piroxicam ranging from 0 - 150 mg/mL were added to each solution. The solutions were shaken for 24 hours at room temperature. After 24 hours, the solutions were filtered using a 0.45 μ m polyvinylidene fluoride membrane and the benzoic acid and piroxicam solution concentrations were analyzed by HPLC.

Equilibrium Co-crystal Solubility

Piroxicam co-crystal equilibrium solubilities in water were determined at room temperature by suspending excess co-crystal in HPLC grade water. The solutions were shaken on an orbital shaker for approximately 24 hours. Solutions were filtered using a 0.45 μm polyvinylidene fluoride membrane and analyzed by HPLC. If necessary, samples were diluted in methanol prior to analysis. The pH of the filtered solution was also measured. Piroxicam solubility was also measured as a control. The remaining solid phase was collected by vacuum filtration, dried at room temperature, and analyzed by XRPD to verify that the solid phase was the co-crystal. Equations 1 and 2 were used to calculate the measured solubilities of the 1:1 piroxicam/acid co-crystals. The fraction of nonionized piroxicam (FP) and acid (FA) were calculated using the Henderson-Hasselbalch equation. Equations 3 and 4 were used to predict co-crystal solubility at various pH values. It is important to note that these equations assume ideal behavior with concentrations replacing activities in the equilibrium constants.

$$K_{sp} = ([Piroxicam]_{eq} * FP / 100) ([Acid]_{eq} * FA / 100) \quad (1)$$

$$S_{CC} = \sqrt{K_{sp}} \quad (2)$$

$$S = \sqrt{K_{sp} \left(1 + \frac{K_{a1,acid}}{[H^+]} + \frac{K_{a1,acid} K_{a2,acid}}{[H^+]^2} \right) \left(1 + \frac{[H^+]}{K_{a1,pirox}} + \frac{K_{a2,pirox}}{[H^+]} \right)} \quad (3)$$

$$S = \sqrt{K_{sp} \left(1 + \frac{K_{a1,acid}}{[H^+]} \right) \left(1 + \frac{[H^+]}{K_{a1,pirox}} + \frac{K_{a2,pirox}}{[H^+]} \right)} \quad (4)$$

Piroxicam and Coformer Aqueous Solution Concentrations by HPLC

Solution concentrations were determined using the HPLC experimental procedure described in Chapter 3.

Results and Discussion

The results from the PBA phase diagram experiments can be seen in Figures 4.1 – 4.3. Figure 4.1 is a plot of the measured benzoic acid solution concentration at equilibrium versus the amount of piroxicam added. Each data point represents an individual solution. From the straight line portion of this plot (inset plot in Figure 4.1), the co-crystal stoichiometry was determined by calculating how much piroxicam and benzoic acid precipitated out of solution (initial acid/piroxicam concentration minus the solution concentration at equilibrium). A 1:1 co-crystal will have the same molar amount for each component. These results confirmed that the piroxicam / benzoic acid co-crystal stoichiometry was 1:1.

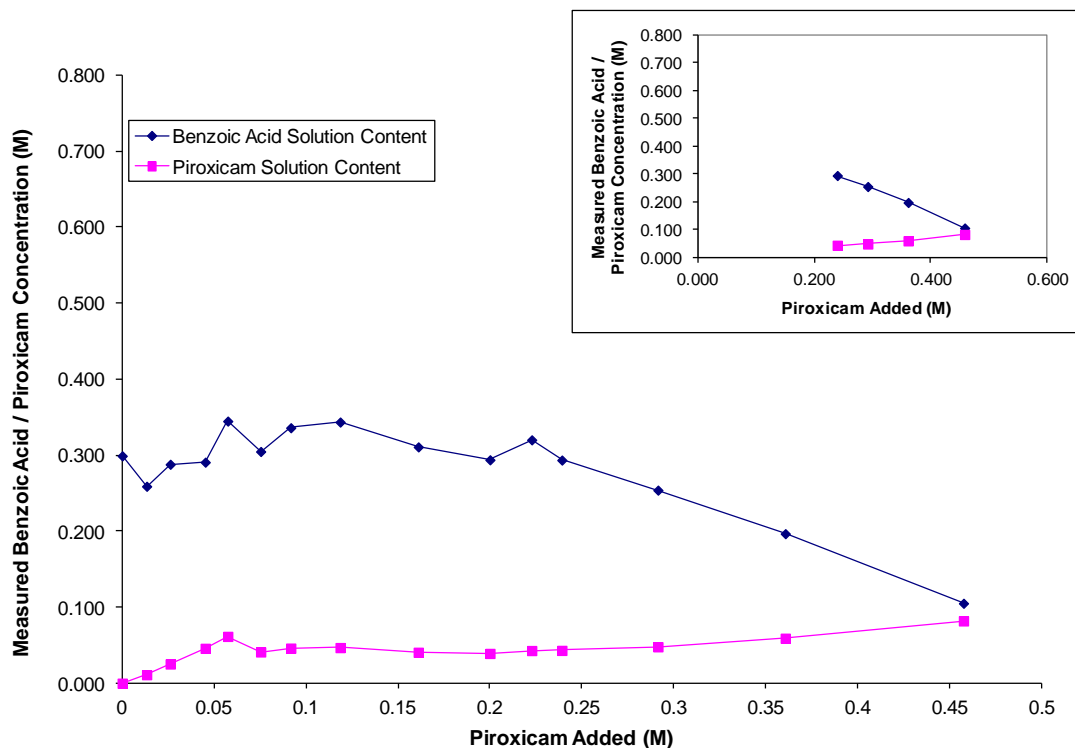


Figure 4.1: Piroxicam / benzoic acid phase diagram.

Following a suggestion from Professor Naír Rodríguez-Hornedo, a plot of the equilibrium solution concentrations of piroxicam versus benzoic acid (Figure 4.2) was made using the data points from the straight line portion in Figure 4.1. From this plot the piroxicam and benzoic acid transition concentrations, $[P]_{tr}$ and $[BA]_{tr}$, were identified where the two lines intersect and were used to determine the co-crystal solubility product, K_{sp} . From the K_{sp} , co-crystal solubility, S_{PBA} , can be determined using Equations 5 and 6.⁵

$$K_{sp} = [P]_{tr} [BA]_{tr} \quad (5)$$

$$S_{PBA} = \sqrt{K_{sp}} \quad (6)$$

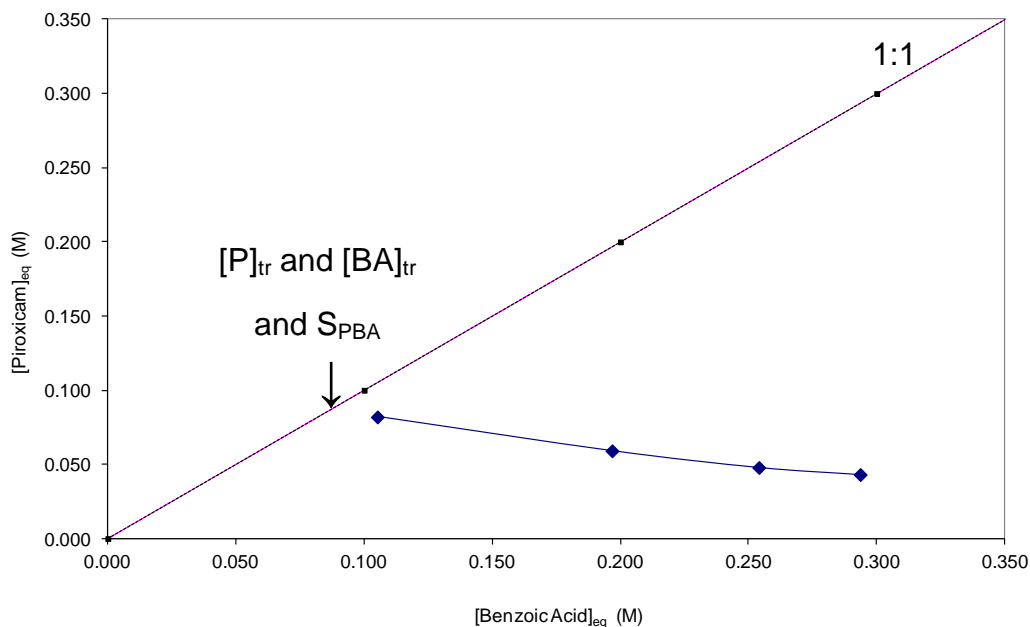


Figure 4.2: Piroxicam / benzoic acid solubility plot.

PBA solubility can also be quantified from a plot of piroxicam concentration versus 1/benzoic acid concentration (Figure 4.3). This plot also gives the K_{sp} as well as the binding constant, K_{11} , where the slope equals the K_{sp} and the intercept equals the $K_{11}K_{sp}$. Using these values, co-crystal solubility was calculated using Equation 7 which incorporates the binding constant, where $[BA]_T$ equals the total benzoic acid concentration (0.94 M).⁵

PBA solubility determined from Figure 4.2 (using Equations 5 and 6) was 0.08 M. The solubility value calculated from Figure 4.3 and Equation 7 was 0.09 M. While these two plots yield similar solubility values, it demonstrates how co-crystal solubility can change by taking into account the binding constant. It is worth mentioning that since these experiments were performed in trifluoroethanol, the transition concentrations and K_{sp} values determined from these

experiments are only relevant to the solubility of PBA in trifluoroethanol and can not be used to calculate co-crystal solubility in other solvents.

$$S_{PBA} = \frac{K_{sp}}{[BA]_T} + K_{11}K_{sp} \quad (7)$$

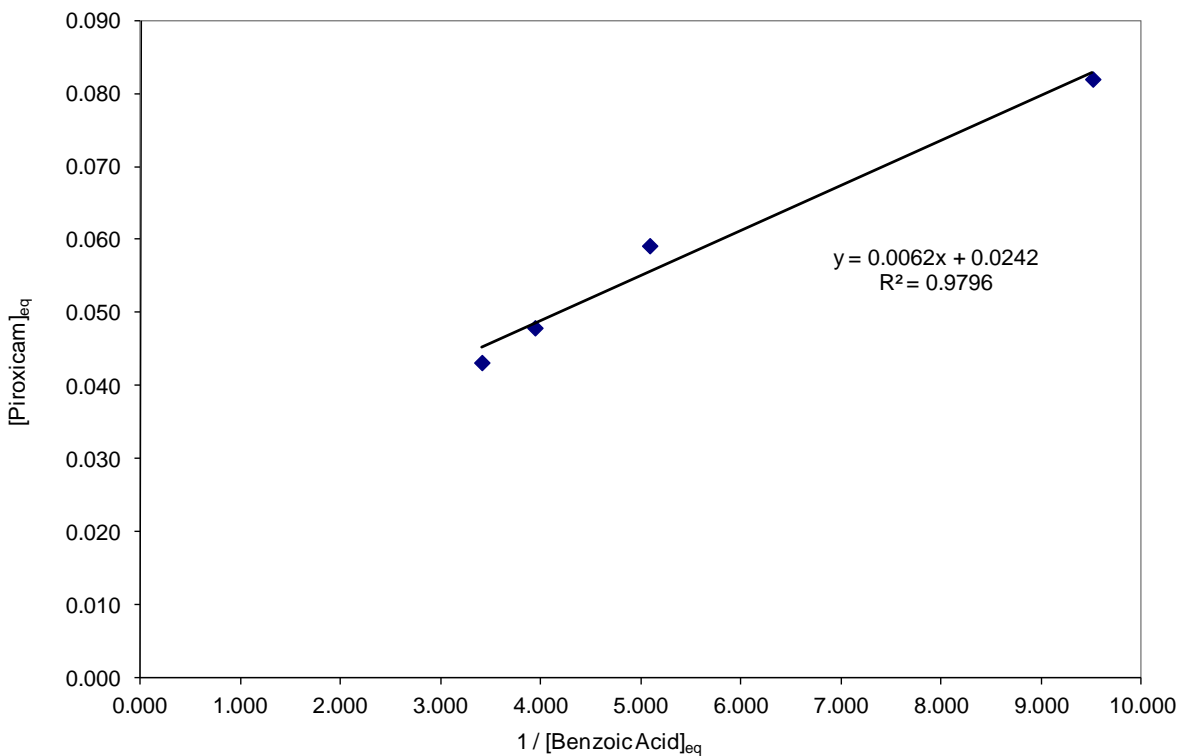


Figure 4.3: Piroxicam / Benzoic acid plot used to determine binding constant.

While co-crystal solubility can be determined from phase diagram experiments, this work is not necessary if co-crystal material is available. A much simpler method is to make a saturated co-crystal solution (with excess co-crystal solid) in the solvent of interest, let it equilibrate, and measure the solution concentration of the drug and cofomer (transition

concentrations).¹ This method was used to determine the aqueous solubility of the piroxicam co-crystals.

The measured solubilities of the piroxicam co-crystals in water at room temperature after 24 hours are listed in Table 4.1 along with the final solution pH values. Co-crystal solubility was dependent on the intrinsic solubility of the coformer (Table 4.1) and solution pH. It was observed that the greater the coformer solubility, the greater the co-crystal solubility. Coformers with higher aqueous solubility (benzoic acid, 4-hydroxy benzoic acid, and gentisic acid) resulted in piroxicam co-crystals with greater solubility than those made with coformers with lower solubility (salicylic acid and saccharin). XRPD patterns of the solid phase after 24 hours confirmed that the remaining solid form was co-crystal and traces of piroxicam monohydrate (XRPD patterns can be found in the appendix). The equilibrium aqueous solubility of PSucA could not be measured because the co-crystal components quickly dissociated when suspended in solution indicating that the co-crystal form was not thermodynamically stable in water. This result is not unexpected given the high aqueous solubility of succinic acid relative to piroxicam (Table 4.1). Co-crystal solubility has been shown to be dependent on the solubility of co-crystal components with coformer solubility about 10-fold higher than drug leading to a co-crystal that is more soluble than drug.¹ Therefore, one could speculate that PSucA is more soluble than piroxicam. This information is also useful for designing a co-crystal that is more soluble.

Table 4.1: Coformer and co-crystal equilibrium solubility in water at room temperature.

Co-crystal	Coformer Solubility, mM (pH)	Coformer pK _a (s)	Co-crystal Solubility (uM) n=3	pH	K _{sp} (M ²)
PBA	26 (2.8)	4.2	310 ± 4.28	3.3	9.60 x 10 ⁻⁸
PSA	13 (2.5)	3.0	68.3 ± 2.83	3.5	4.66 x 10 ⁻⁹
P4hBA	38 (3.0)	4.5, 9.3	275 ± 13.1	3.6	7.57 x 10 ⁻⁸
PSacc	17 (1.8)	2.0	142 ± 2.27	2.5	2.03 x 10 ⁻⁸
PGA	130 (1.9)	3.0	291 ± 1.50	2.7	8.49 x 10 ⁻⁸
PSucA	620 (2.0)	4.2, 5.6	nd	nd	nd

*nd = no data.

The aqueous solubilities of the co-crystals were measured in unbuffered water; therefore, a change in pH was observed due to the dissociation of the acidic co-crystal components. Because solution pH was not controlled, the measured co-crystal solubilities could not be directly compared to piroxicam solubility alone (also measured in unbuffered water). Equations have been derived to calculate and predict co-crystal solubility and stability in water based on solution pH, solubility product, and dissociation constant(s) of the co-crystal components.^{7,9} The K_{sp} calculated from experimentally measured co-crystal solubility at one pH can be used to predict co-crystal solubility at other pH values. A saturated solution of piroxicam in water has a pH value of 6.9. To compare to the measured piroxicam solubility (Table 4.2), the co-crystal solubilities were predicted at pH 6.9 (Table 4.2) using equations 3 or 4. At pH 6.9, the co-crystal solubilities were predicted to be about 225 (4-hydroxy benzoic acid co-crystal) to 2000 times (saccharin co-crystal) more soluble than piroxicam. An attempt was made to measure the equilibrium solubilities of the co-crystals at pH 6.9 to compare to the predicted values; however, this was not feasible because the solution pH could not be controlled independently. Despite increases in buffer concentration, the solution pH was driven by the acid coformer concentration.

Furthermore, the co-crystals completely dissociated to piroxicam monohydrate and coformer. In other words, the co-crystals were not thermodynamically stable at pH 6.9.

Table 4.2 Co-crystal predicted solubility at pH 6.9.

Compound	Solubility (mM)	Co-crystal/Piroxicam Solubility Ratio
Piroxicam	0.16	--
PBA	55	344
PSA	50	313
P4hBA	36	225
PSacc	320	2000
PGA	220	1375

The pH-dependency of the solubility of pharmaceutical acids and bases has been well established.¹⁰ As a zwitterionic drug, piroxicam solubility is higher at pH values below its pK_{a1} (1.8) and above its pK_{a2} (5.1). In its neutral form, between pH 1.8 and 5.1, piroxicam has its lowest solubility. Since piroxicam solubility is affected by pH, piroxicam equilibrium solubility was measured at pH 2, 3, and 4 in order to compare to the equilibrium co-crystal solubilities (measured at pH 2.5 – 3.3). The results can be seen in Figure 4.4. With the exception of the PSA co-crystal, all co-crystals had a significant solubility advantage over piroxicam between pH 2-4.

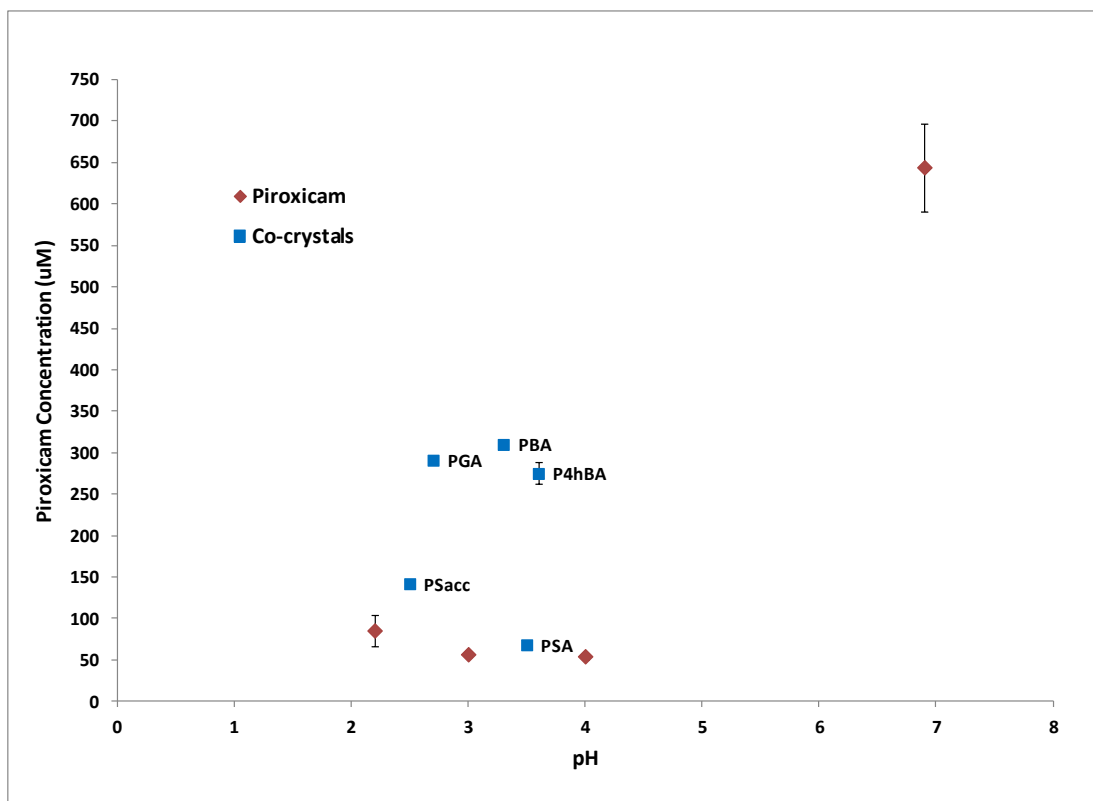


Figure 4.4: Piroxicam pH-dependent solubility and measured co-crystal solubility, n=3.

Conclusions

A method developed by Rodríguez-Hornedo et. al.^{1,5,6} to measure co-crystal equilibrium solubility was applied to determine piroxicam co-crystal solubility in water at room temperature. Further research builds on these principles and allows one to measure and predict co-crystal solubility and stability as a function of pH,^{7,10} These methods were applied to predict piroxicam co-crystal solubility at pH 6.9, a region in which the piroxicam co-crystals were not stable. Except for the PSA co-crystal at low pH, all co-crystals had a solubility advantage over piroxicam at pH 2 - 4 and 6.9.

Equilibrium solubility measurement and solubility prediction methods applied in this research are extremely useful because (1) they enable co-crystal solubility and pH dependent solubility to be measured and predicted from a single experiment using very little material (approximately 30 – 50 mg in this study) and (2) they allow co-crystal solubility to be predicted in pH regions where the co-crystal and/or co-crystal components are not stable.¹⁰

References

1. Good DJ, Rodríguez-Hornedo N. 2009. Solubility advantage of pharmaceutical cocrystals. *Cryst Growth Des* 9(5):2252-2264.
2. Blagden N, de Matas M, Gavan PT, York P. 2007. Crystal engineering of active pharmaceutical ingredients to improve solubility and dissolution rates. *Adv Drug Deliv Rev* 59(7):617-630.
3. Basavoju S, Boström D, Velaga P. 2006. Pharmaceutical cocrystals and salts of norfloxacin. *Cryst Growth Des* 6(12):2699-2708.
4. Stanton MK, Bak A. 2008. Physicochemical properties of pharmaceutical co-crystals: A case study of ten AMG 517 co-crystals. *Cryst Growth Des* 8(10):3856-3862.
5. Nehm SJ, Rodríguez-Spong B, Rodríguez-Hornedo N. 2006. Phase solubility diagrams of cocrystals are explained by solubility product and solution complexation. *Cryst Growth Des* 6(2):592-600.
6. Rodríguez-Hornedo N, Nehm SJ, Seefeldt KF, Pagán-Torres Y, Falkiewicz CJ. 2005. Reaction crystallization of pharmaceutical molecular complexes. *Molecular Pharmaceutics* 3(3):362-367.
7. Bethune SJ, Huang N, Jayasanka A, Rodríguez-Hornedo N. 2009. Understanding and predicting the effect of cocrystal components and pH on cocrystal solubility. *Cryst Growth Des* 9(9):3976-3988.
8. Haddad AF, Sciarron BJ, Higuchi T. 1959. Formation of complexes by N,N'-dimethyl-diketobenzodiazines in nonaqueous solutions. *J Amer Pharm Assoc* 48(10):588-591.
9. Reddy SL, Bethune SJ, Kampf JW, Rodríguez-Hornedo N. 2009. Co-crystals and salts of gabapentin: pH dependent co-crystal stability and solubility. *Cryst Growth Des* 9(1):378-385.
10. Stahl PH, Wermuth CG. 2002. *Handbook of Pharmaceutical Salts: Properties, Selection, and Use*. Wiley-VCH, Weinheim.

CHAPTER 5. Co-crystal Intrinsic Dissolution and Rat Pharmacokinetics

Purpose of the Research Performed

The purpose of the research performed in this chapter was to measure the dissolution rates of the piroxicam co-crystals at physiological pH, to determine co-crystal *in-vivo* bioavailability, and to establish possible correlations between dissolution and pharmacokinetic data.

Introduction

Dissolution testing is used by formulation scientists to assist in choosing among drug candidate solid state forms and formulations as well as to establish possible *in vivo* / *in vitro* correlations between release of the drug from the dosage form and drug absorption.^{1,2} Evaluation of dissolution profiles is especially important for Class II drugs since dissolution for these substances is assumed to be rate limiting step to *in vivo* absorption.^{3,4}

Intrinsic dissolution studies are often carried out using a Woods Apparatus comprised of rotating disks of compacted powder of the API immersed in dissolution test media.⁵ This method affords advantages over powder dissolution methods because the exposed area of the disk is constant and thus dissolution variability from particle size is eliminated during the dissolution period.

The solubility advantage of co-crystals has been shown to correlate with increased dissolution and bioavailability.⁶⁻⁸ Piroxicam co-crystal solubility was significantly greater than piroxicam. Therefore, in order to assess whether this solubility advantage correlates with

increased dissolution and oral exposure, intrinsic dissolution profiles for the co-crystals were generated in biorelevant media at pH 1.2 and 6.8. The effect of buffer concentration on co-crystal dissolution rate was also evaluated. Finally, co-crystals were dosed orally in rat to determine co-crystal bioavailability and draw correlations, if any, between the *in vivo* results and *in vitro* dissolution data.

Experimental

Intrinsic Dissolution

A miniature Wood's Apparatus (Distek 2100C, North Brunswick, NJ) was used to measure the dissolution rate of the co-crystals in US Pharmacopeia buffers at pH 1.2 (0.07 M HCl/ 0.03 M NaCl) and 6.8 (0.05 M monobasic potassium phosphate/0.03 M NaOH).⁹ Dissolution rates were also measured in 0.1 M monobasic potassium phosphate at pH 6.8. Approximately 10 - 15 mg of co-crystal was compressed in a punch die at 400 psi for one minute. All dissolution studies were performed in 100 mL of solution at 37°C. Paddle rotation speed was 100 rpm. Time points were collected for up to 2 hours and piroxicam concentrations were analyzed by HPLC (see Chapter 3 experimental for HPLC method). Piroxicam dissolution rates were calculated by plotting the cumulative amount of piroxicam dissolved per unit area (Equation 8) versus time. The piroxicam reference standard dissolution profile was also determined as a control. Bulk solution pH was measured at the end of the experiments and the left over pellet was analyzed by XRPD to verify that the solid state of each co-crystal was the same as the starting material.

$$Amt.Dissolved = \left\{ \left(\frac{Std.Conc. \times SampleArea}{Ave.Std.Area} \right) \times SampleVolume \right\} \div PelletSurfaceArea \quad (8)$$

*Std. Conc. = 0.1 mg/mL

*Sample Area = HPLC Peak Area Response

*Ave. Std. Area = Std. Conc. HPLC Peak Area Response

*Sample Volume = 100 mL

*Pellet Surface Area = 0.031 cm²

Rat Pharmacokinetics

Adult male Sprague Dawley (Charles River, Kingston, New York) rats were used in all experiments. The rats were fasted overnight prior to oral dose administration. Intravenous administration was via the lateral tail vein and oral doses were administered by gavage. Piroxicam and piroxicam co-crystals were orally dosed in capsules at 5 mg/kg piroxicam equivalents. Piroxicam was also dosed intravenously at 1 mg/kg in DMSO/Solutol®/PBS (3/30/67) in order to calculate bioavailability. For blood collection, each rat (unanesthetized) was placed in a clear Plexiglas® restraining tube and blood samples (approximately 0.25 mL) were drawn from a lateral tail vein into heparinized collection tubes. Blood samples were collected out to six hours. The blood samples were placed on wet ice until centrifuged to separate plasma. The plasma fraction was transferred into clean dry tubes, frozen on dry ice and stored at approximately -20°C pending analysis.

Piroxicam plasma concentration was determined by LC/MS/MS (an integrated Cohesive Technologies LX-2 series liquid chromatography system coupled with an Applied Biosystems MDS-SCIEX 4000 Qtrap mass spectrometer, Foster City, CA). Plasma proteins were

precipitated with acetonitrile containing an internal standard (alprenolol). Calibration standards were prepared in rat plasma ranging from 10 – 10000 ng/mL. WinNonLin® was used to calculate pharmacokinetic parameters.

Statistics

A one-way analysis of variance (ANOVA) test was performed to demonstrate statistical significance. $p < 0.05$ was considered statistically significant.

Results and Discussion

Intrinsic Dissolution

The dissolution profiles for piroxicam and the co-crystals at pH 6.8 and at pH 1.2 are shown in Figures 5.1-5.5. Dissolution rates were determined from the slopes of the linear regression lines and are listed in Table 5.1. The piroxicam reference standard dissolution rates measured were in agreement with previous reports.²

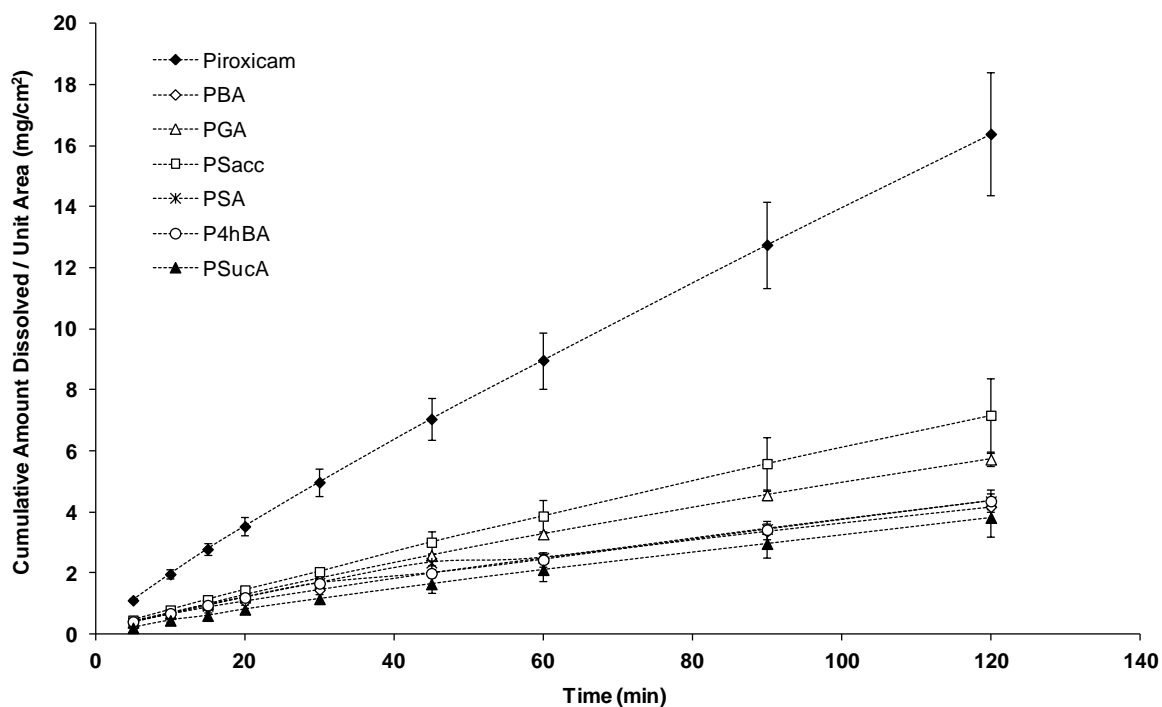


Figure 5.1: Piroxicam and co-crystal dissolution profiles in 0.05 M phosphate buffer, pH 6.8.

Dissolution at pH 6.8. At pH 6.8, all co-crystals had significantly lower dissolution rates than piroxicam alone (Table 5.1). These results are most likely due to a drop in pH occurring at the solid-liquid interface. The interfacial pH is affected by the degree of dissociation of the acid or base at the interface, which is determined by the concentration and pK_a of the acid.¹⁰ As the acid coformer dissociates, hydrogen ions are released thus lowering the pH of the diffusion layer relative to that of the bulk solution. Since piroxicam at pH 6.8 is acidic, the lower interfacial pH suppresses the solubility and thus dissolution rate. The pH 6.8 dissolution data illustrates that a co-crystal will quickly dissociate during dissolution experiments performed in pH regions where the drug and coformer are ionized. Once the co-crystal dissociates, the dissolution rate is driven

by the intrinsic solubility of the drug as function of pH.¹⁰ These results reveal the importance of understanding the acid/base properties of both drug and coformer and how they can impact the overall dissolution rate of the drug. Furthermore, it emphasizes the need to stabilize the co-crystal to prevent dissociation and achieve the solubility and dissolution advantages of the co-crystal form¹¹.

Table 5.1: Piroxicam dissolution rates at pH 1.2 and 6.8 at 37°C ($\mu\text{g}/\text{min}/\text{cm}^2$).

Compound	pH 1.2 ^a	pH 6.8 (0.05M) ^b
Piroxicam	54 ± 7.0	130 ± 17
PBA	62 ± 7.5	32 ± 1.5
PSA	48 ± 18	34 ± 2.1
P4hBA	66 ± 5.1	33 ± 3.2
PSacc	42 ± 12	59 ± 11
PGA	40 ± 3.6	46 ± 2.1
PSucA	25 ± 7.9	31 ± 5.0

^a 30 minute dissolution rate.

^b 2 hour dissolution rate.

Previous research has shown that dissolution behavior can be affected by buffer concentration.¹² Therefore, in an attempt to dampen pH changes within the diffusion layer, potassium phosphate buffer concentration was doubled to 0.1 M. The dissolution profiles are shown in Figure 5.2. While the dissolution rates of the co-crystals were still significantly lower than piroxicam alone, the increased buffer concentration appeared to give a small boost to the dissolution rates (Figure 5.3), which was significant for the PBA and PSA co-crystals. The $\text{pK}_a(\text{s})$ and intrinsic solubility of the acid as well as the pK_a of the buffer are important to take into account when interpreting the dissolution data; therefore, the equilibrium solubilities of piroxicam and the acids were measured in the dissolution media and are listed along with their $\text{pK}_a(\text{s})$ in Table 5.2. Solubility in 0.1 M potassium phosphate buffer was not determined due to

limited material for some of the acids but one would expect the solubility to be comparable to 0.05 M. The PSucA co-crystal dissolution rate in these buffer conditions was not determined because based on the results for the other co-crystals, it was concluded that the dissolution behavior of PSucA would be similar.

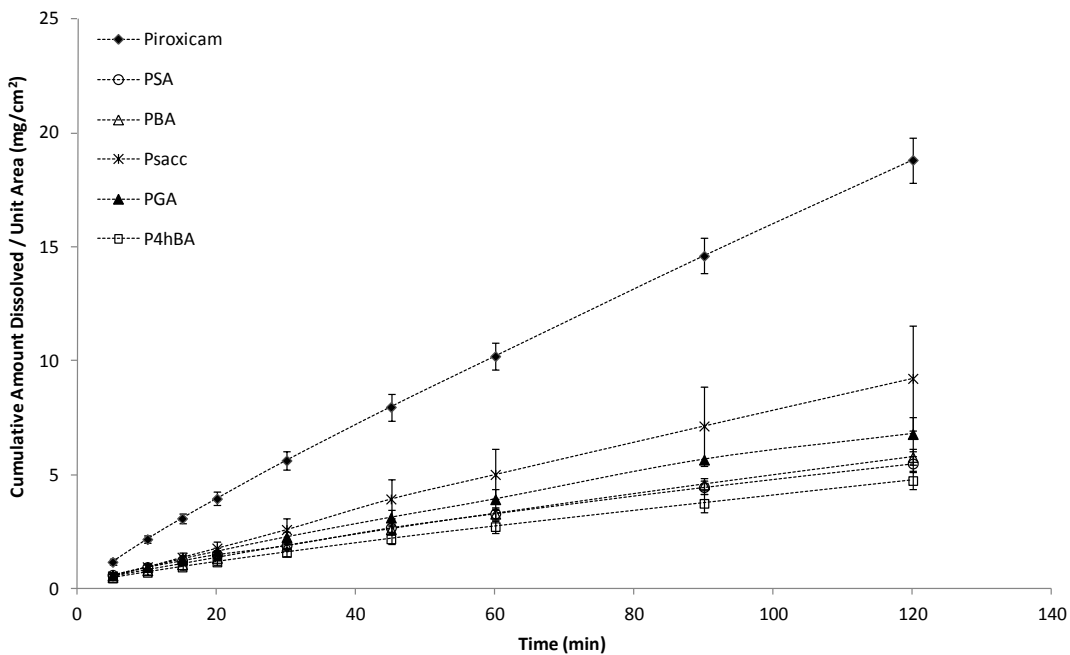


Figure 5.2: Piroxicam and co-crystal dissolution profiles in 0.1 M phosphate buffer, pH 6.8.

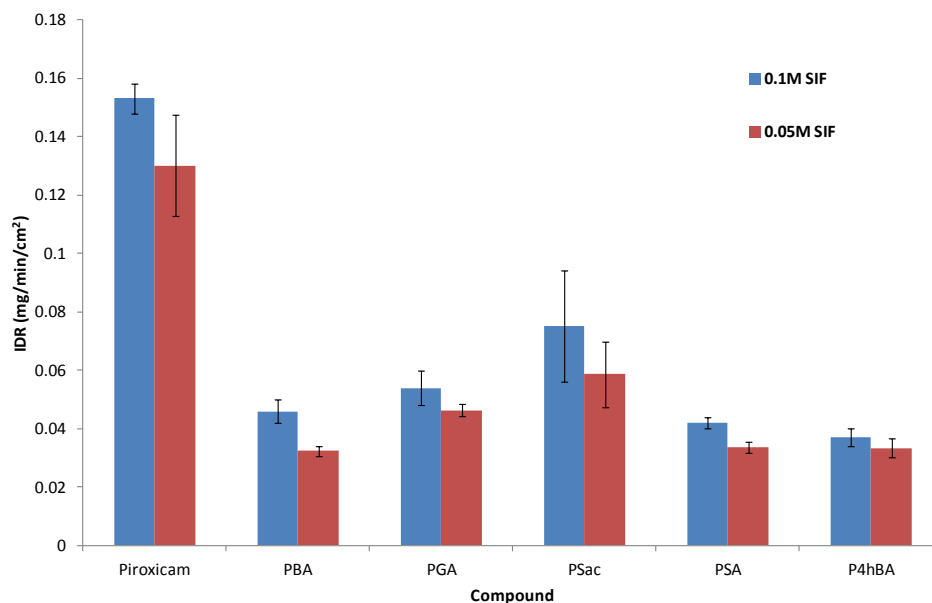


Figure 5.3: Dissolution rate comparison in 0.05 M and 0.1 M buffer, pH 6.8.

Table 5.2: Piroxicam and coformer solubility in biorelevant media (mM).

Compound	pH 1.2	pH 6.8 (0.05M)	pK _a (s)
Piroxicam	0.36	1.20	1.8, 5.1
Gentisic Acid*	118.43	129.76	3.0
4-hydroxy Benzoic Acid	54.75	85.64	4.5, 9.3
Salicylic Acid	13.88	48.25	3.0
Saccharin	9.93	59.33	2.0
Benzoic Acid	42.78	67.23	4.2

*Solution not completely saturated due to limited material.

No significant changes in piroxicam dissolution rate were observed for the PGA and P4hBA co-crystals with an increase in buffer concentration. This can be explained by dissolution rate dependency on the intrinsic solubility of the acids and pH. Acids with higher solubilities, i.e. gentisic acid and 4-hydroxy benzoic acid, are less sensitive to buffer concentration and pH because they are so soluble that they “self-buffer” the pH in the diffusion

layer.¹² In other words, high concentrations of hydrogen ions are released in solution from these acids which consume all the unprotonated form of the buffer. Benzoic acid and salicylic acid have lower solubilities and therefore are less able to self-buffer the diffusion layer pH. The co-crystals with these acid cofomers (PBA and PSA) have piroxicam dissolution rates that are affected more by an increase in buffer concentration.

Dissolution at pH 1.2. Dissolution experiments were also conducted at pH 1.2. The results are shown in Figure 5.3. After 45 minutes, there was a great deal of variability between the three pellets for each co-crystal so it was difficult to draw conclusions for the complete two hour dissolution period; however, differences were observed within the first 30 minutes (Figure 5.4). In the first 30 minutes for the PBA and P4hBA co-crystals, the cumulative amount of piroxicam dissolved per unit area for each individual time point was significantly greater than piroxicam (Figure 5.5). The piroxicam dissolution rate for these co-crystals (Table 5.1) also appeared to be slightly improved; however, it was not statistically different at the 95% confidence interval (PBA, $p = 0.2$ and P4hBA, $p = 0.07$).

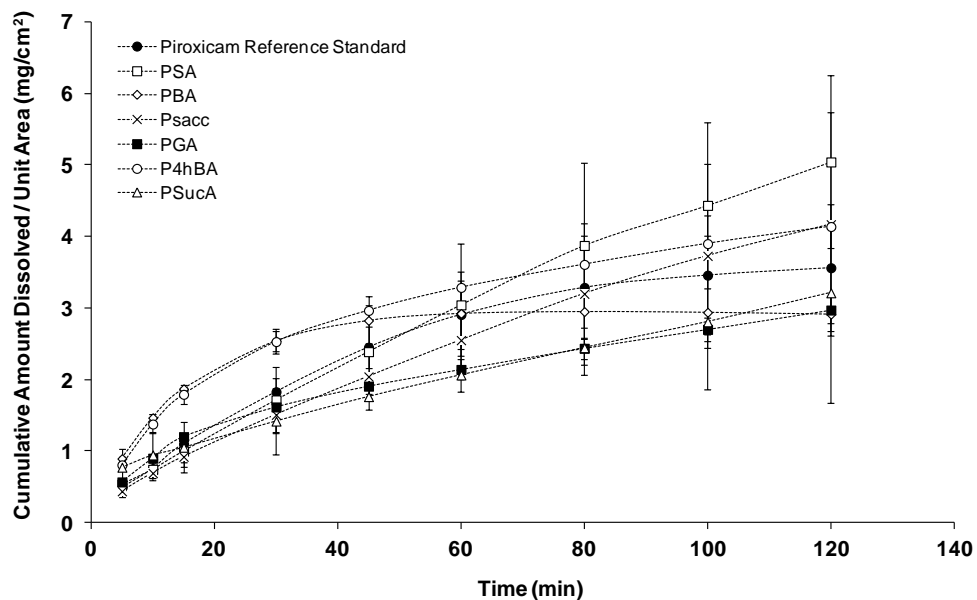


Figure 5.3: Piroxicam and co-crystal 2 hour dissolution profiles at pH 1.2.

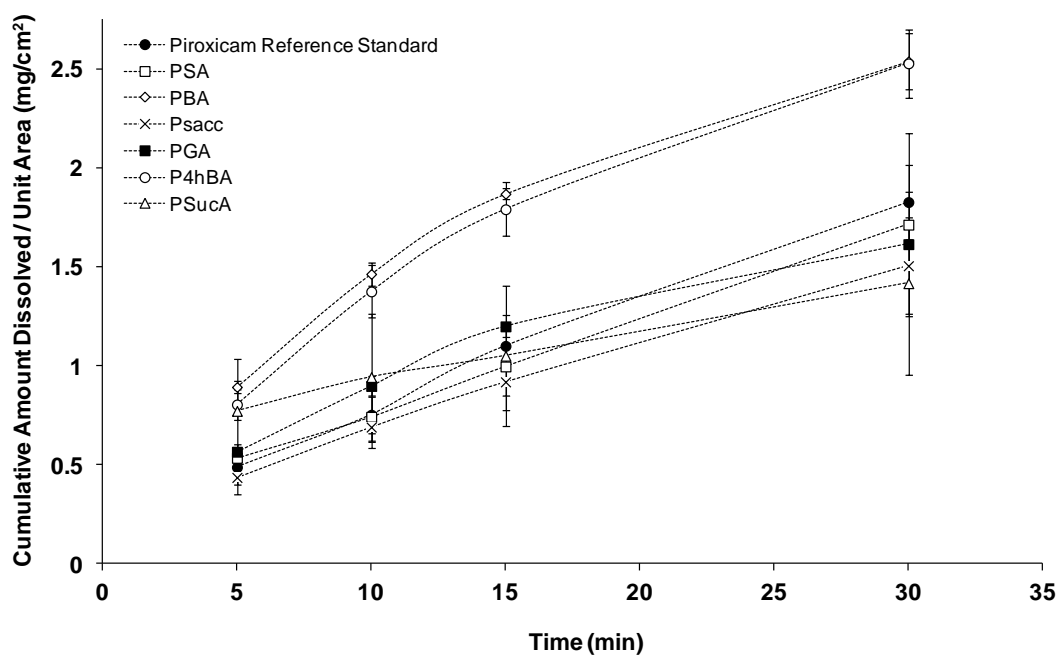


Figure 5.4: Piroxicam and co-crystal 30 minute dissolution profiles at pH 1.2.

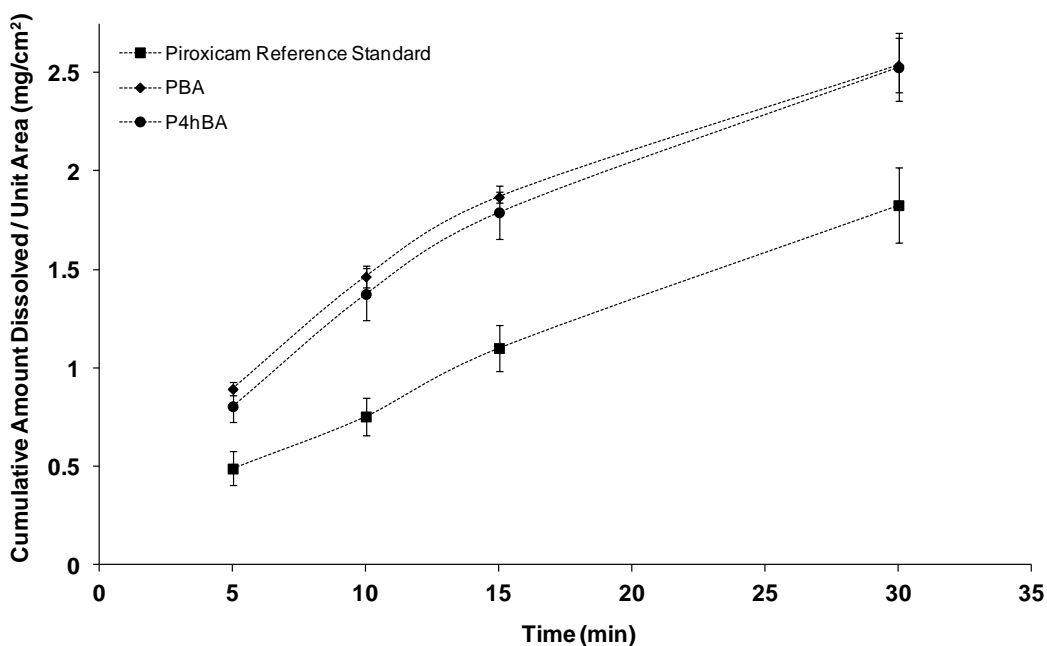


Figure 5.5: Piroxicam, PBA, and P4hBA 30 minute dissolution profiles at pH 1.2

The dissolution results at pH 1.2 can be explained by examining the solubility and pK_a of the acid cofomers. Benzoic acid and 4-hydroxy benzoic acid have pK_a values over four and in a solution at pH 1.2, all the acid species should be in the unionized form. Saccharin, gentisic acid, and salicylic acid, however, have lower pK_a values around 2 - 3 which are much closer to pH 1.2. It is possible that there was a small percentage of these acids in the ionized form. As previously stated, dissociation of the acid liberates hydrogen ions and therefore lowers the pH of the diffusion layer relative to the bulk solution pH. The intrinsic solubilities of the acids also contribute to dissolution rate. Benzoic acid and 4-hydroxy benzoic acid were about five times more soluble than salicylic acid and saccharin in the dissolution media. Gentisic acid and succinic acid were the most soluble of all the acid cofomers; however, the gentisic acid and

succinic acid co-crystals did not significantly boost the piroxicam dissolution rate. This could be explained if there were some fraction of the acid dissociating that changes the pH of the diffusion layer and thus the dissolution rate.

Pharmacokinetics

Solubility is one of the many physiochemical factors that affect oral absorption of a drug.¹³ As a Class II drug (high permeability, low solubility), the *in vivo* absorption rate of piroxicam is limited by its low solubility.¹⁴ Therefore, based on the co-crystal solubility results, one might expect the co-crystals to have higher bioavailability. The oral exposure profiles and calculated six hour rat bioavailability for piroxicam and the co-crystals can be seen in Figure 5.6 and Table 5.3. Statistical analysis (ANOVA, $p>0.05$) revealed that co-crystal bioavailability was not different than piroxicam. Additional pharmacokinetic data not listed in this chapter can be found in the appendix.

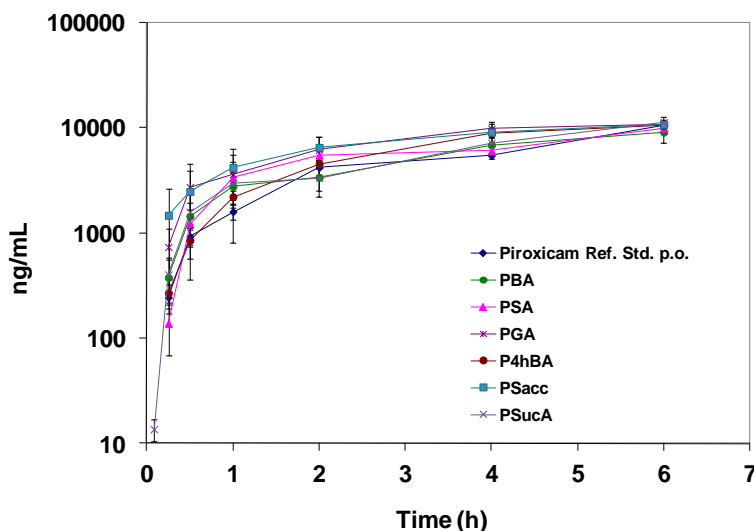


Figure 5.6: Piroxicam 6 hour rat plasma levels after oral capsule dosing (n=3).

Table 5.3: Piroxicam and co-crystal 6 hour bioavailability (n=3).

Compound	Bioavailability (%) \pm sem
Piroxicam Reference Standard	30 \pm 2
PBA	31 \pm 5
PSA	34 \pm 1
PGA	44 \pm 7
P4hBA	38 \pm 3
PSacc	44 \pm 9
PSucA	40 \pm 6

The gentisic acid and saccharin co-crystals appeared to possibly give a slight boost to piroxicam plasma levels within the first hour. Therefore, a one hour PK study with additional time points was conducted for piroxicam and the gentisic acid and saccharin co-crystals to confirm these results. These results are shown in Figure 5.7. No significant differences were observed compared to piroxicam for the saccharin co-crystal. Piroxicam exposure from the gentisic acid co-crystal appeared to be greater within the first 30 minutes but was not significantly different ($p=0.3$).

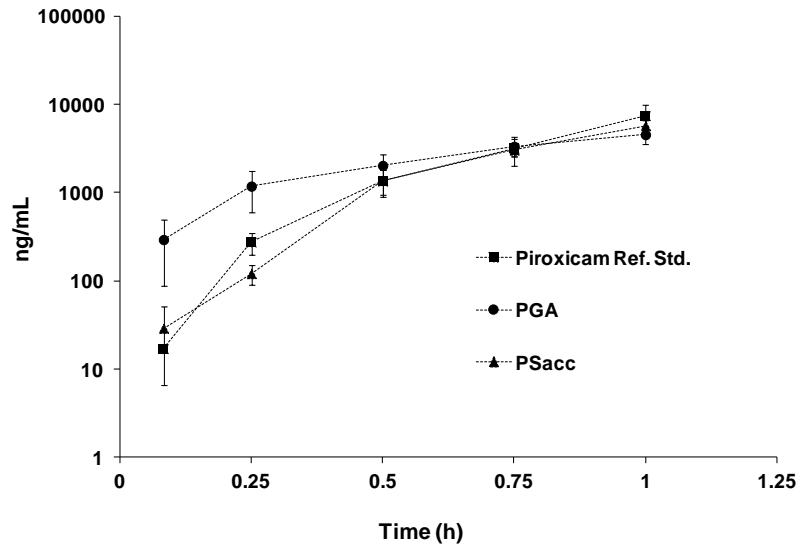


Figure 5.7: Piroxicam 1 hour rat plasma levels after oral capsule dosing (n=6).

Overall the pharmacokinetic data was variable and no significant differences were observed between the co-crystals and piroxicam. It is likely that the co-crystals quickly dissociated as the capsules dissolved in the stomach. Improved oral exposure has been reported for co-crystals that have been formulated to stabilize the co-crystal form.¹⁵ It is possible that stabilizing the piroxicam co-crystals with a formulation could result in increased oral exposure.

Conclusions

Piroxicam dissolution rates appeared to be most dependent on interfacial pH, which was driven by the intrinsic solubility and dissociation constant(s) of the cofomer. This effect was most apparent at pH 6.8 with piroxicam co-crystal dissolution rates significantly lower than piroxicam alone. At pH 1.2, piroxicam co-crystal dissolution rates were similar to free piroxicam. In this pH region ionization of the co-crystal components was negligible so as the co-crystal dissociates, one would expect the piroxicam dissolution rate from the co-crystals to be similar to free piroxicam.

Overall, the *in vivo* data correlated well with the *in vitro* intrinsic dissolution results at pH 1.2. This is not unexpected given that the capsules were dosed directly into the stomach, which has a presumed pH of 1 - 2. Physiological factors including the site of absorption, gastrointestinal blood flow, and gastric emptying also play an important role in oral absorption. These variables make it difficult to completely understand the absorption processes occurring *in vivo* for the co-crystals. Furthermore, it is probable that the co-crystals quickly dissociated *in vivo* which would hinder any potential increases in bioavailability from the co-crystal form. In

future studies formulation strategies to stabilize a co-crystal should be studied in order to fully utilize the solubility advantage of co-crystals.

References

1. Dressman JB, Amidon GL, Reppas C, Shah VP. 1998. Dissolution testing as a prognostic tool for oral drug absorption: Immediate release dosage forms. *Pharm Res* 15(1):11-22.
2. Yu LX, Carlin AS, Amidon GL, Hussain AS. 2004. Feasibility studies of utilizing disk intrinsic dissolution rate to classify drugs. *International J Pharm* 270:221-227.
3. Varma MVS, Khandavilli S, Ashokraj Y, Jain A, Dhanikula A, Sood A, Thomas NS, Pillai O, Sharma P, Gandhi R, Agrawal S, Nair V, Panchagnula R. 2004. Biopharmaceutic classification system: A scientific framework for pharmacokinetic optimization in drug research. *Current Drug Metabolism* 5(5):375-388.
4. Galia E, Nicolaides E, Hörter D, Löbenberg R, Reppas C, Dressman JB. 1998. Evaluation of various dissolution media for predicting *in vivo* performance of class I and II drugs. *Pharm Res* 15(5):698-705.
5. Wood JH, Syarto JE, Letterman H. 1965. Improved holder for disk intrinsic dissolution rate studies. *J Pharm Sci* 54(7):1068.
6. Blagden N, de Matas M, Gavan PT, York P. 2007. Crystal engineering of active pharmaceutical ingredients to improve solubility and dissolution rates. *Adv Drug Deliv Rev* 59(7):617-630.
7. Stanton MK, Kelly RC, Colletti A, Kiang YH, Langley M, Munson EJ, Peterson ML, Roberts J, Wells M. 2010. Improved pharmacokinetics of AMG 517 through co-crystallization part 1: Comparison of two acids with corresponding amide co-crystals. *J Pharm Sci* 99(9):3769-3778.
8. Jung MS, Kim JS, Kim MS, Alhalaweh A, Cho W, Hwang SJ, Velaga SP. 2010. Bioavailability of indomethacin-saccharin co-crystals. *J Pharmacy and Pharmacology* 62(11):1560-1568.
9. Avdeef AT, Tsinman O. 2008. Miniaturized rotating disk intrinsic dissolution rate measurement: Effects of buffer capacity in comparisons to traditional Wood's apparatus. *Pharm Research* 25(11):2613-2627.
10. Mooney KG, Mintun MA, Himmelstein KJ, Stella VJ. 1981. Dissolution kinetics of carboxylic acids I: Effect of pH under unbuffered conditions. *J Pharm Sci* 70(1):13-22.
11. Shiraki K, Takata N, Takano R, Hayashi Y, Terada K. 2008. Dissolution improvement and the mechanism of the improvement from cocrystallization of poorly water-soluble compounds. *Pharm Res* 25(11):2581-2592.
12. Mooney KG, Mintun MA, Himmelstein KJ, Stella VJ. 1981. Dissolution kinetics of carboxylic acids II: Effect of buffers. *J Pharm Sci* 70(1):22-32.
13. Rogge MC, Taft DR. 2005. *Preclinical Drug Development (Drugs and the Pharmaceutical Sciences)*. 1st ed.: Taylor and Francis Group, Florida.

14. Takamatsu N, Welage LS, Idkaidek NM, Liu D, Lee PI, Hayashi Y, Rhie JK, Lennernäs H, Barnett JL, Shah VP, Lesko L, Amidon GL. 1997. Human intestinal permeability of piroxicam, propranolol, phenylalanine, and PEG 400 determined by Jejunal perfusion. *Pharm Res* 14(9):1127-1132.
15. Stanton MK, Kelly RC, Colletti A, Kiang YH, Langley M, Munson EJ, Peterson ML, Roberts J, Wells M. 2010. Improved pharmacokinetics of AMG 517 through co-crystallization part 1: Comparison of two acids with corresponding amide co-crystals. *J Pharm Sci* 99(9):3769-3778.

CHAPTER 6. Final Conclusions and Future Considerations

In this thesis, co-crystal methodology and behavior was explored to better understand co-crystal technology and assess the feasibility of creating co-crystals in an early development setting to address API solubility issues. Slow evaporation methods to create co-crystals on a large scale were quickly abandoned because the method proved to be too time consuming and often produced a mixture of products and not pure co-crystal. However, slow evaporation methods are still useful for discovering new co-crystal forms on a small scale.

Reaction crystallization proved to be the method of choice for this project to produce scalable batches of pure co-crystals. Using this method, co-crystal formation could be visibly observed and co-crystals often formed very quickly. The reaction process was also easily controlled and the results were reproducible for small and large batches of co-crystals. It was discovered that co-crystal yield could be optimized while conserving API and coformer material by suspending the least soluble component in a saturated solution of the more soluble component.

Equilibrium co-crystal solubility measurement techniques developed by Nair Rodríguez-Hornedo and colleagues were successfully applied to measure co-crystal solubility. Measuring co-crystal equilibrium solubility is very useful as a means to screen for a co-crystal that is more soluble than the API. Additionally, this information can be used to estimate co-crystal solubilities in pH regions where the co-crystal may not be stable. It is also valuable knowledge that can be used to both formulate the co-crystal and/or assess whether it is necessary to stabilize the co-crystal through formulation techniques.

The intrinsic dissolution results for the piroxicam co-crystals demonstrated the need to understand the pH solubility and stability of the co-crystal and the co-crystal components and how this data will affect the overall dissolution rate of the API. Any rapid dissociation of the co-crystal is likely to reduce the solubility advantage and may cause suppression of the dissolution of the API due to the acid/base properties of the co-crystal components. Both intrinsic dissolution and PK results reiterate the fact that the piroxicam co-crystals created herein will dissociate within targeted *in vivo* pH regions; therefore, formulation work is likely required to stabilize these co-crystals in order to achieve an increase in bioavailability.

CHAPTER 7. Appendix

Slow Evaporation Solid State Data

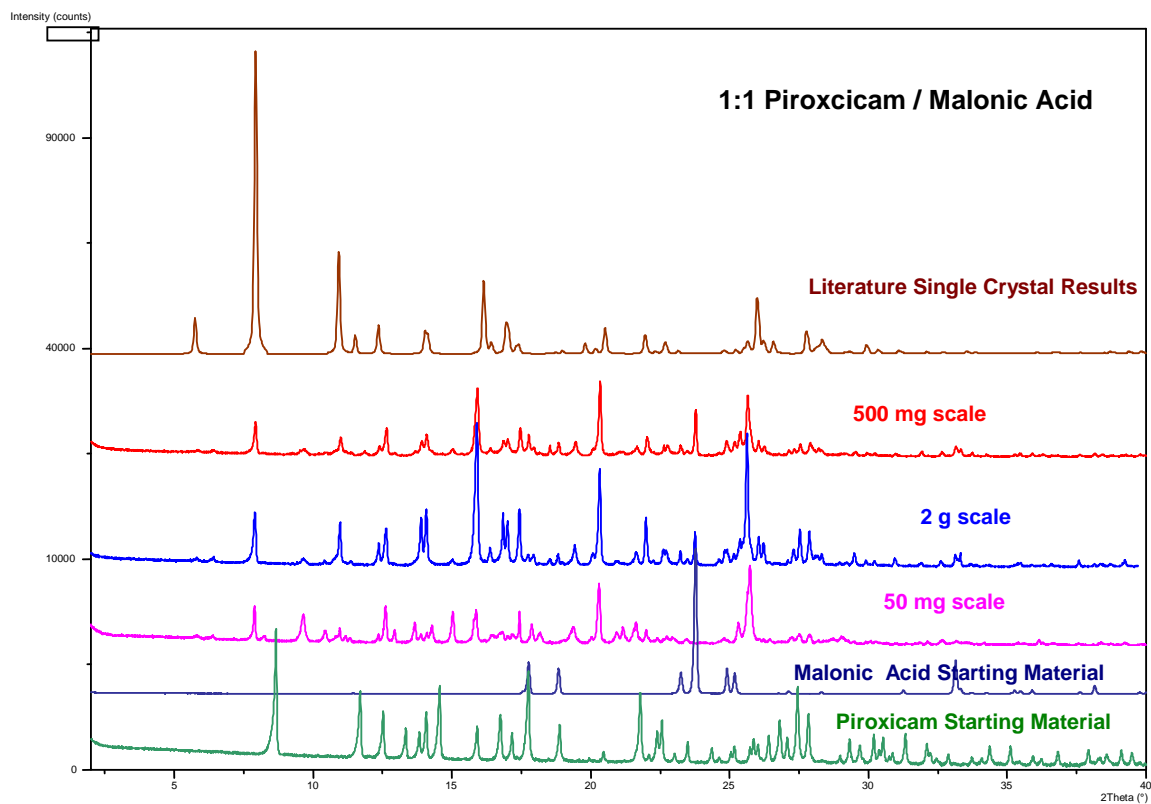


Figure 7.1: XRPD patterns for 1:1 piroxicam/malonic acid and starting materials.

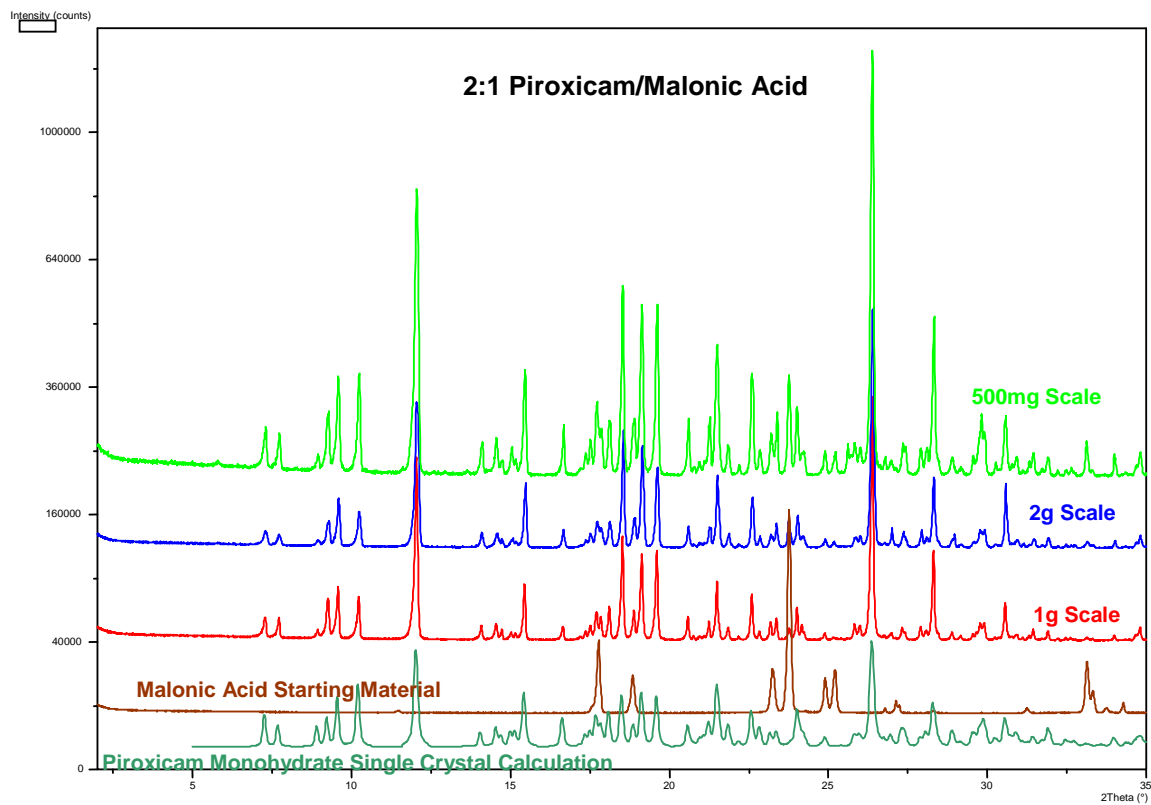


Figure 7.2: XRPD patterns for 2:1 piroxicam/malonic acid and starting materials.

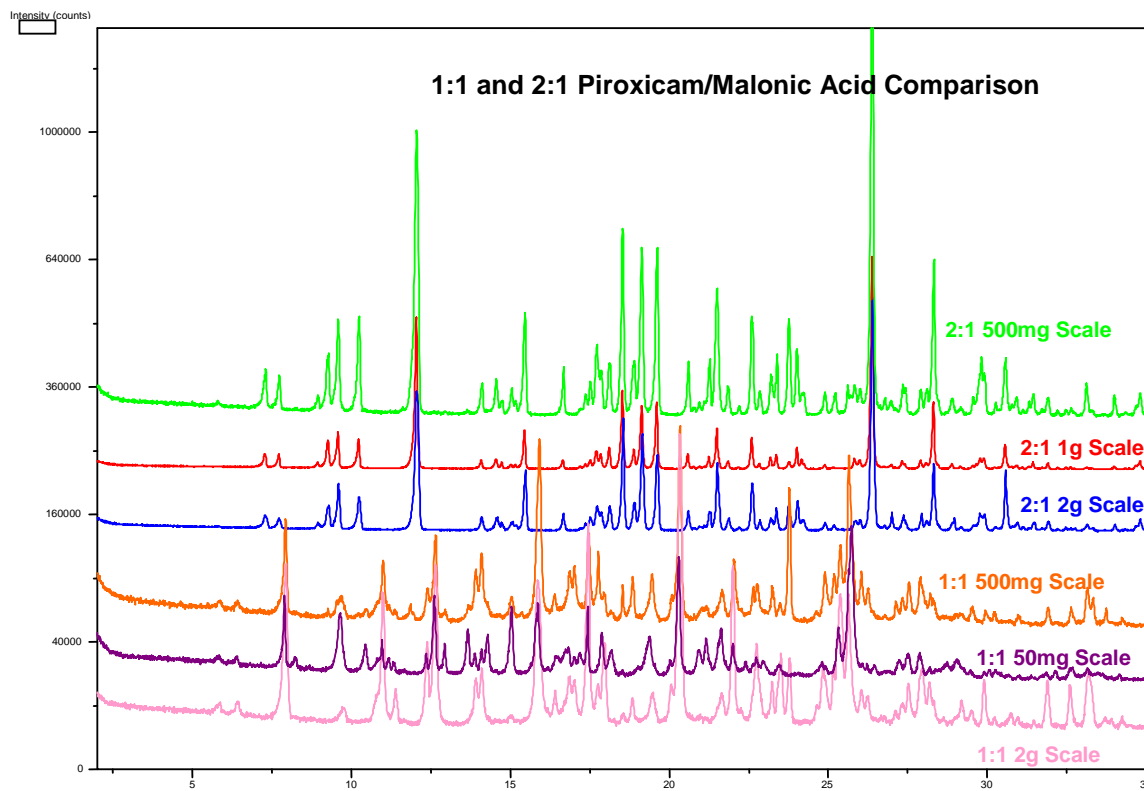


Figure 7.3: 1:1 and 2:1 piroxicam/malonic acid XRPD comparison.

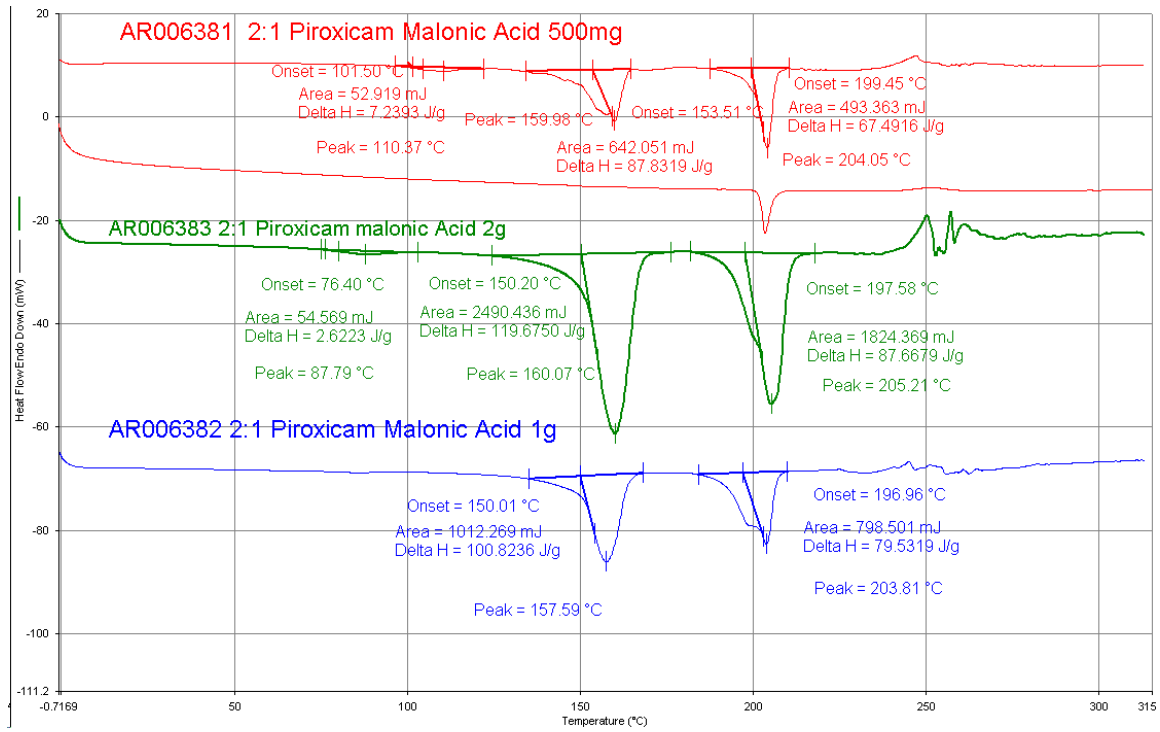


Figure 7.4: 2:1 piroxicam/malonic acid DSC thermograms.

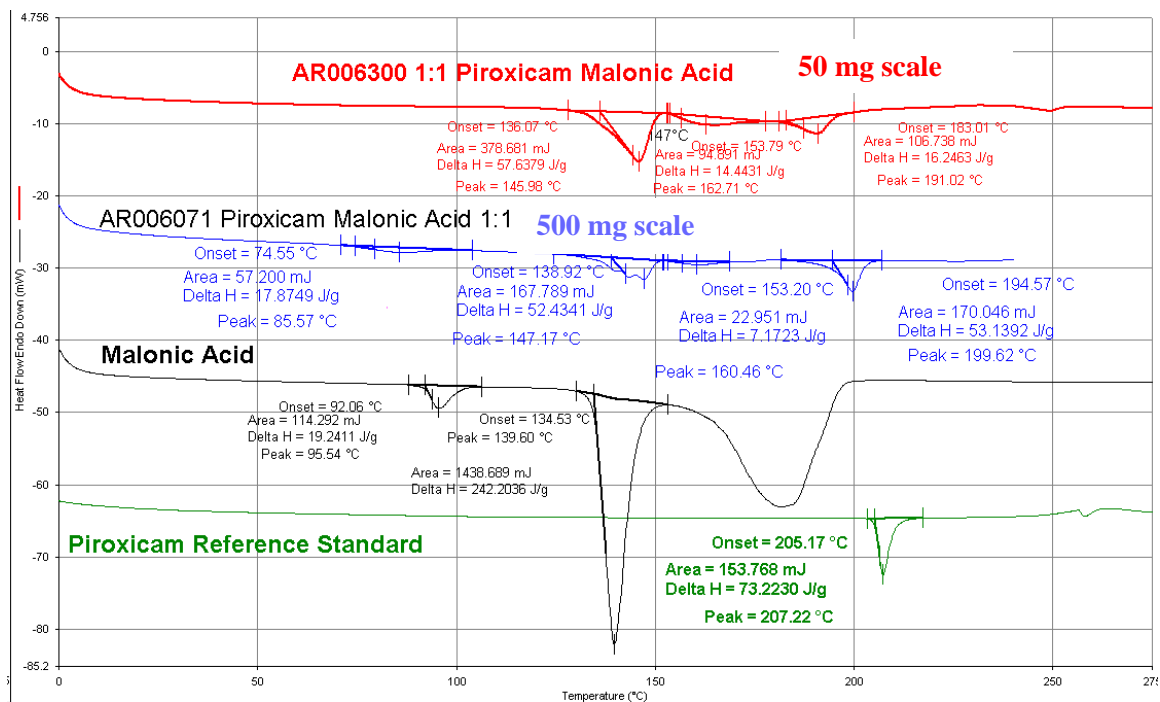


Figure 7.5: 1:1 piroxicam/malonic acid DSC thermograms (50 and 500 mg scales).

Filename: ...3 1:1 Piroxicam Malonic Acid xxx.drd
Operator ID: Steve Bierlmaier
Sample ID: AR006153 1:1 Piroxicam Malonic Acid
Sample Weight: 5.930 mg
Comment: RB2861-40

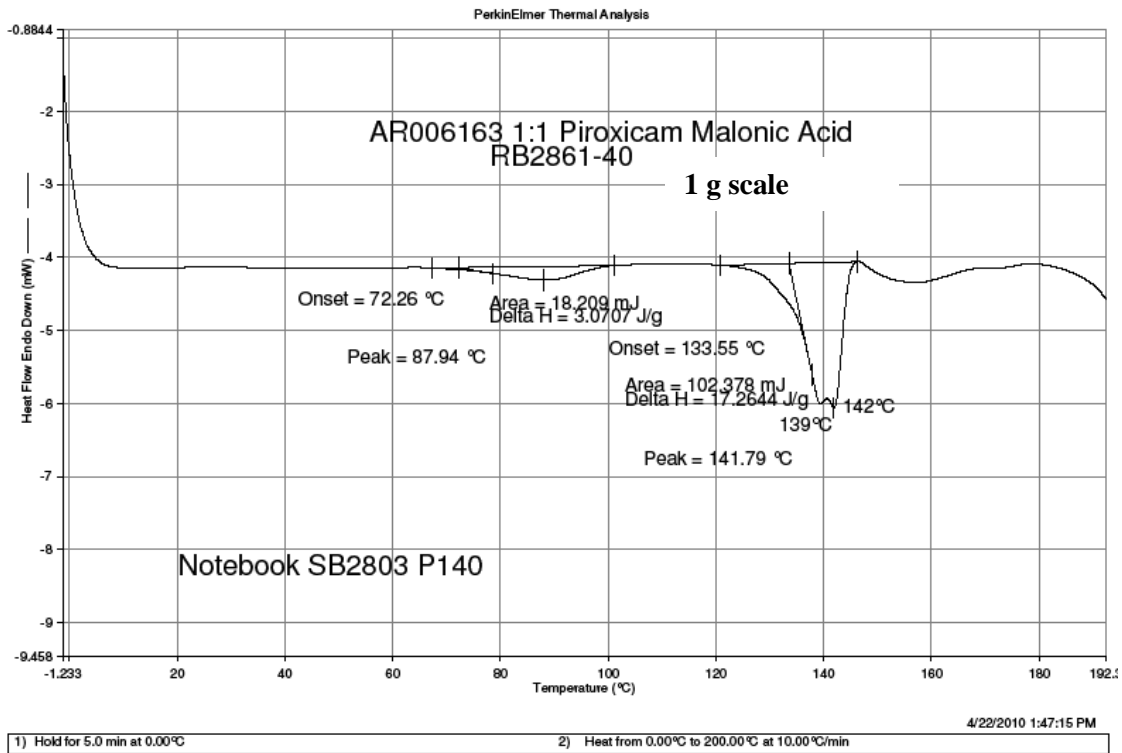


Figure 7.6: 1:1 piroxicam/malonic acid DSC thermogram (1 gram scale).

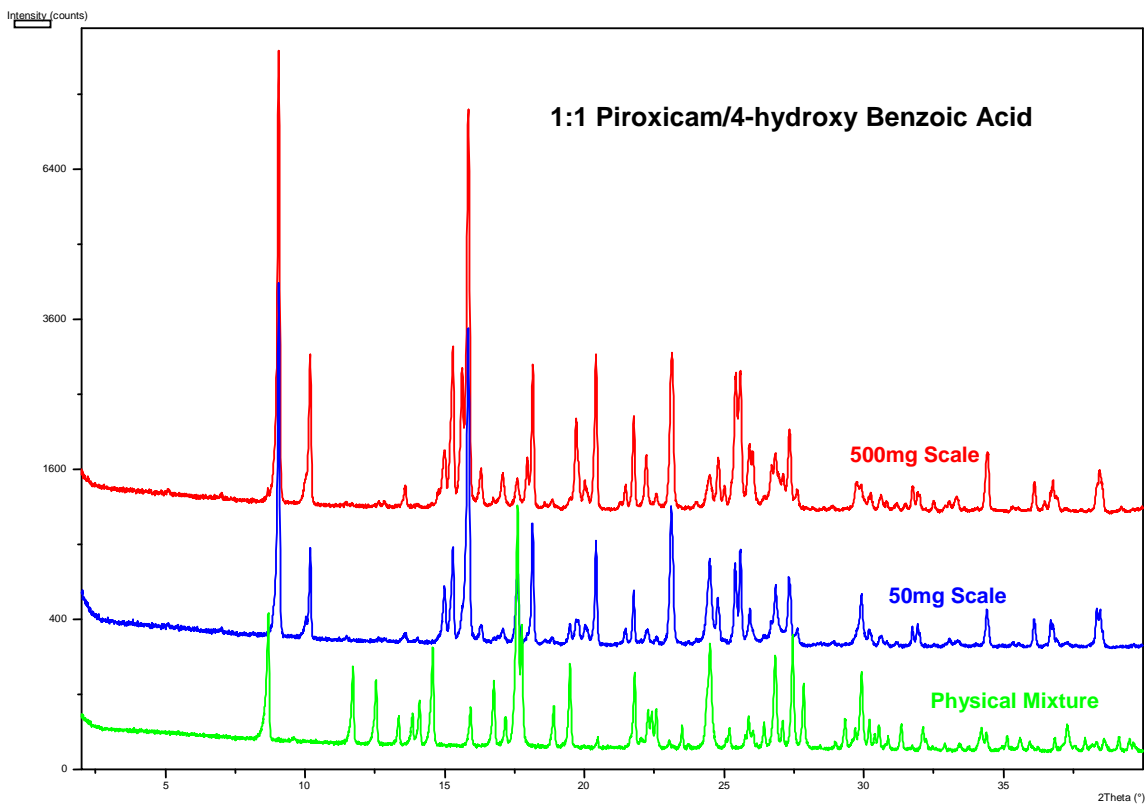


Figure 7.7: XRPD patterns for 1:1 piroxicam/4-hydroxy benzoic acid and physical mixture.

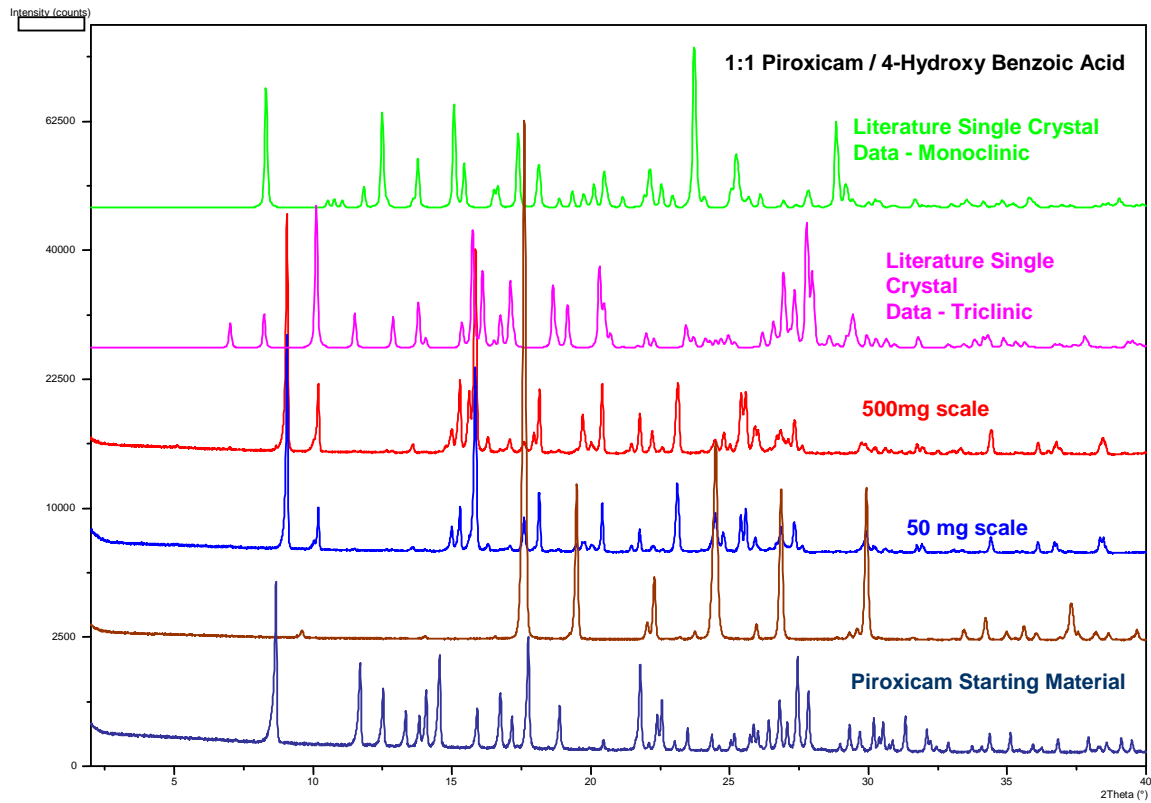


Figure 7.8: XRPD patterns for 1:1 piroxicam/4-hydroxy benzoic acid and starting materials.

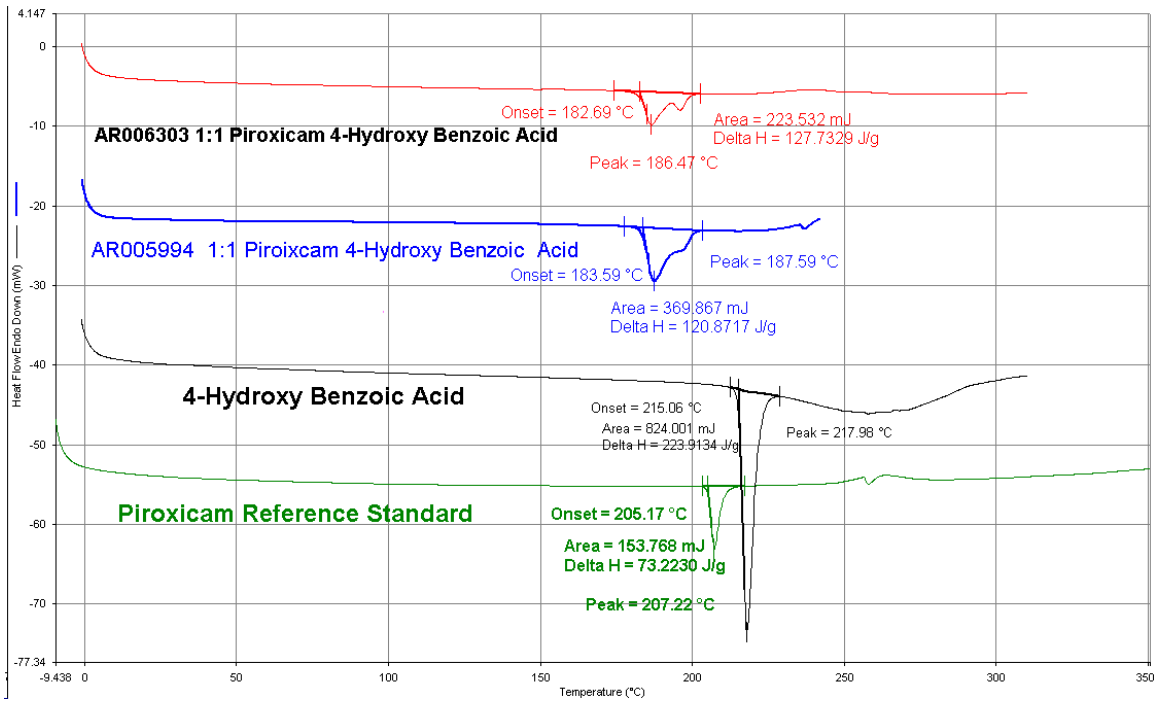


Figure 7.9: 1:1 piroxicam/4-hydroxy benzoic acid DSC thermograms.

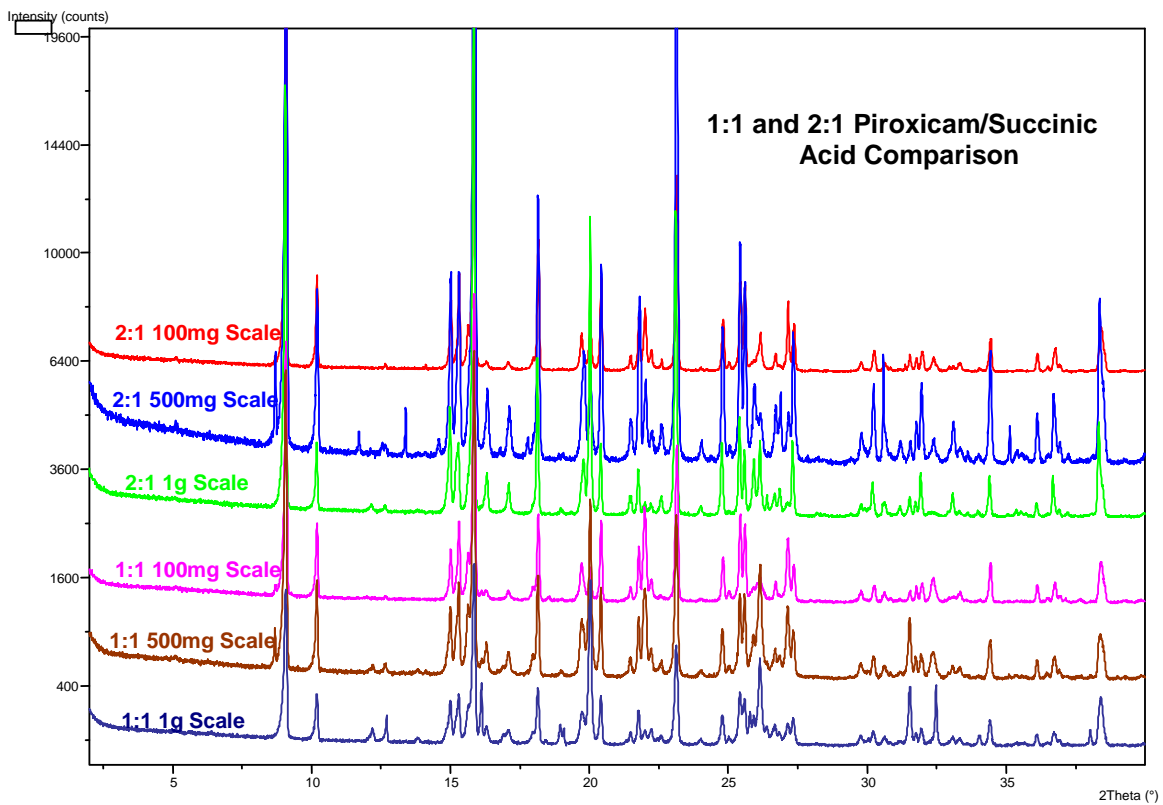


Figure 7.10: 1:1 and 2:1 piroxicam/succinic acid XRPD pattern comparison.

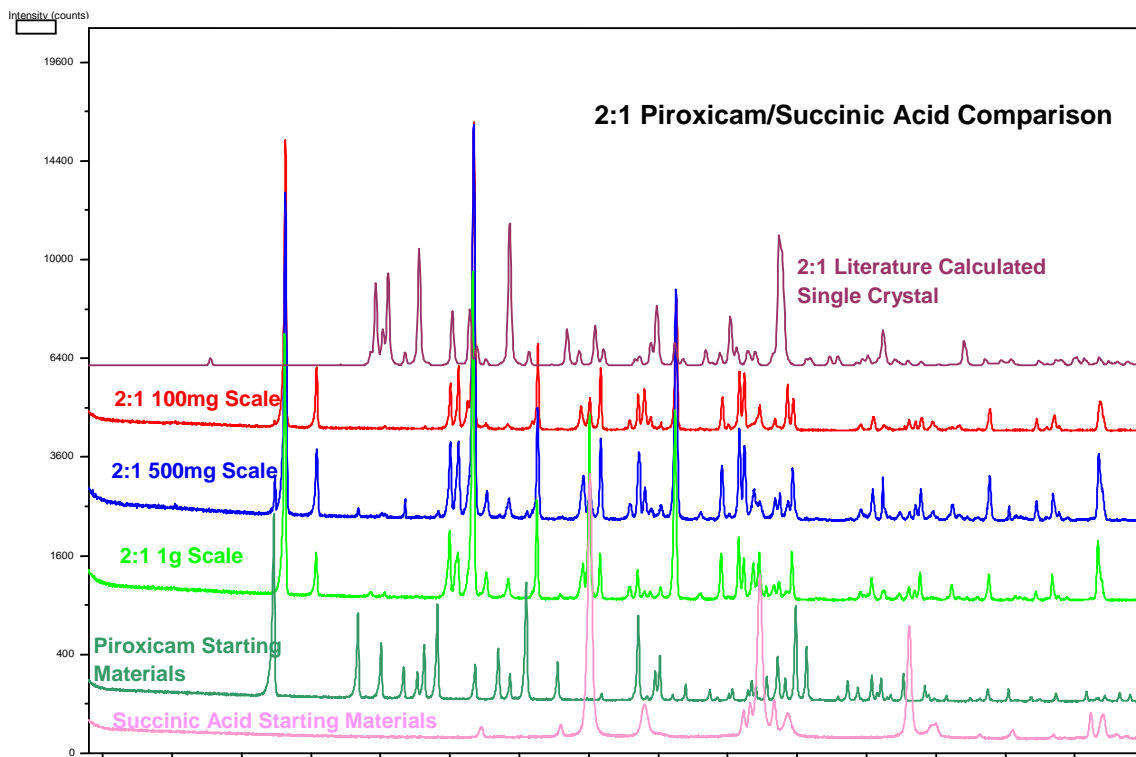


Figure 7.11: XRPD patterns for 2:1 piroxicam/succinic acid and starting materials.

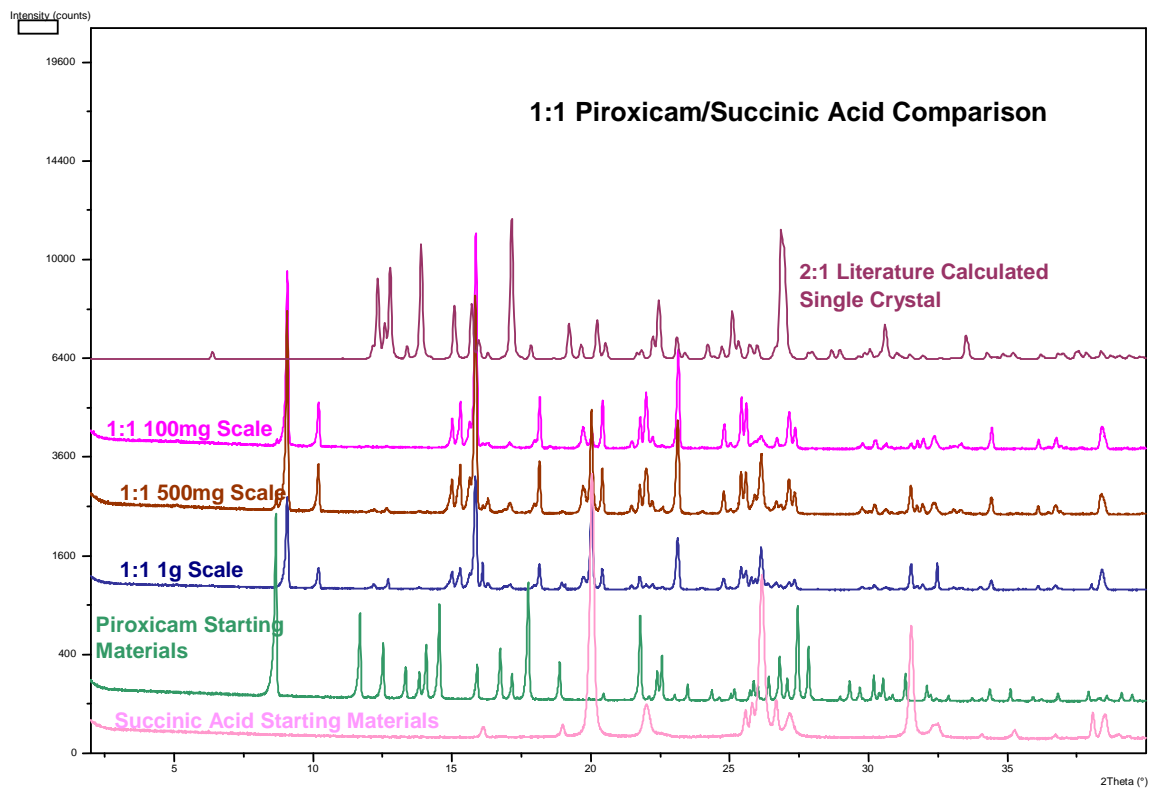


Figure 7.12: XRPD patterns for 1:1 piroxicam/succinic acid and starting materials.

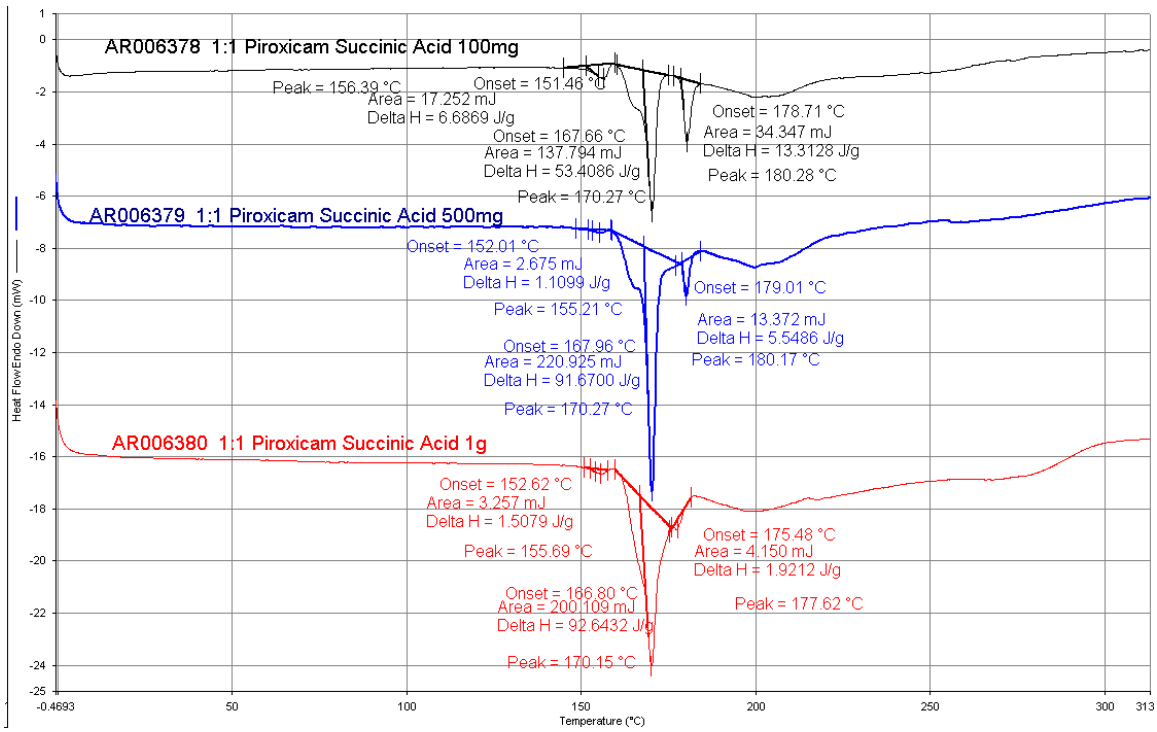


Figure 7.13: 1:1 piroxicam/succinic acid DSC thermograms.

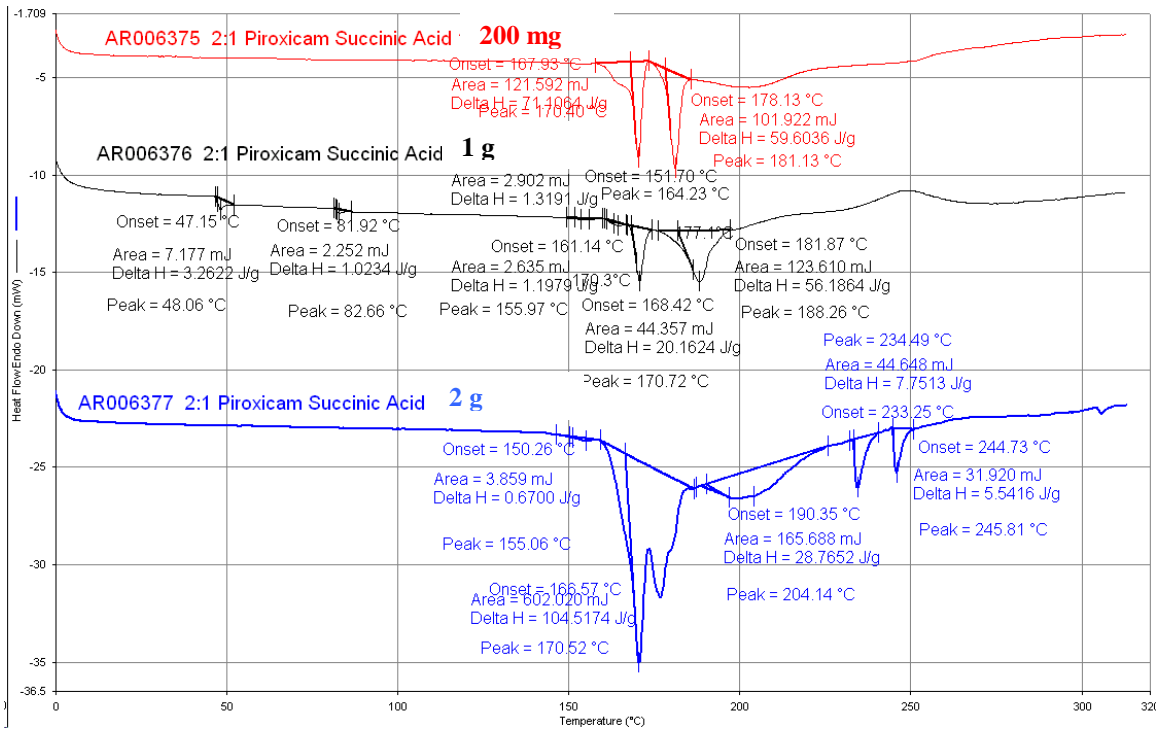


Figure 7.14: 2:1 piroxicam/succinic acid DSC thermograms.

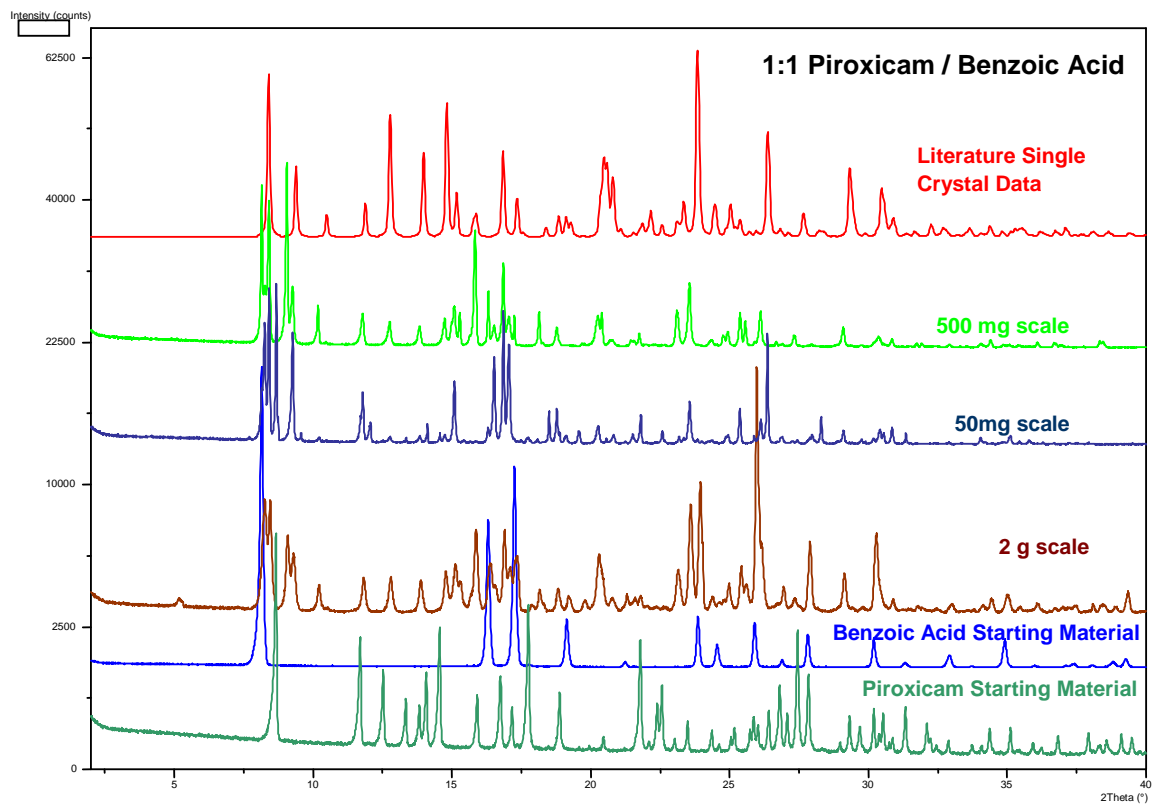


Figure 7.15: XRPD patterns for 1:1 piroxicam/benzoic acid and starting materials.

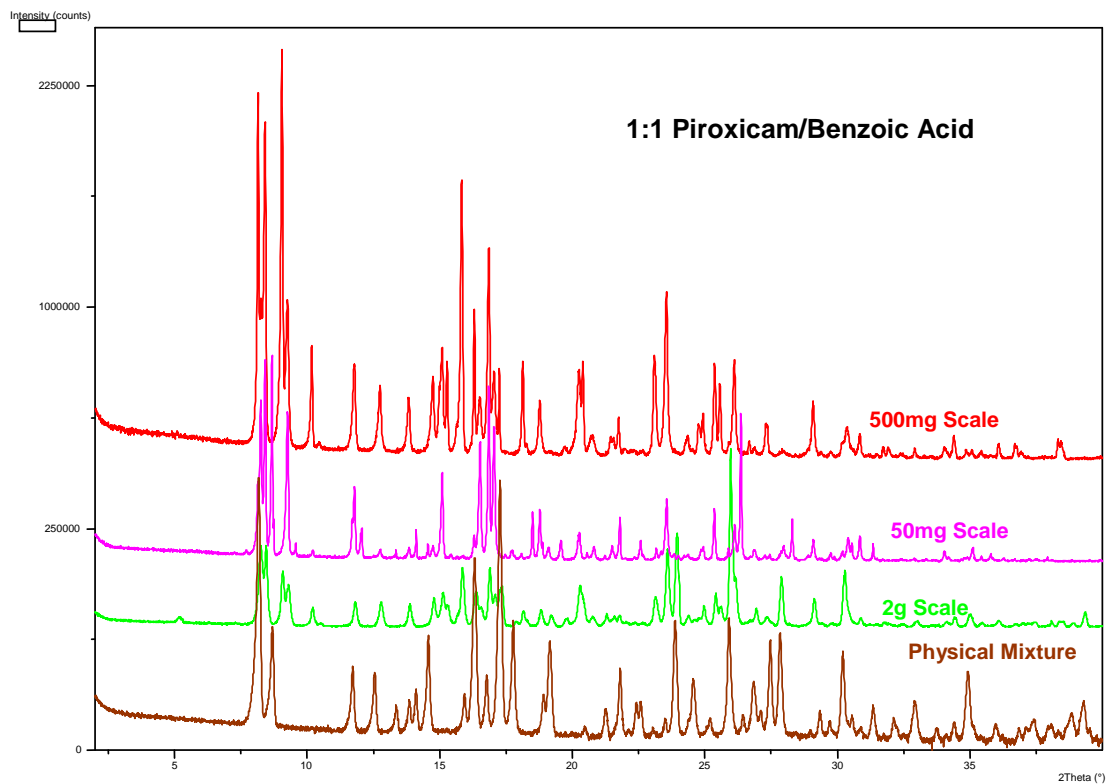


Figure 7.16: XRPD patterns for 1:1 piroxicam/benzoic acid and physical mixture.

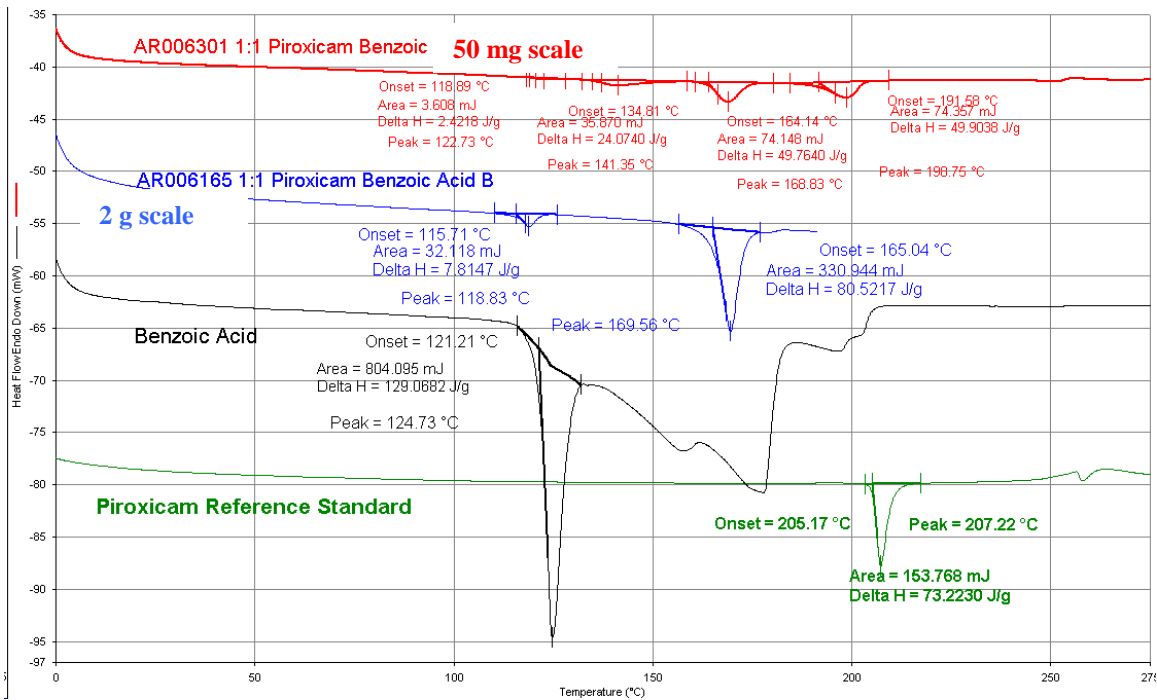
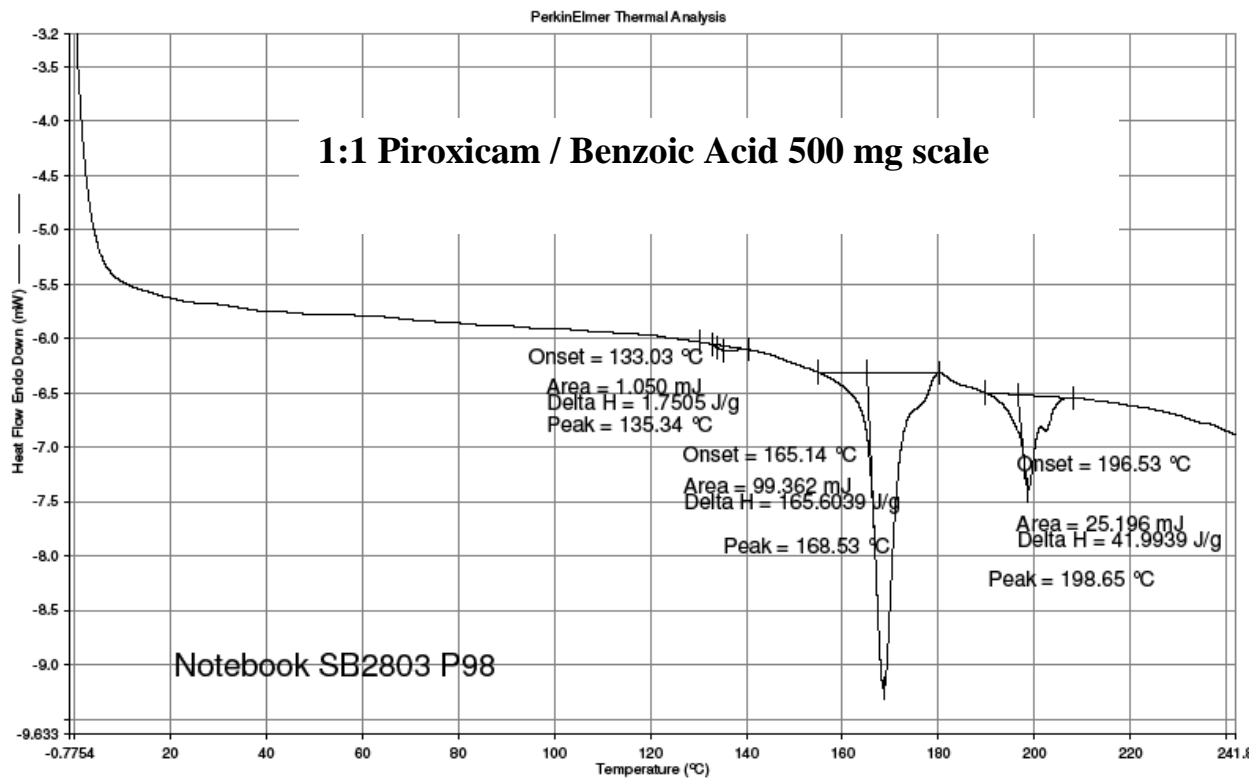


Figure 7.17: 1:1 piroxicam/benzoic acid DSC thermograms (50 mg and 2 g scales).

Filename: ...5 1 1 pirocam benzoic Acid 3B.drd
Operator ID: Steve Bierlmaier
Sample ID: AR005995 AR0059994 1:1 pirocam benzoic Acid 3B
Sample Weight: 0.600 mg
Comment: RB2862-36



2/25/2010 9:29:53 AM

1) Hold for 5.0 min at 0.00°C

2) Heat from 0.00°C to 250.00°C at 10.00°C/min

Figure 7.18: 1:1 piroxicam/benzoic acid DSC thermograms (500 mg scale).

Reaction Crystallization Solid State Data

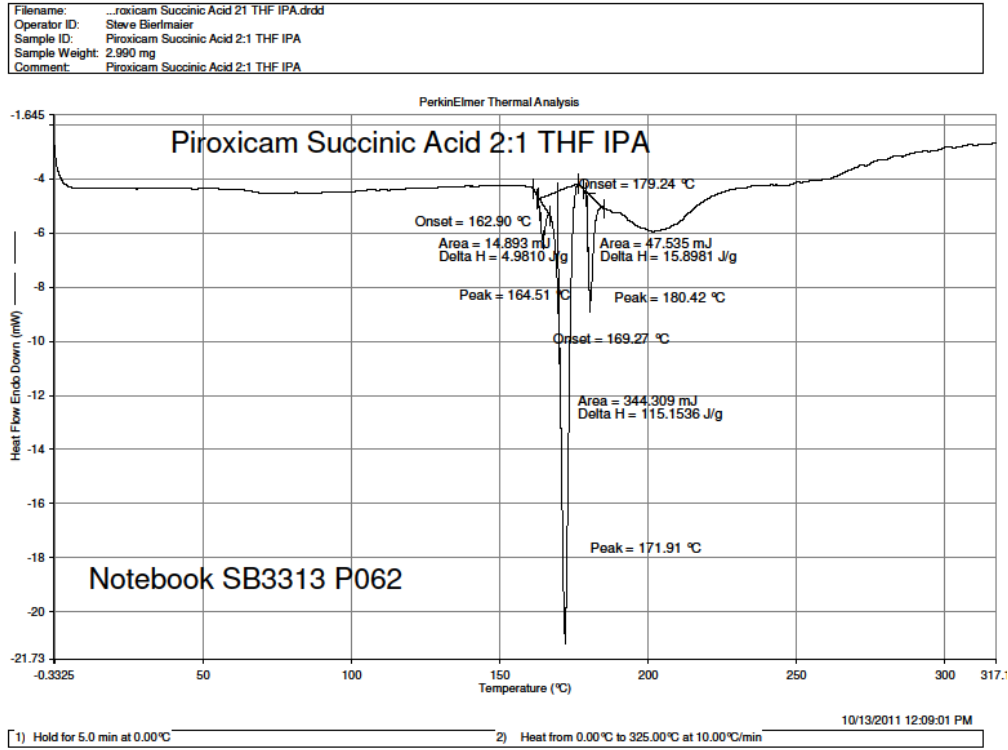


Figure 7.19: 2:1 piroxicam/succinic acid co-crystal DSC thermogram (2:1 THF/IPA solvent).

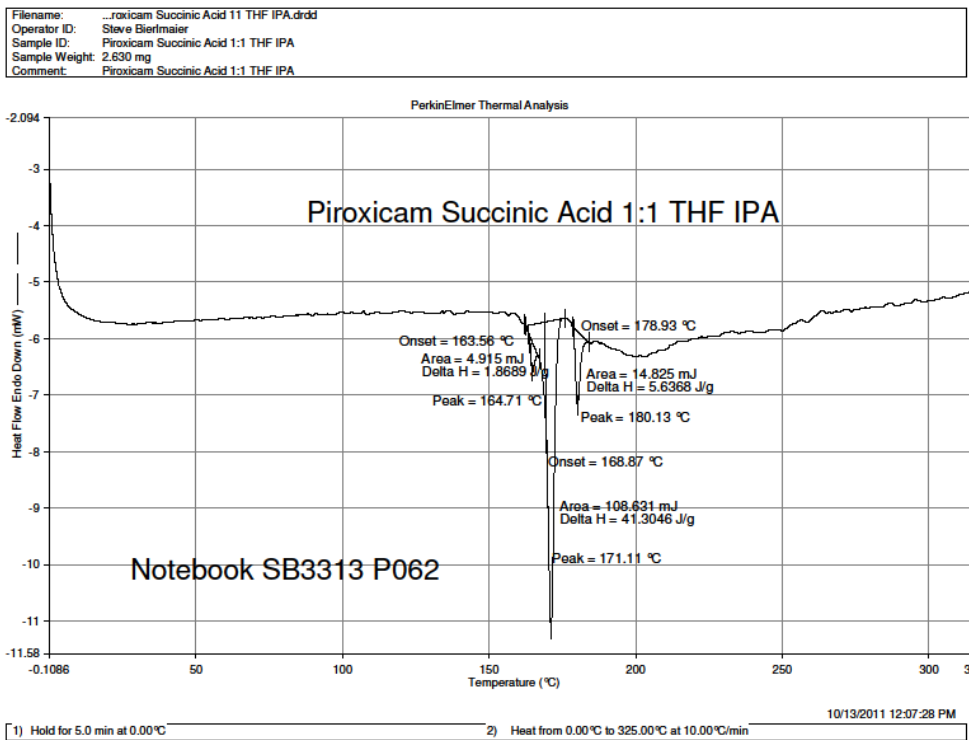


Figure 7.20: 2:1 piroxicam/succinic acid co-crystal DSC thermogram (1:1 THF/IPA solvent).

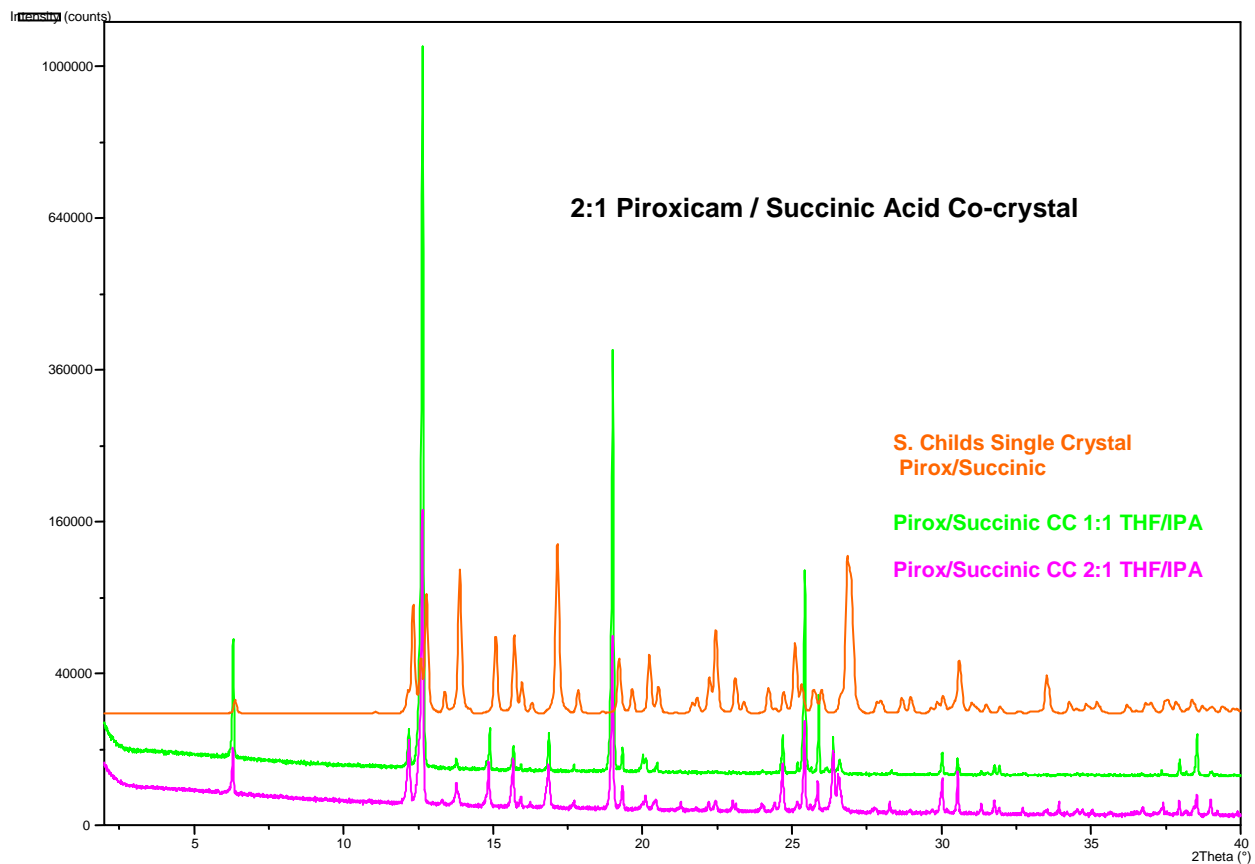
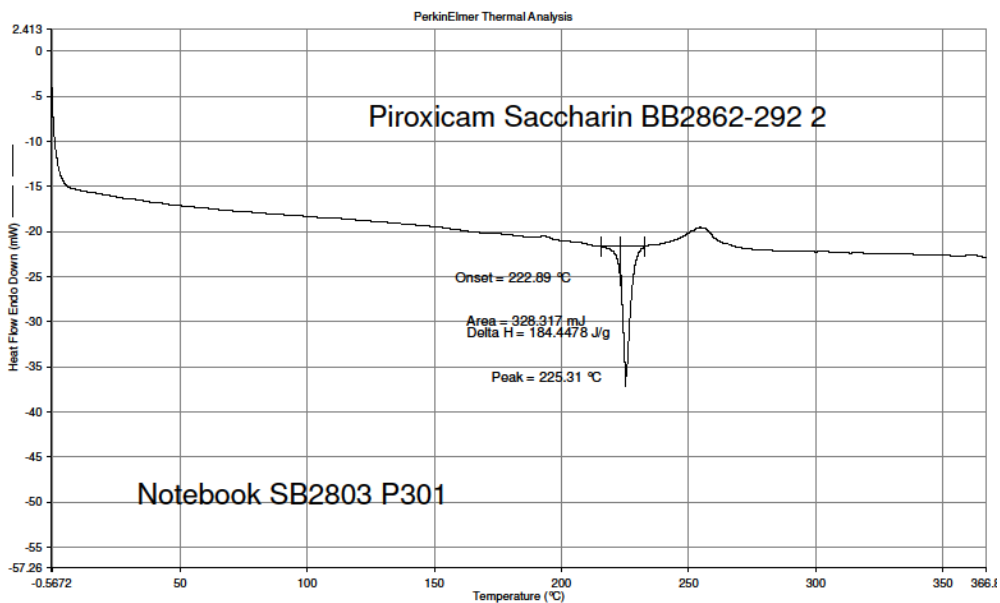


Figure 7.21: XRPD patterns for 2:1 piroxicam/succinic acid co-crystals made with 1:1 and 2:1 THF/IPA solvents.

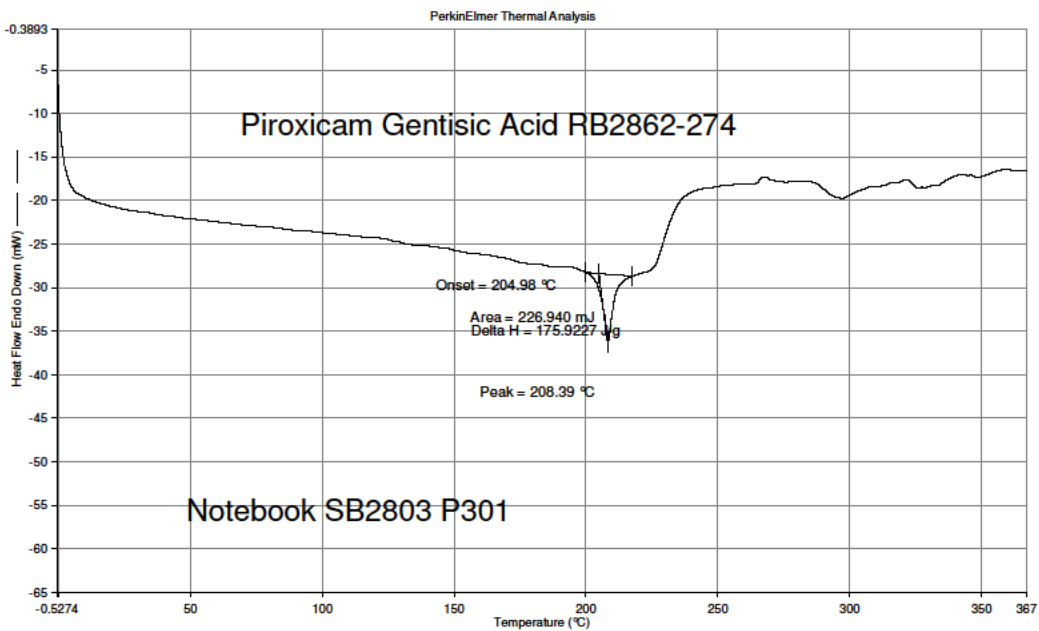
Filename: C:\...Piroxicam Saccharin BB2862-292 2.drd
Operator ID: Steve Biermaier
Sample ID: Piroxicam Saccharin BB2862-292 2
Sample Weight: 1.780 mg
Comment: Piroxicam Saccharin BB2862-292 2



1) Hold for 5.0 min at 0.00°C
2) Heat from 0.00°C to 375.00°C at 10.00°C/min
3/29/2011 3:33:00 PM

Figure 7.22: 1:1 piroxicam/saccharin co-crystal DSC thermogram.

Filename: ...roxicam Gentisic Acid RB2862-274.drd
Operator ID: Steve Biermaier
Sample ID: Piroxicam Gentisic Acid RB2862-274
Sample Weight: 1.290 mg
Comment: Piroxicam Gentisic Acid RB2862-274



3/16/2011 10:55:04 AM
1) Hold for 5.0 min at 0.00°C 2) Heat from 0.00°C to 375.00°C at 10.00°C/min

Figure 7.23: 1:1 piroxicam/gentisic acid co-crystal DSC thermogram.

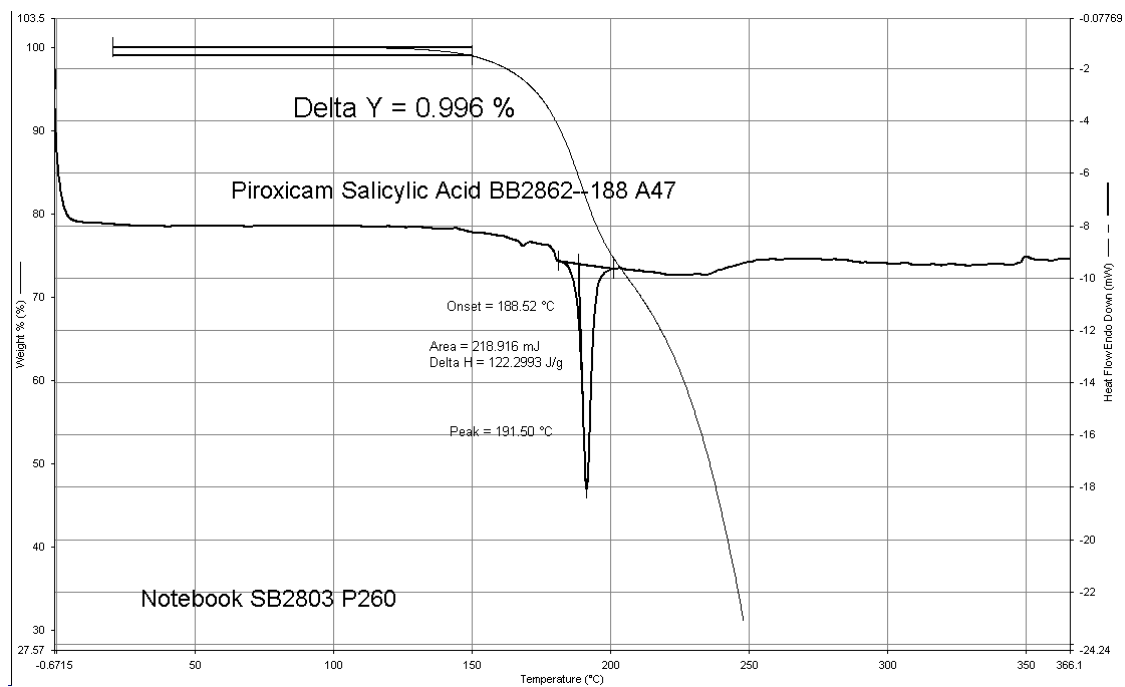


Figure 7.24: 1:1 piroxicam/salicylic acid co-crystal DSC thermogram and TGA overlay.

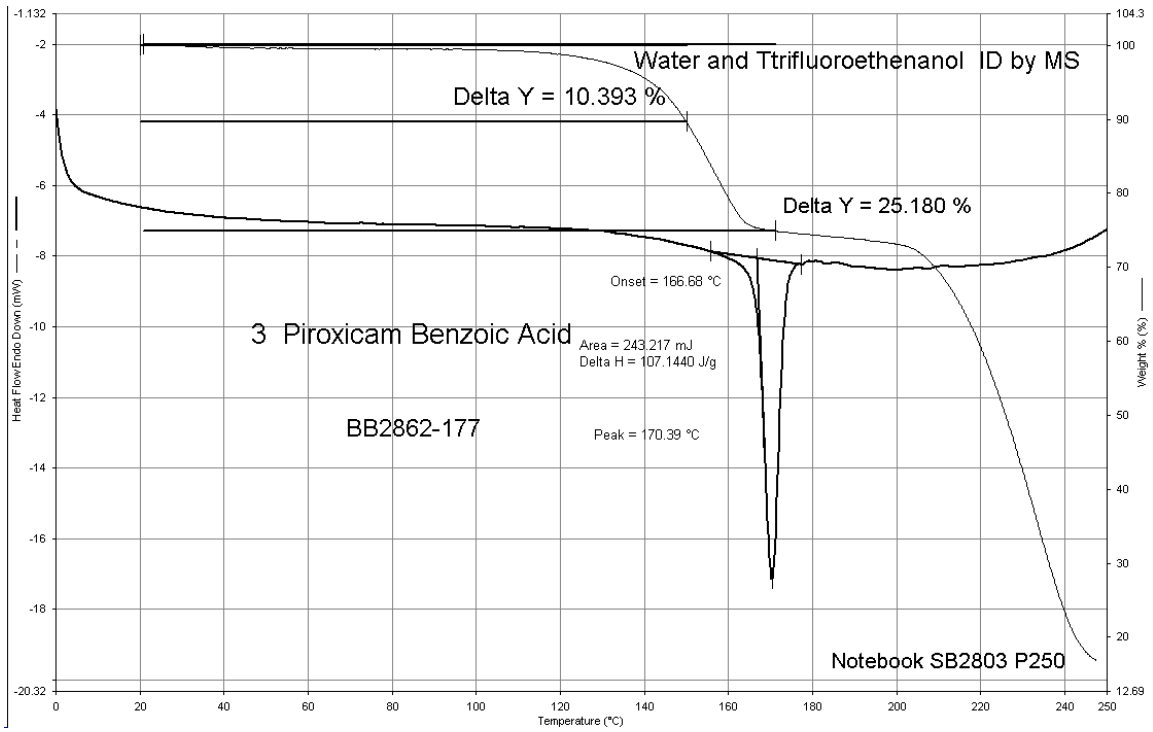


Figure 7.25: 1:1 piroxicam/benzoic acid co-crystal DSC thermogram and TGA overlay.

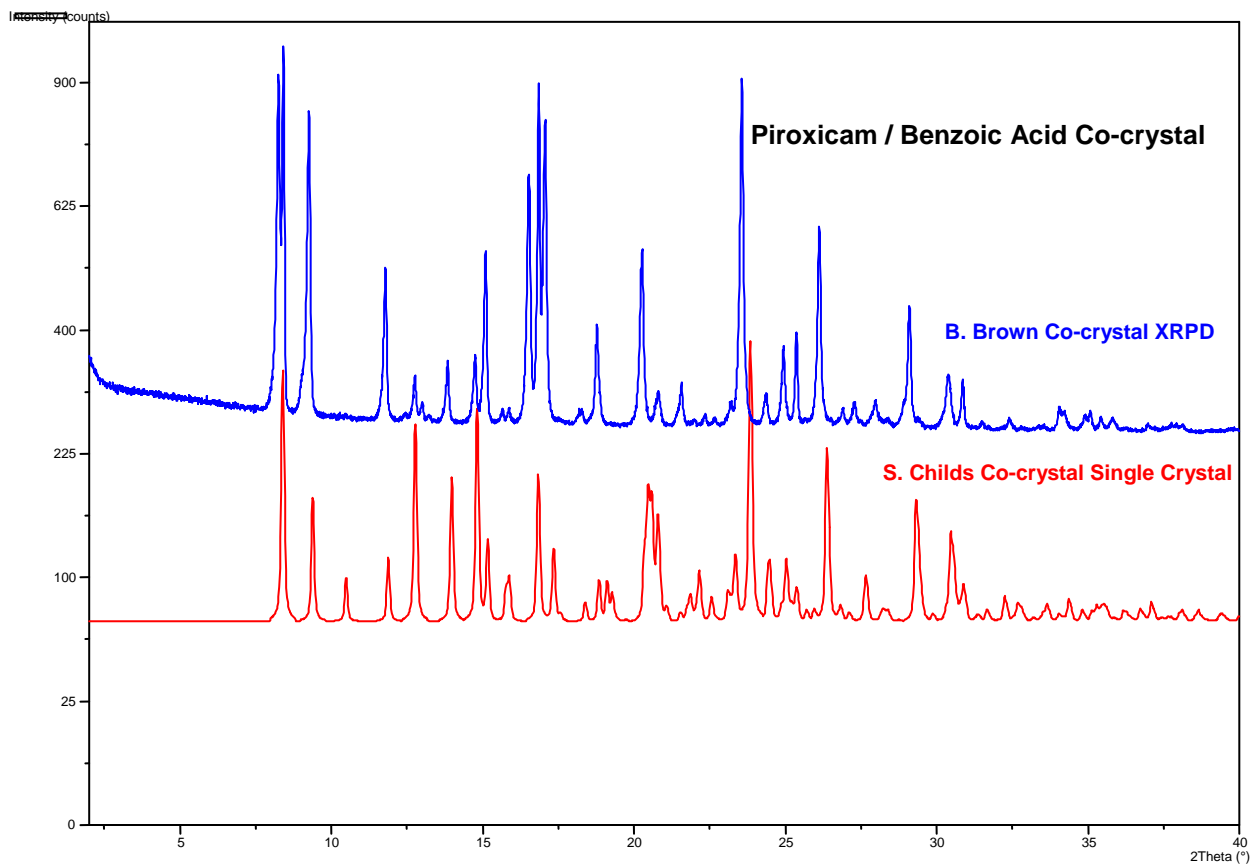


Figure 7.26: 1:1 piroxicam/benzoic acid co-crystal XRPD pattern comparison with Childs reference co-crystal.

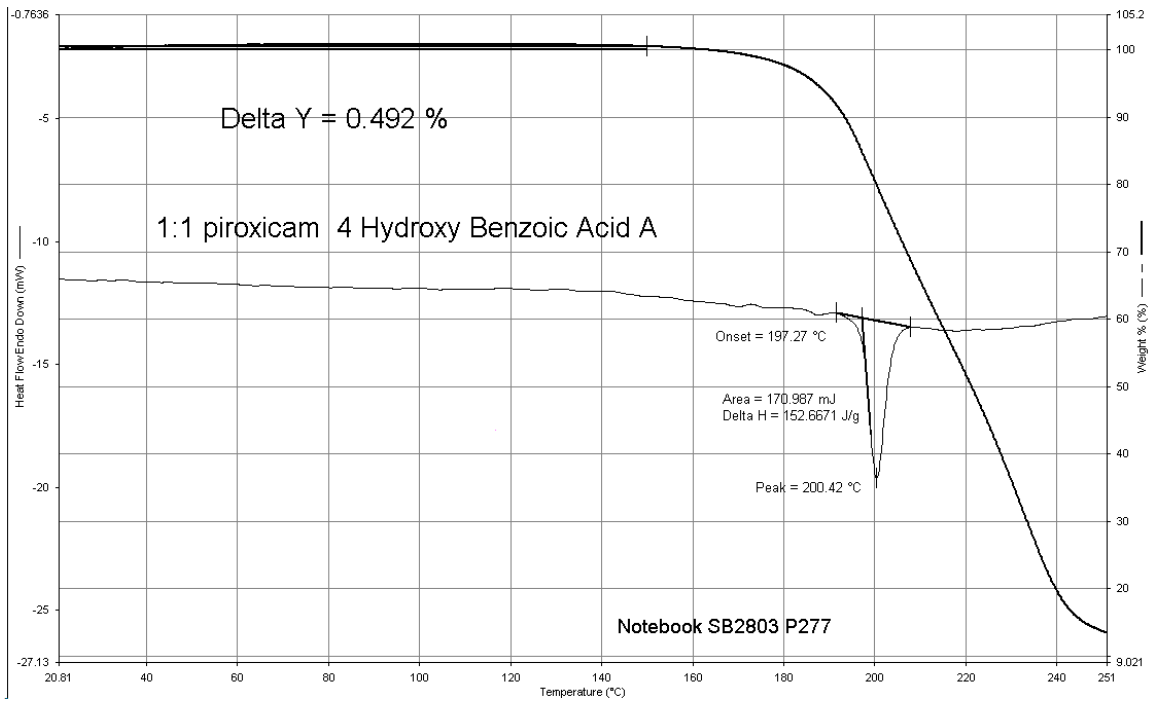


Figure 7.27: 1:1 piroxicam/4-hydroxy benzoic acid co-crystal DSC thermogram and TGA overlay.

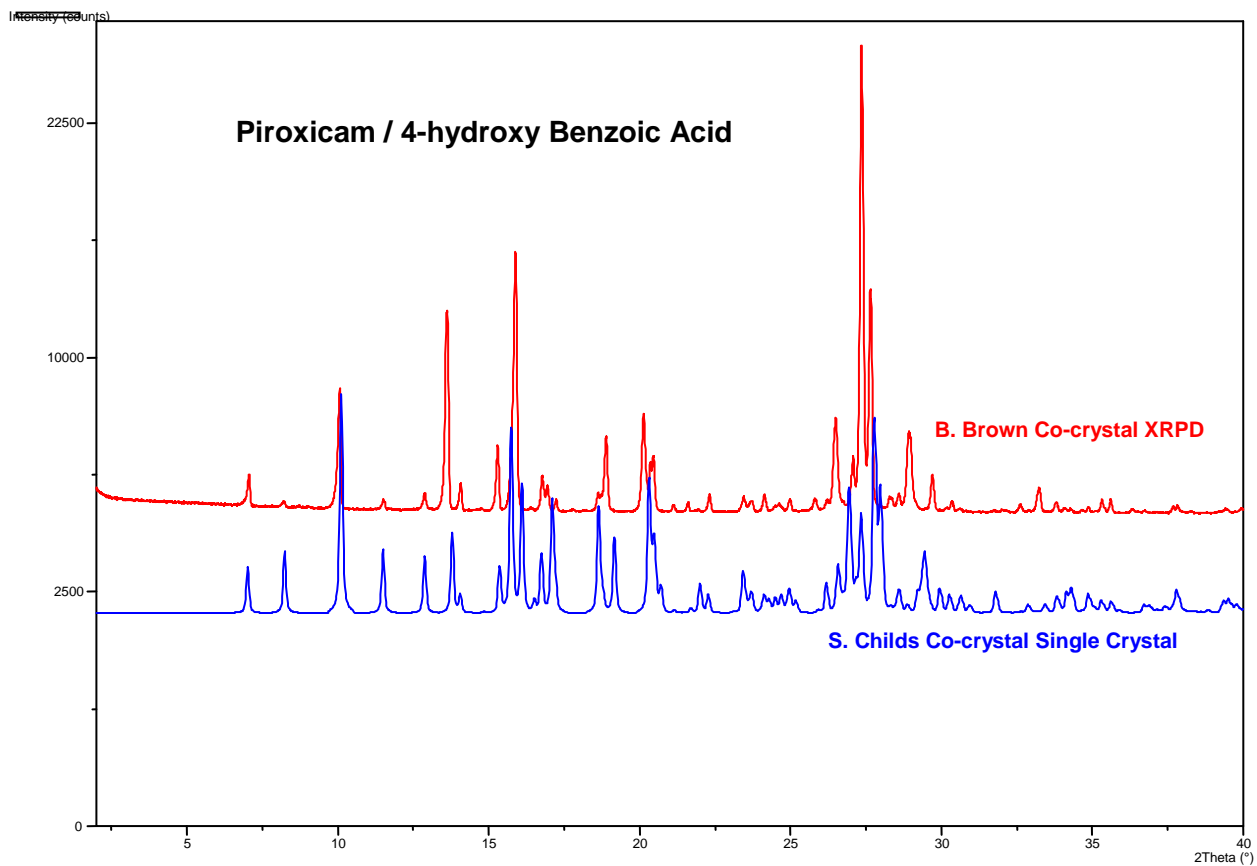


Figure 7.28: 1:1 piroxicam/4-hydroxy benzoic acid co-crystal XRPD pattern comparison with Childs reference co-crystal.

Co-crystal Solubility XRPD Patterns

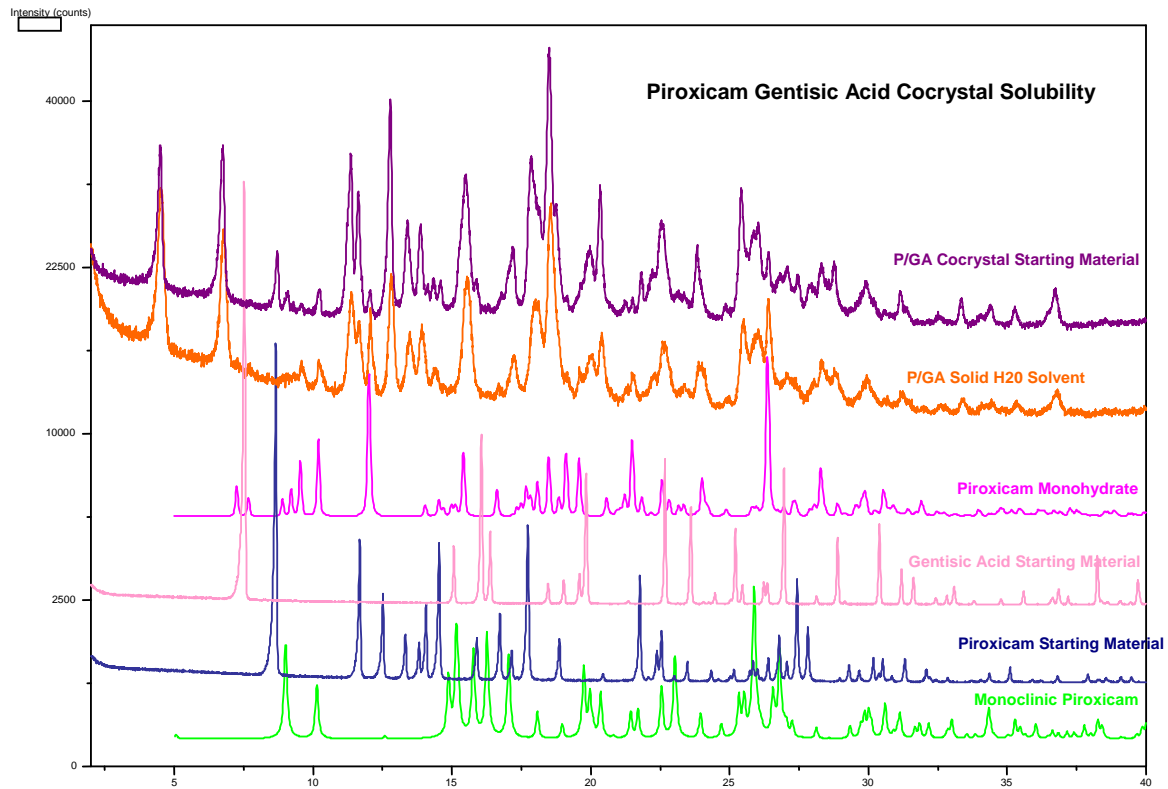


Figure 7.29: 1:1 piroxicam/gentisic acid co-crystal XRPD pattern after aqueous solubility experiments.

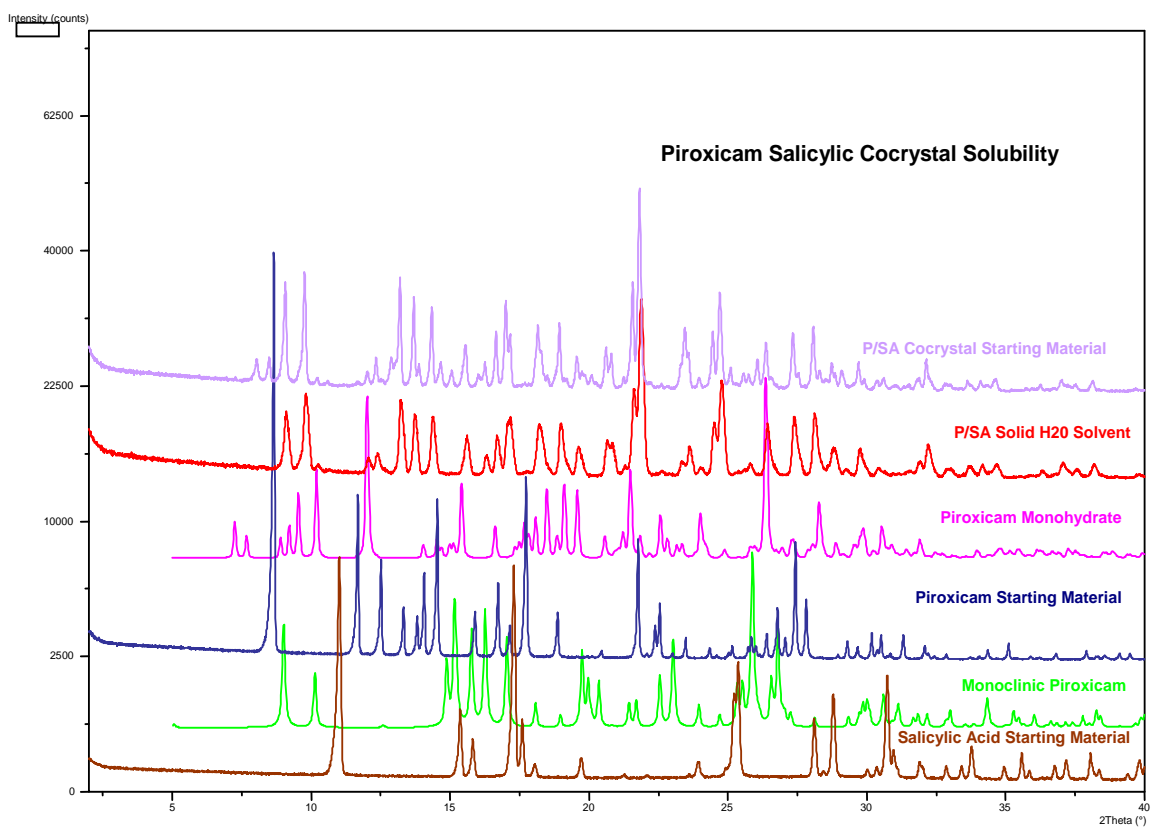


Figure 7.30: 1:1 piroxicam/salicylic acid co-crystal XRPD pattern after aqueous solubility experiments.

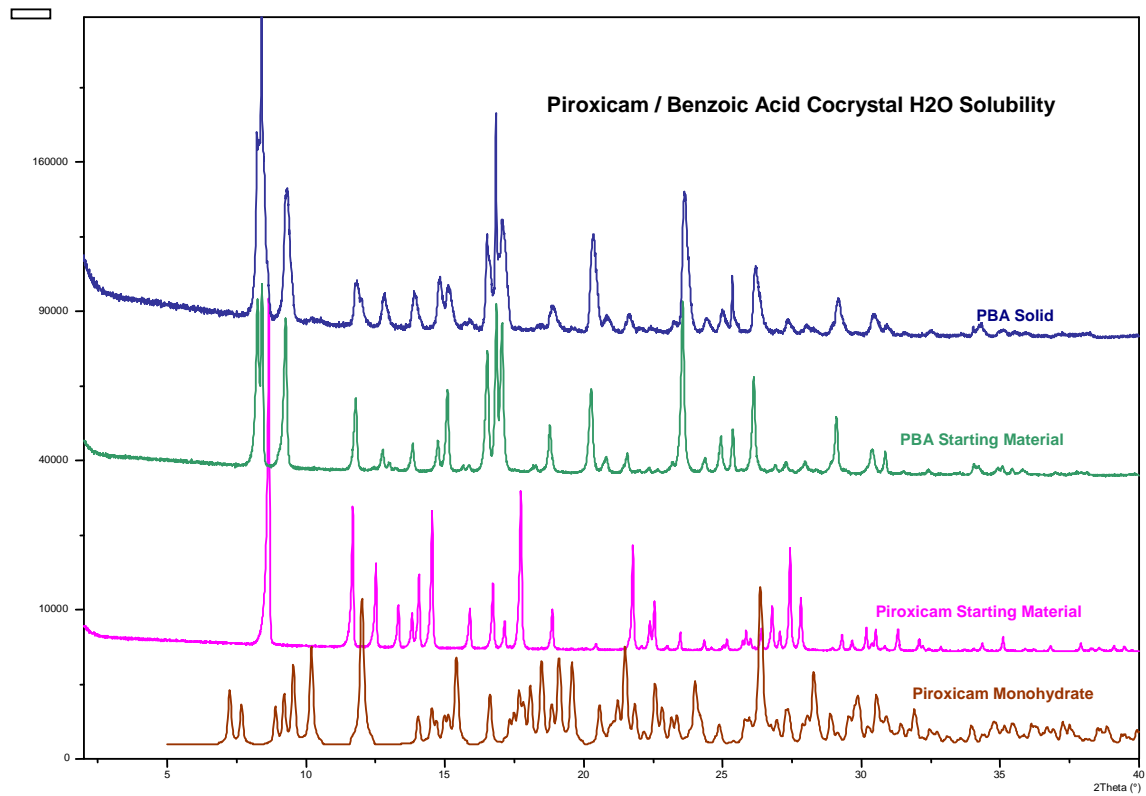


Figure 7.31: 1:1 piroxicam/benzoic acid co-crystal XRPD pattern after aqueous solubility experiments.

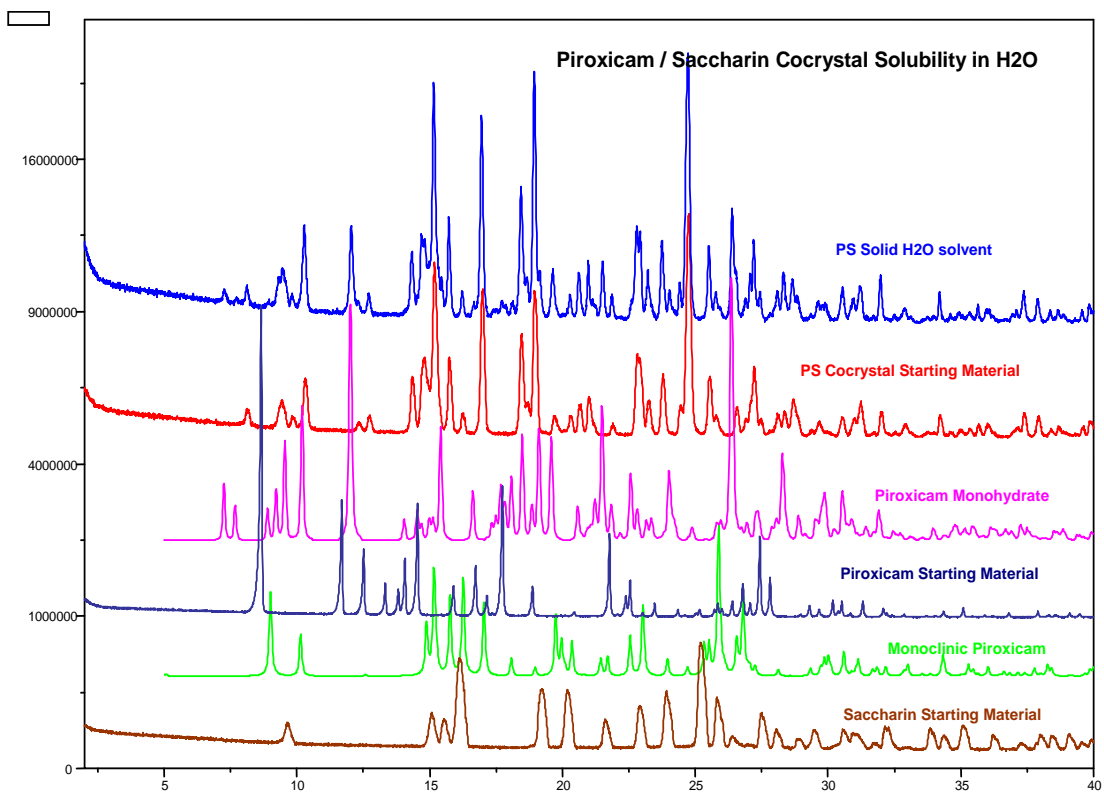


Figure 7.32: 1:1 piroxicam/saccharin co-crystal XRPD pattern after aqueous solubility experiments.

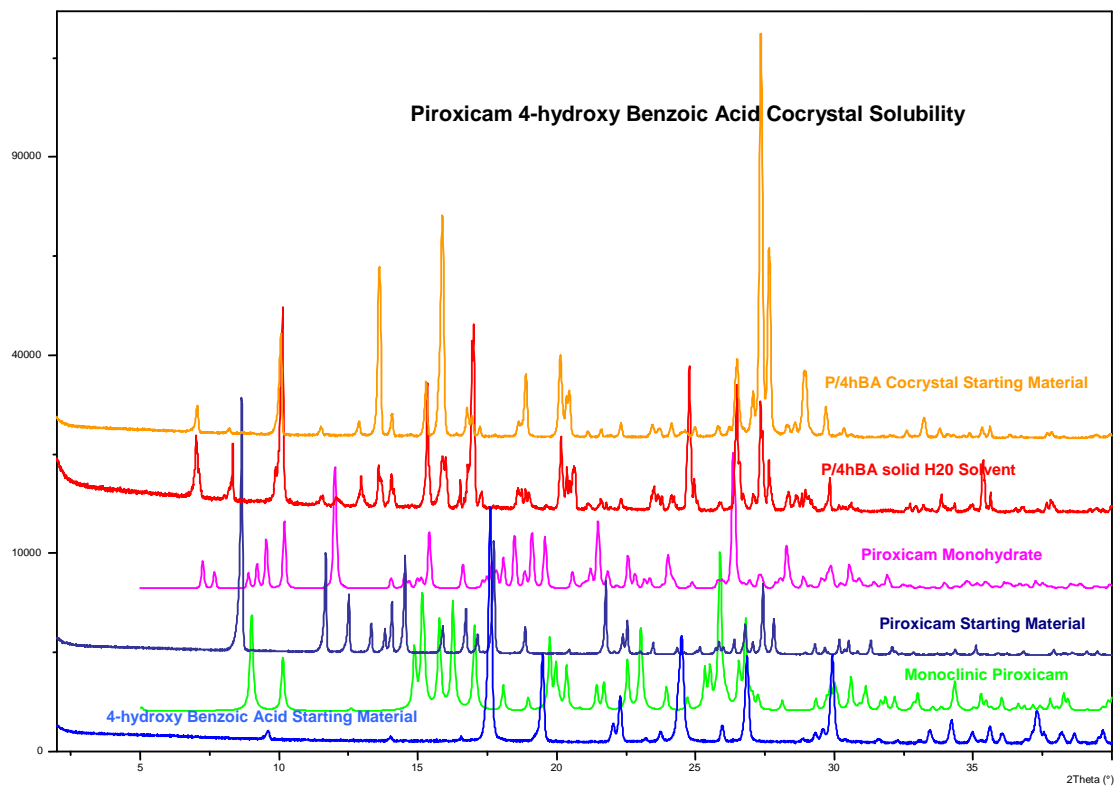


Figure 7.33: 1:1 piroxicam/4-hydroxy benzoic acid co-crystal XRPD pattern after aqueous solubility experiments.

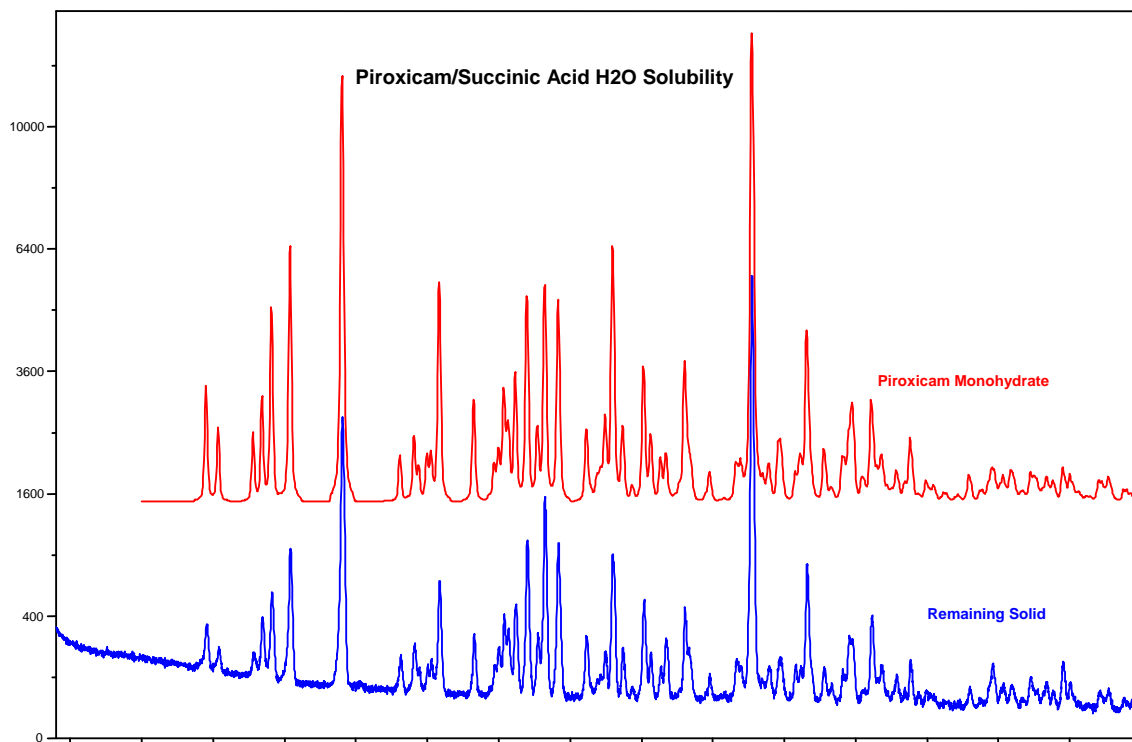


Figure 7.34: 1:1 piroxicam/succinic acid co-crystal XRPD pattern after aqueous solubility experiments.

Co-crystal Intrinsic Dissolution XRPD Patterns

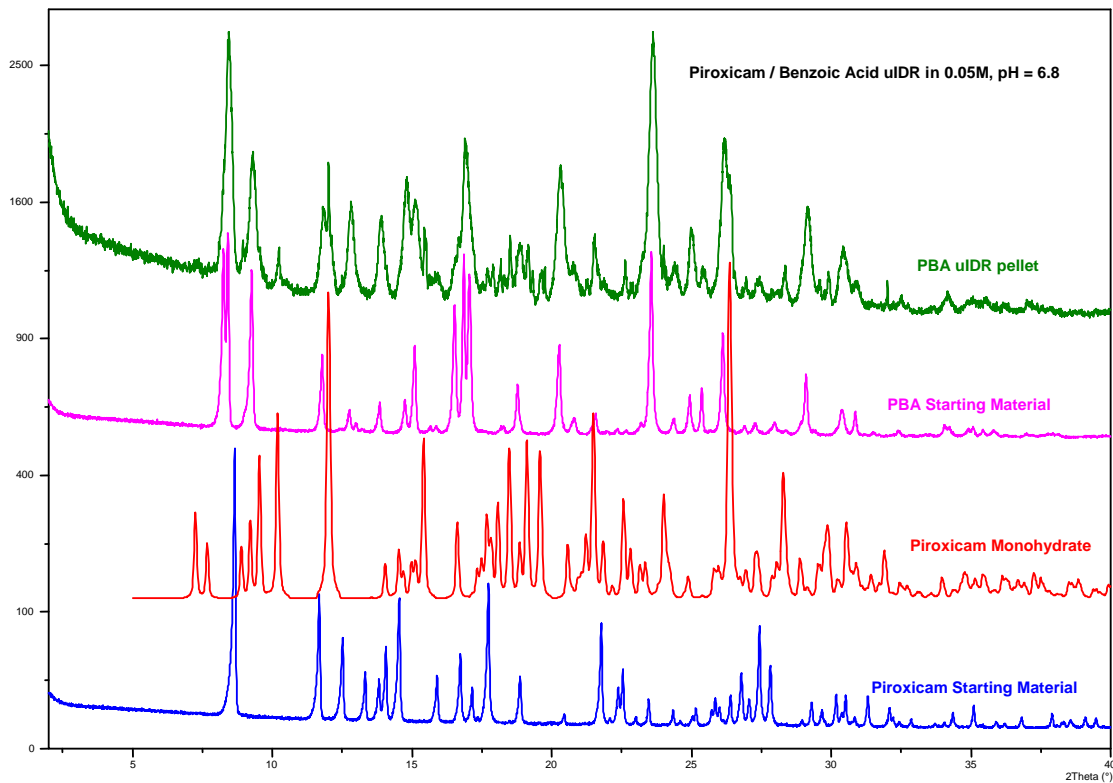


Figure 7.35: 1:1 piroxicam/benzoic acid co-crystal XRPD pattern after intrinsic dissolution experiments (0.05M buffer, pH 6.8).

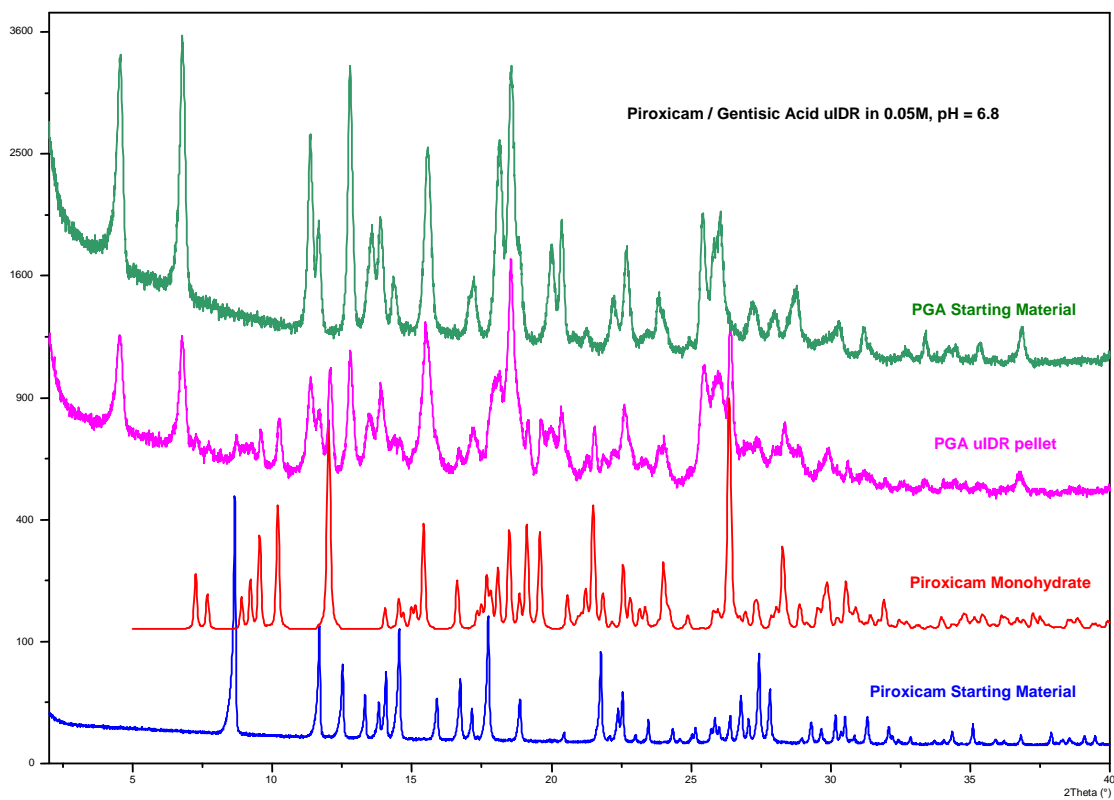


Figure 7.36: 1:1 piroxicam/gentisic acid co-crystal XRPD pattern after intrinsic dissolution experiments (0.05M buffer, pH 6.8).

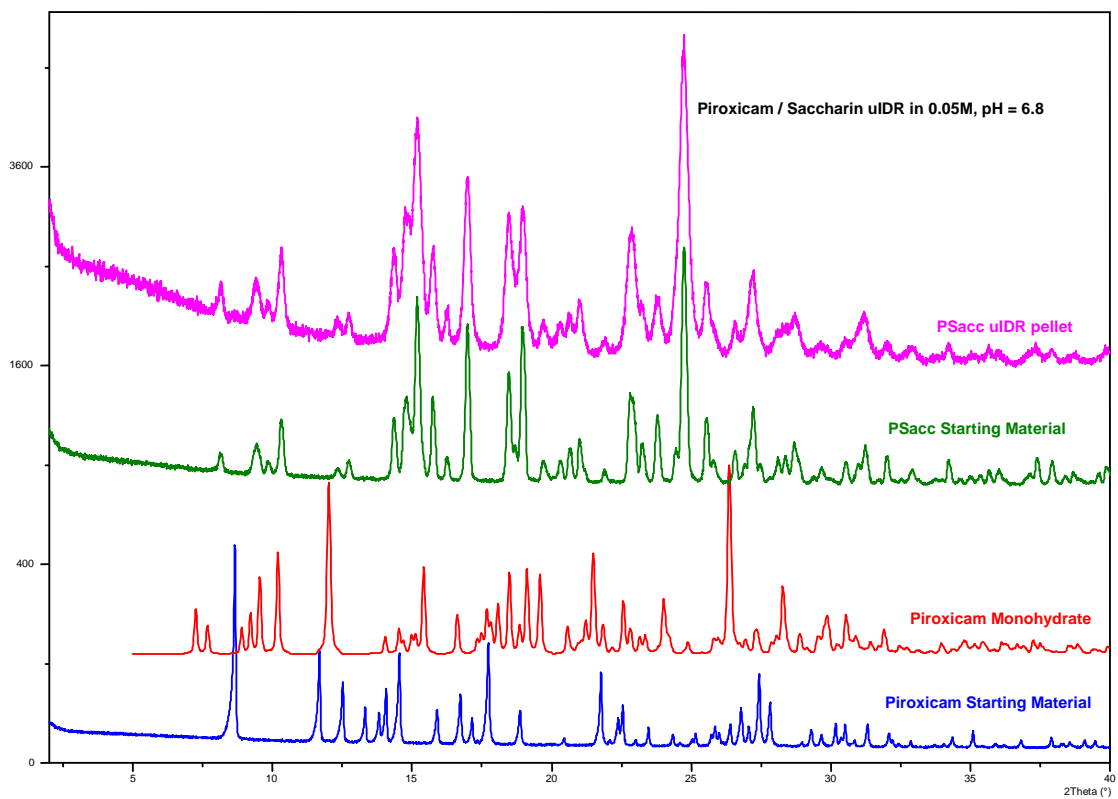


Figure 7.37: 1:1 piroxicam/saccharin co-crystal XRPD pattern after intrinsic dissolution experiments (0.05M buffer, pH 6.8).

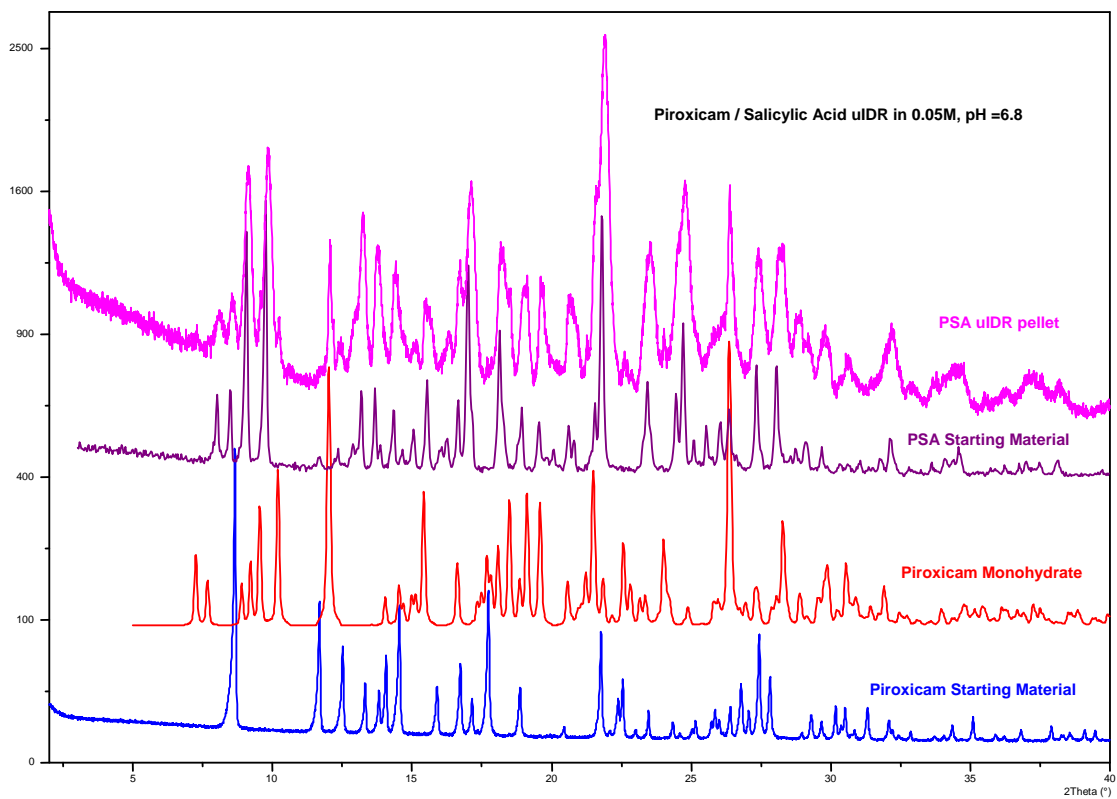


Figure 7.38: 1:1 piroxicam/salicylic acid co-crystal XRPD pattern after intrinsic dissolution experiments (0.05M buffer, pH 6.8).

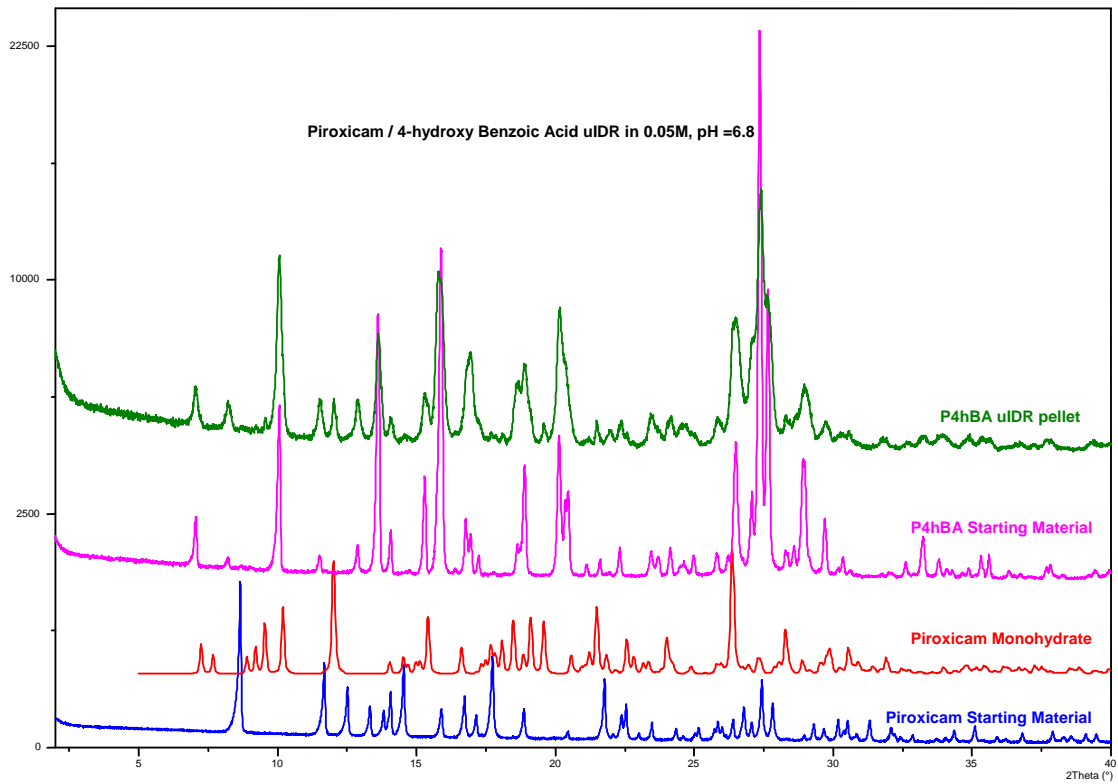


Figure 7.39: 1:1 piroxicam/4-hydroxy benzoic acid co-crystal XRPD pattern after intrinsic dissolution experiments (0.05M buffer, pH 6.8).

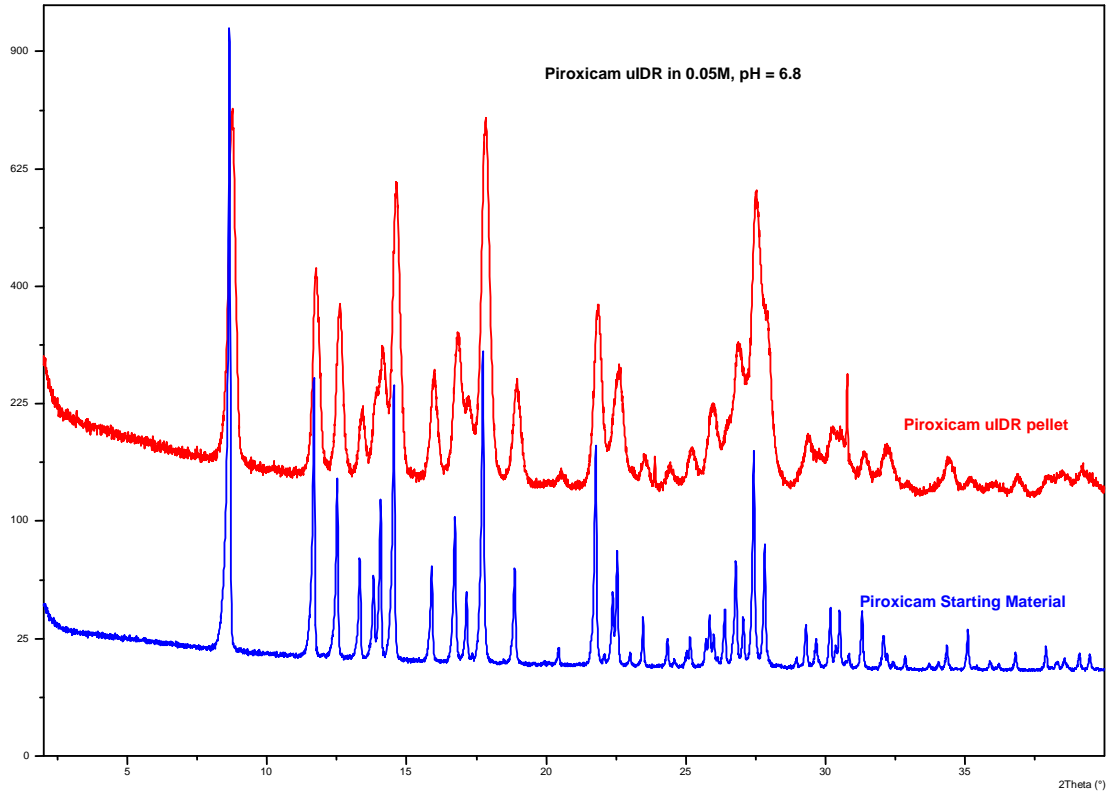


Figure 7.40: Piroxicam reference standard XRPD pattern after intrinsic dissolution experiments (0.05M buffer, pH 6.8).

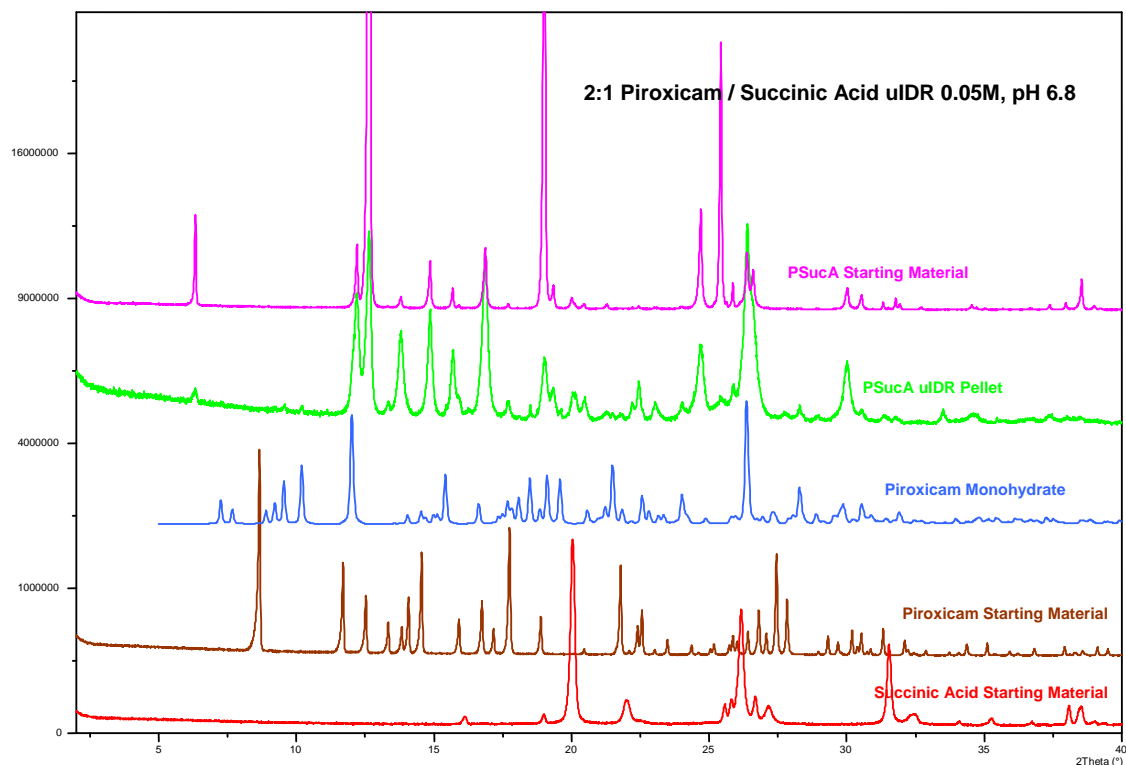


Figure 7.41: 2:1 piroxicam/succinic acid co-crystal XRPD pattern after intrinsic dissolution experiments (0.1M buffer, pH 6.8).

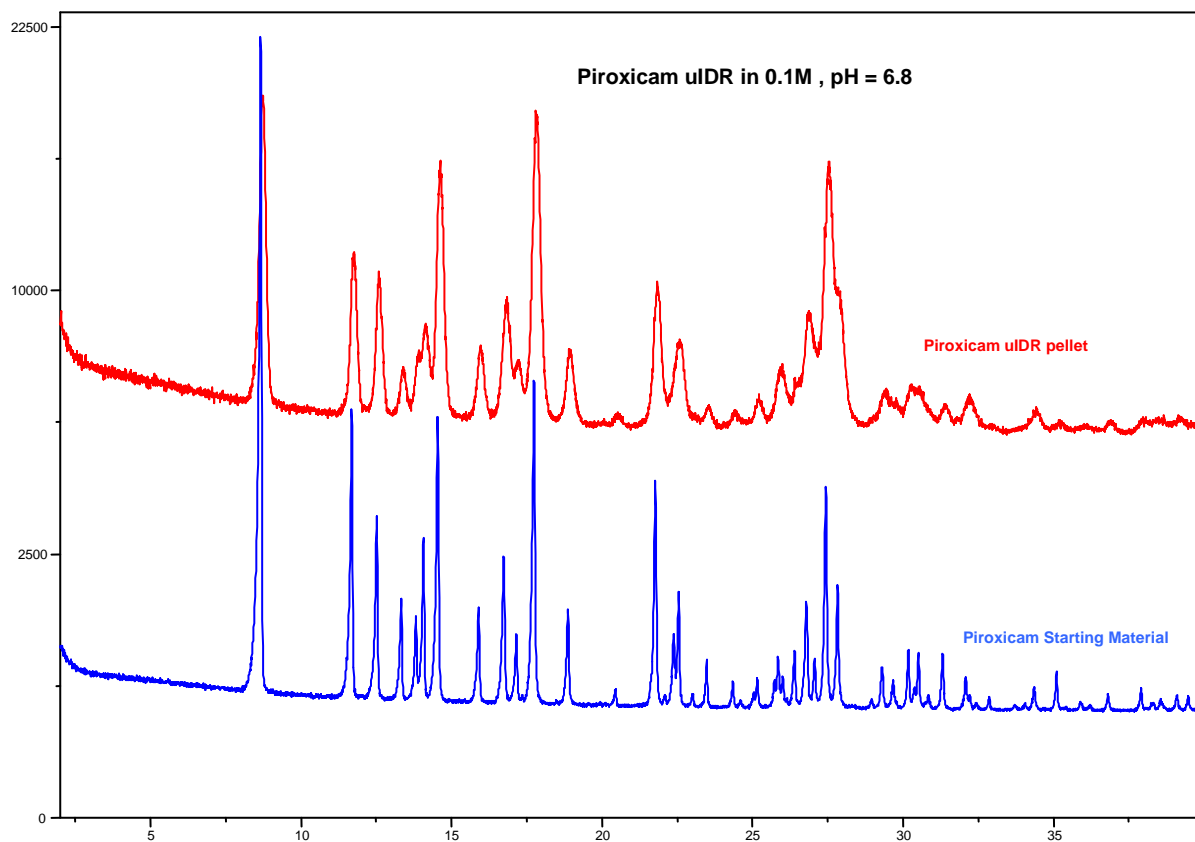


Figure 7.42: Piroxicam reference standard XRPD pattern after intrinsic dissolution experiments (0.1M buffer, pH 6.8).

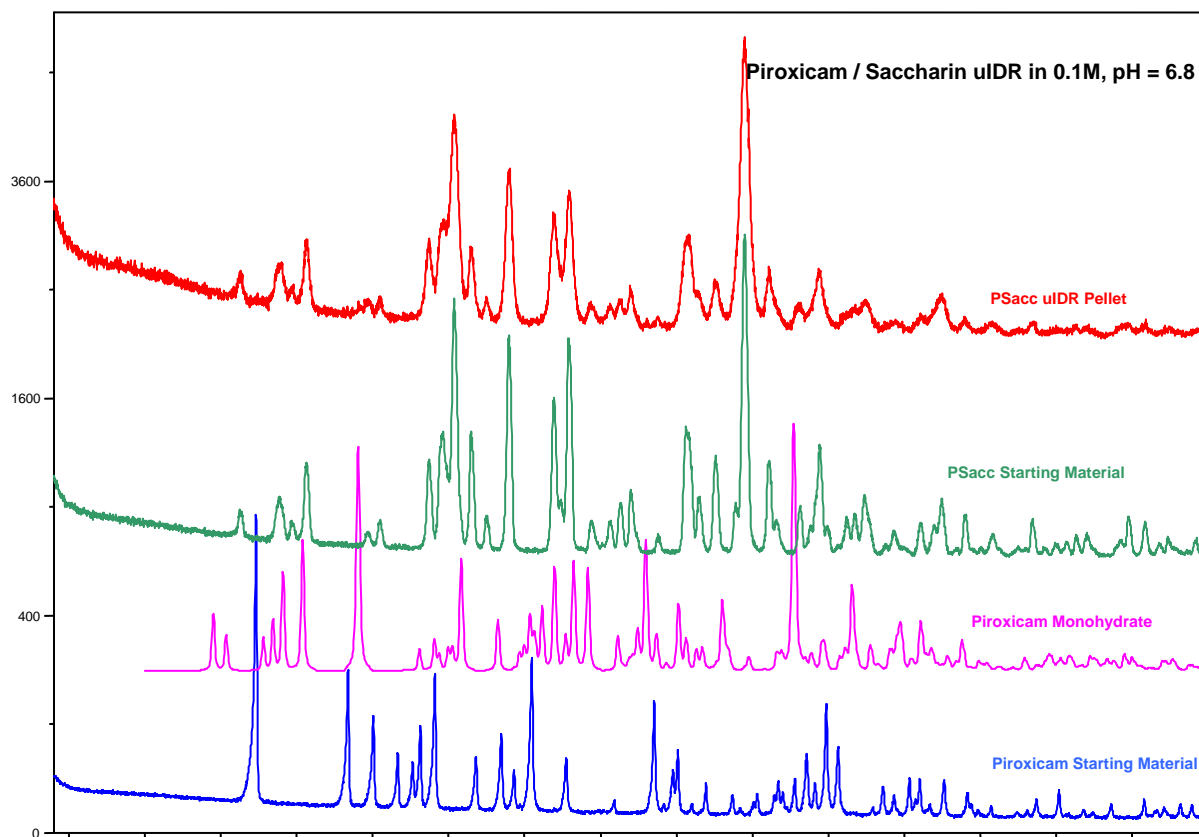


Figure 7.43: 1:1 piroxicam/saccharin co-crystal XRPD pattern after intrinsic dissolution experiments (0.1M buffer, pH 6.8).

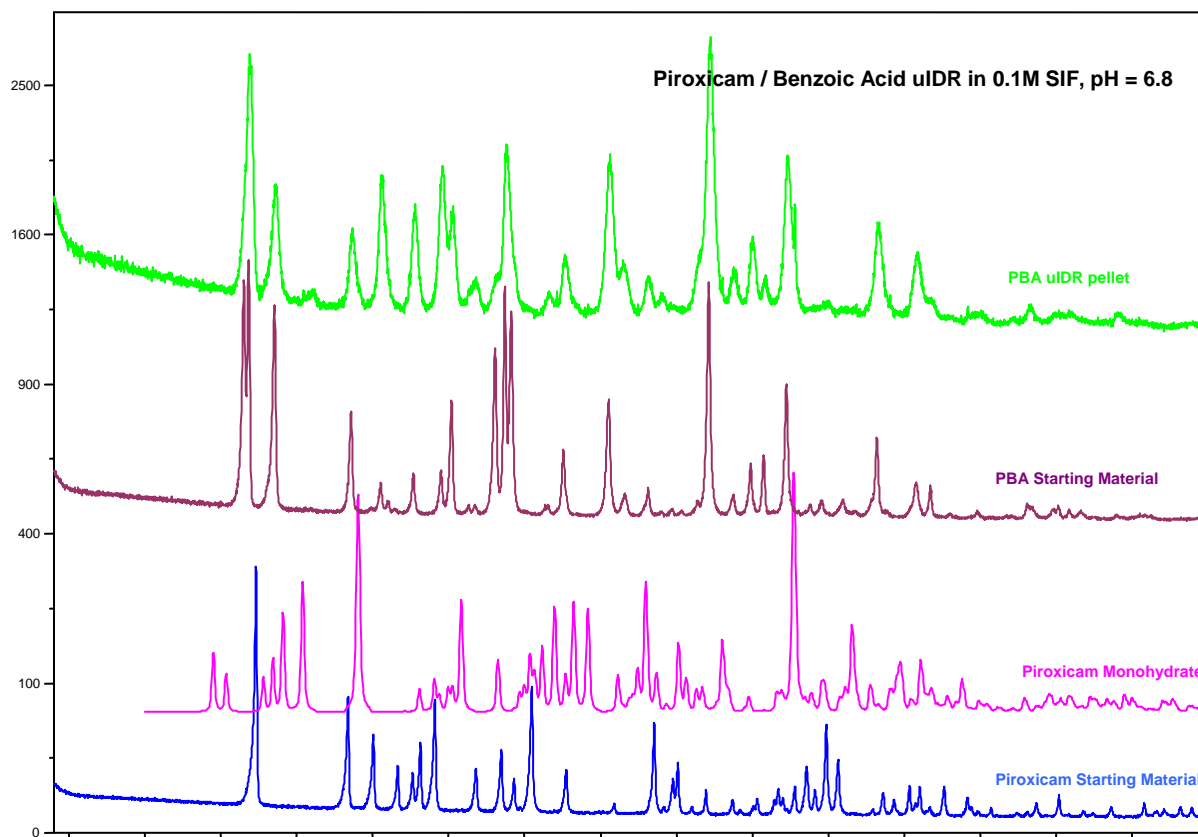


Figure 7.44: 1:1 piroxicam/benzoic acid co-crystal XRPD pattern after intrinsic dissolution experiments (0.1M buffer, pH 6.8).

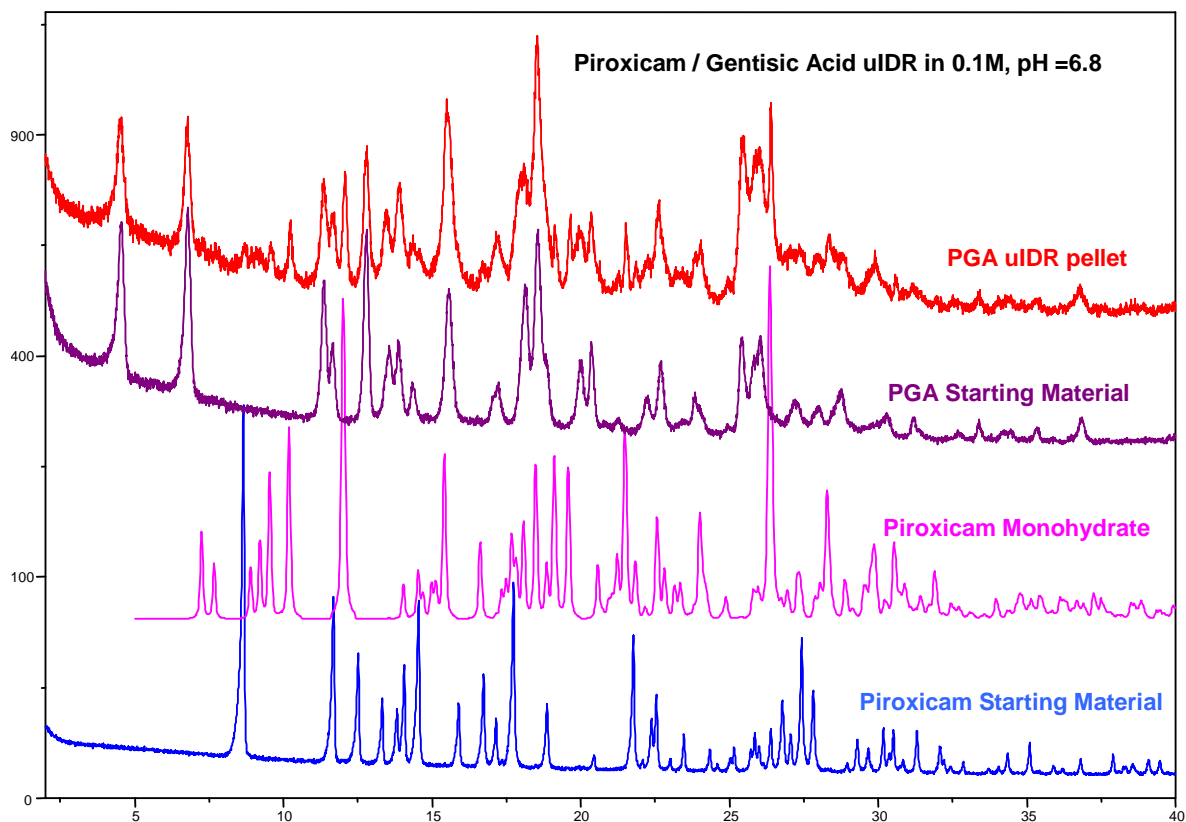


Figure 7.45: 1:1 piroxicam/gentisic acid co-crystal XRPD pattern after intrinsic dissolution experiments (0.1M buffer, pH 6.8).

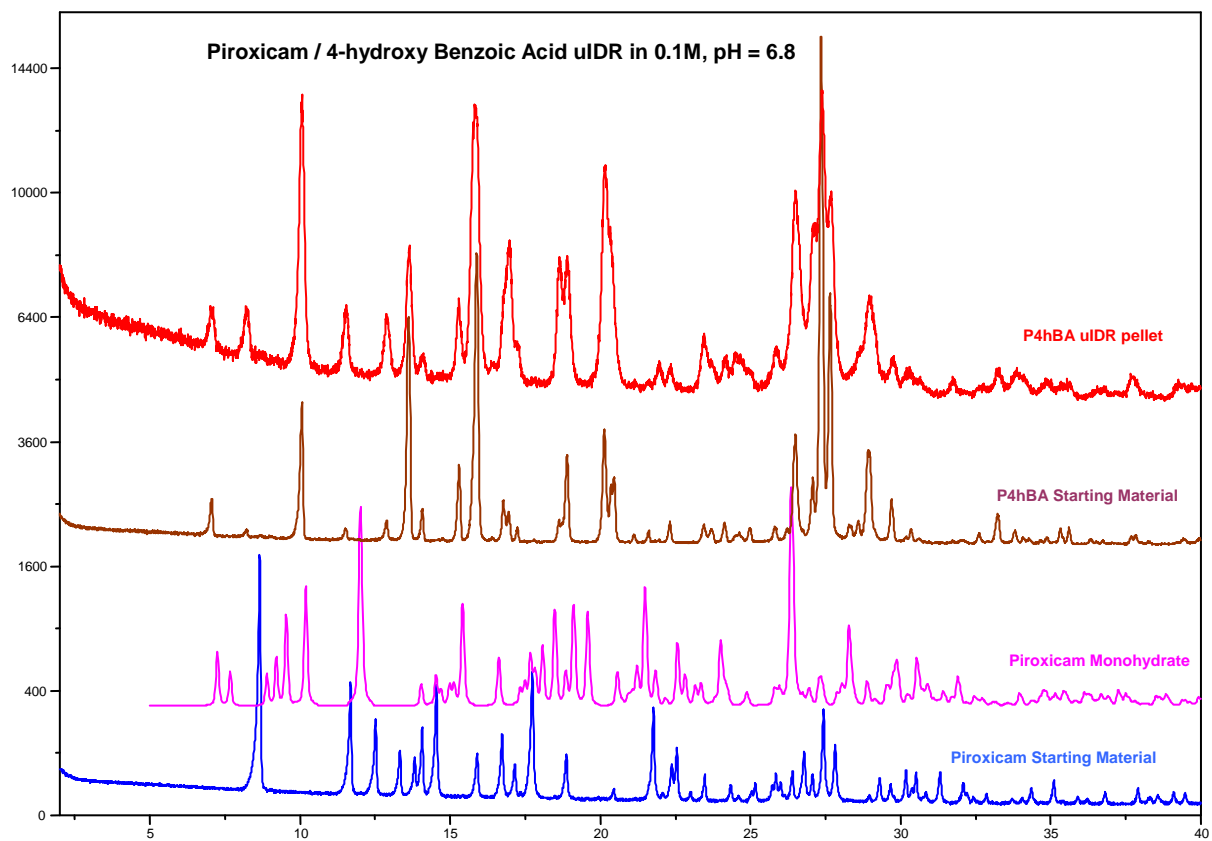


Figure 7.46: 1:1 piroxicam/4-hydroxy benzoic acid co-crystal XRPD pattern after intrinsic dissolution experiments (0.1M buffer, pH 6.8).

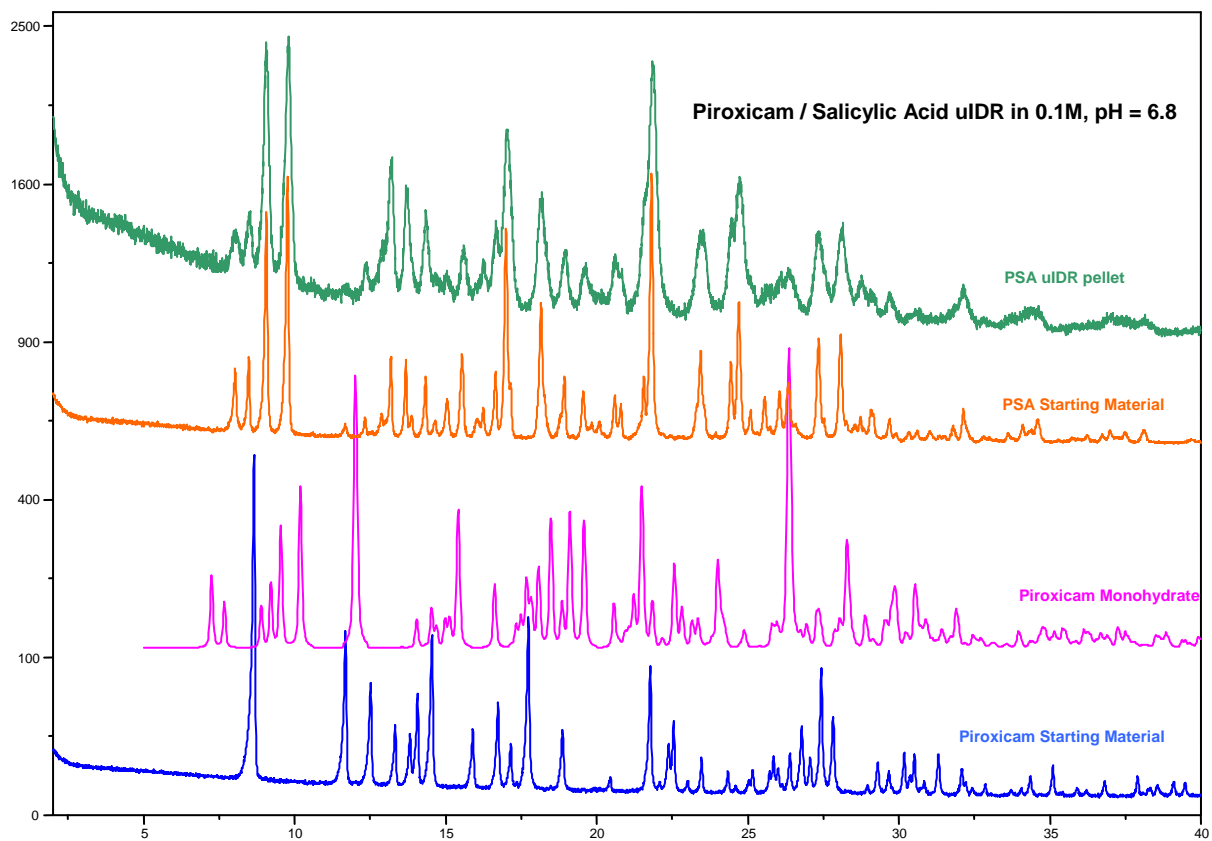


Figure 7.47: 1:1 piroxicam/salicylic acid co-crystal XRPD pattern after intrinsic dissolution experiments (0.1M buffer, pH 6.8).

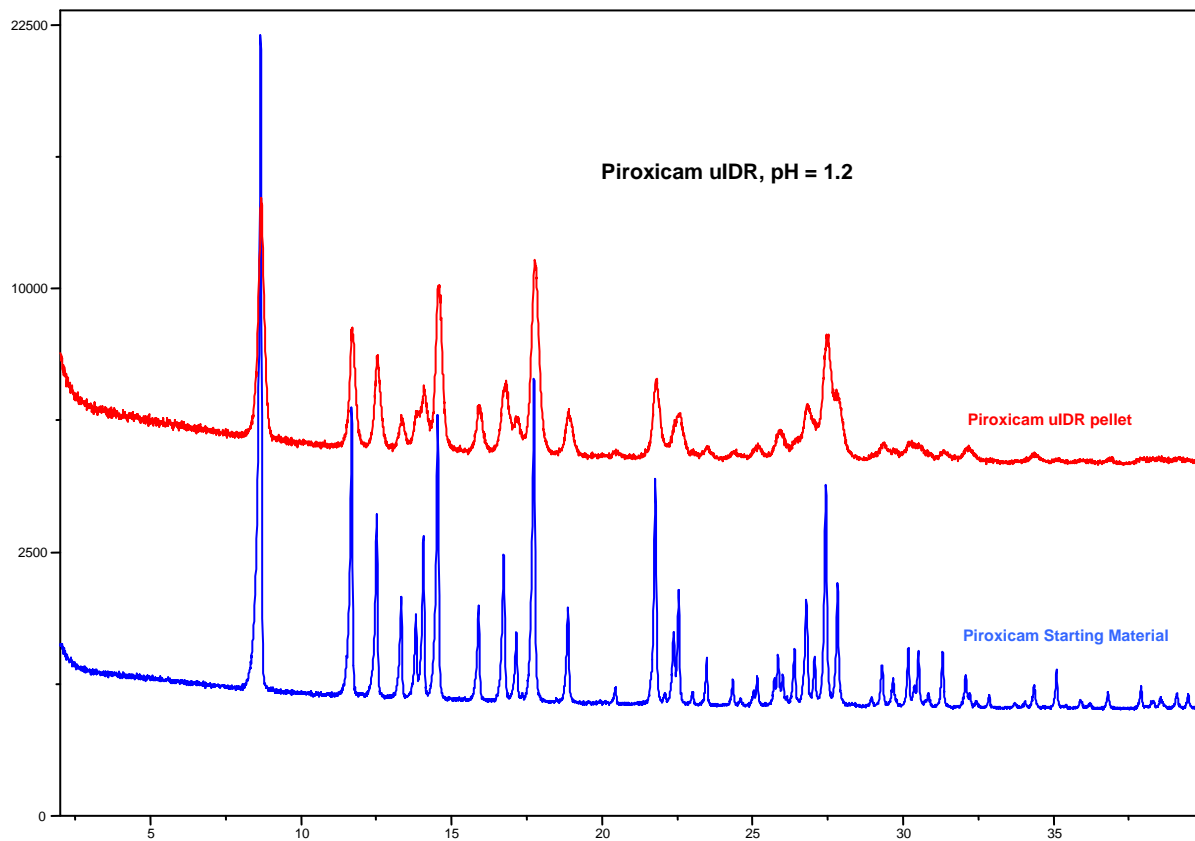


Figure 7.48: Piroxicam reference standard XRPD pattern after intrinsic dissolution experiments (pH 1.2).

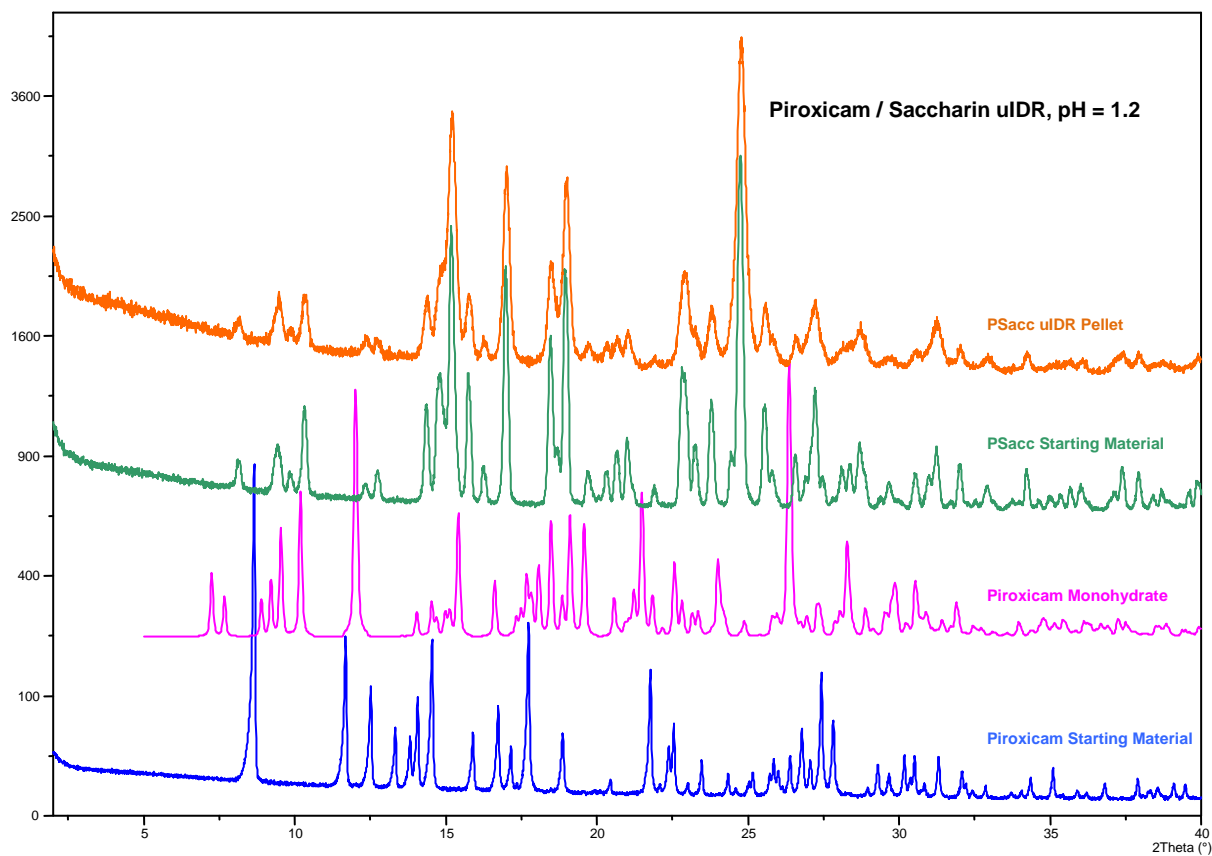


Figure 7.49: 1:1 piroxicam/saccharin co-crystal XRPD pattern after intrinsic dissolution experiments (pH 1.2).

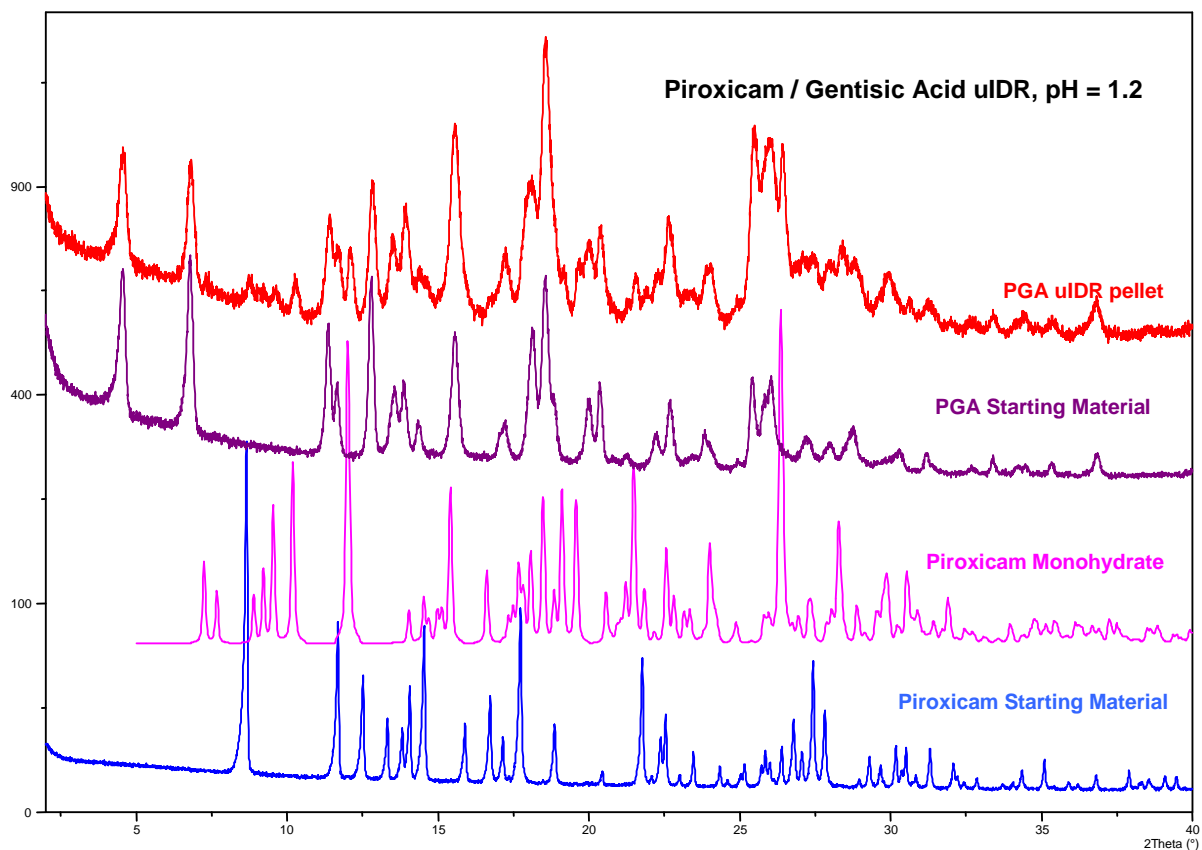


Figure 7.50: 1:1 piroxicam/gentisic acid co-crystal XRPD pattern after intrinsic dissolution experiments (pH 1.2).

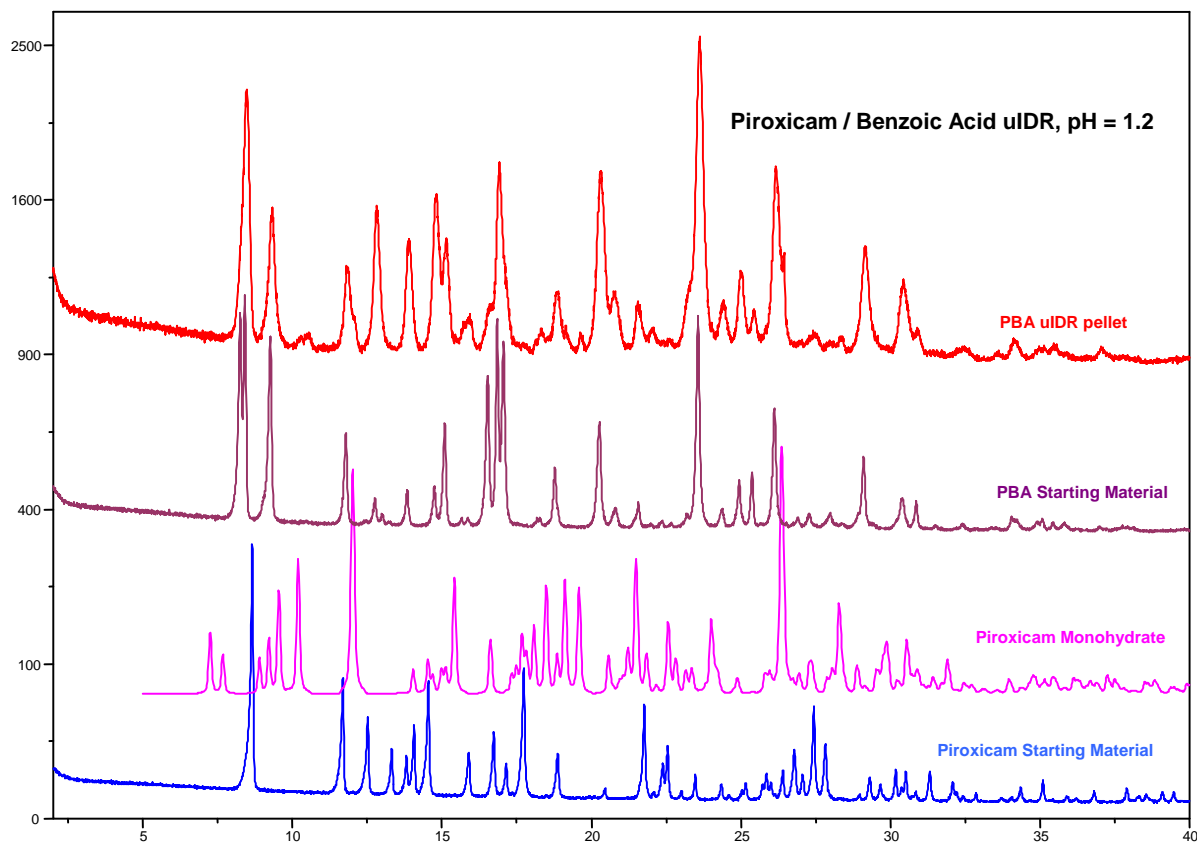


Figure 7.51: 1:1 piroxicam/benzoic acid co-crystal XRPD pattern after intrinsic dissolution experiments (pH 1.2).

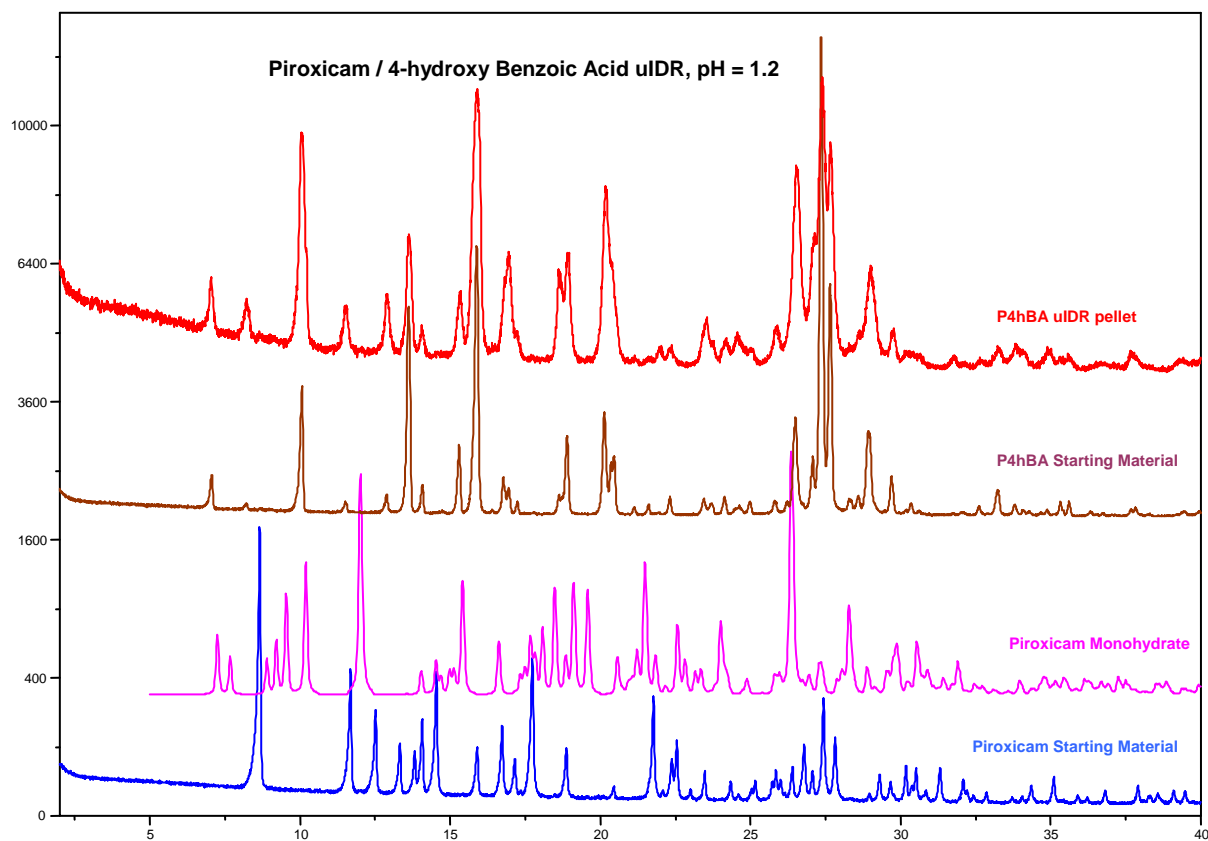


Figure 7.52: 1:1 piroxicam/4-hydroxy benzoic acid co-crystal XRPD pattern after intrinsic dissolution experiments (pH 1.2).

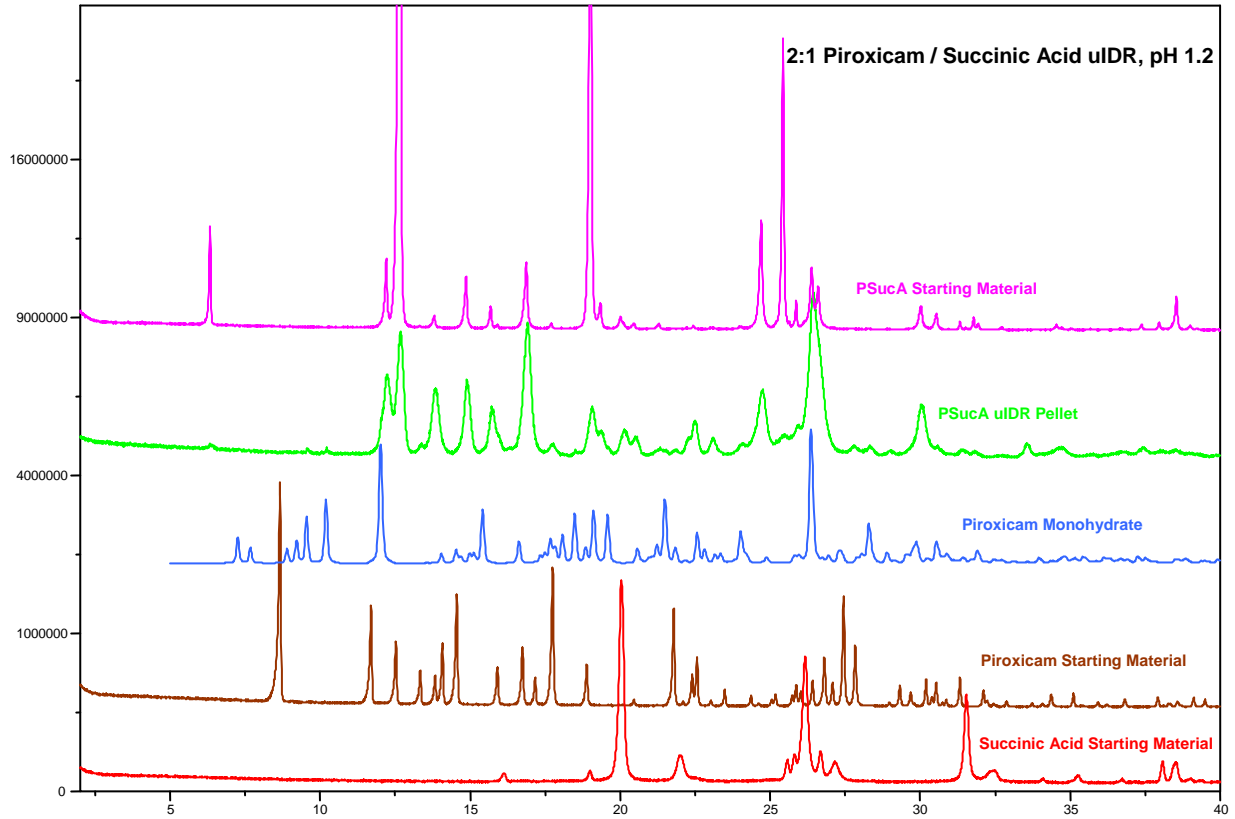


Figure 7.53: 2:1 piroxicam/succinic acid co-crystal XRPD pattern after intrinsic dissolution experiments (pH 1.2).

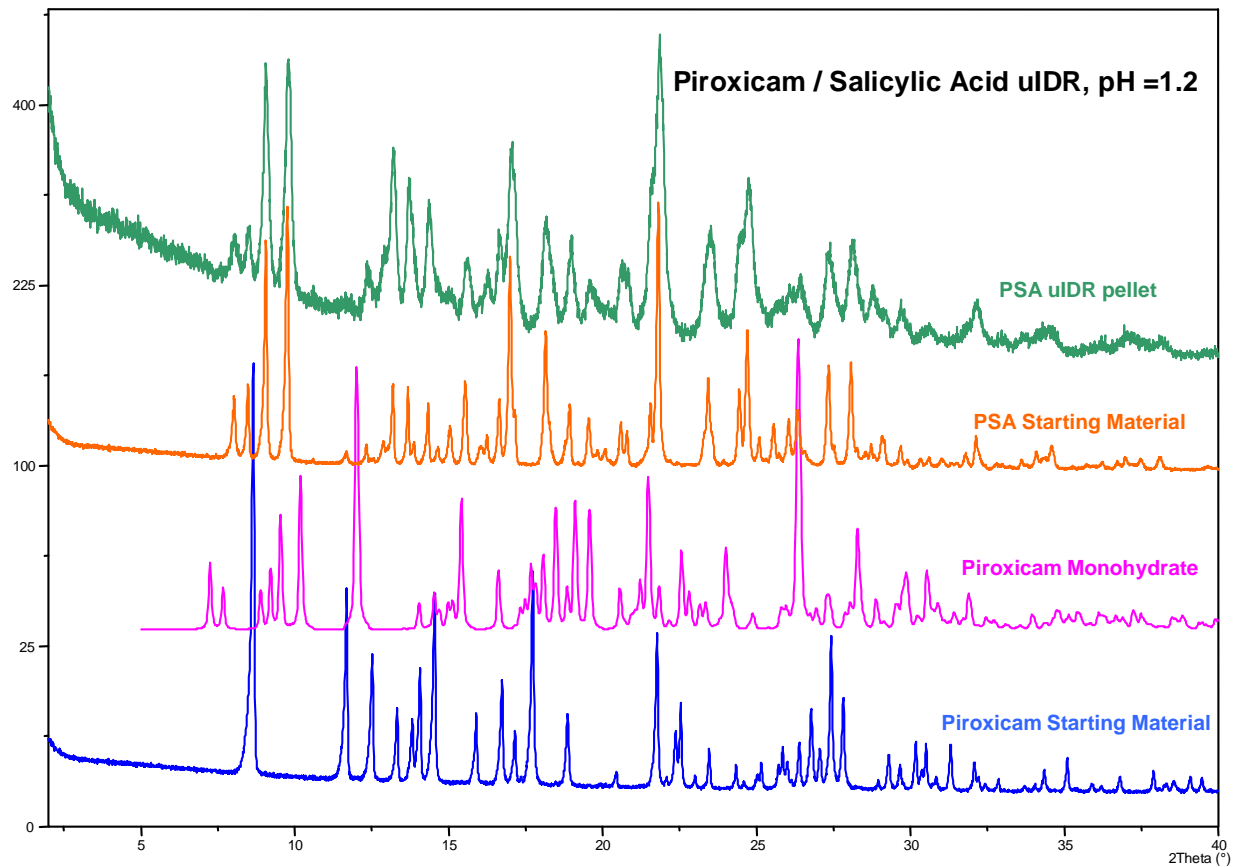


Figure 7.54: 1:1 piroxicam/salicylic acid co-crystal XRPD pattern after intrinsic dissolution experiments (pH 1.2).

Pharmacokinetic Data

Plasma Levels of Piroxicam in Rat 1 mg/kg i.v., 5 mg/kg p.o. Capsules

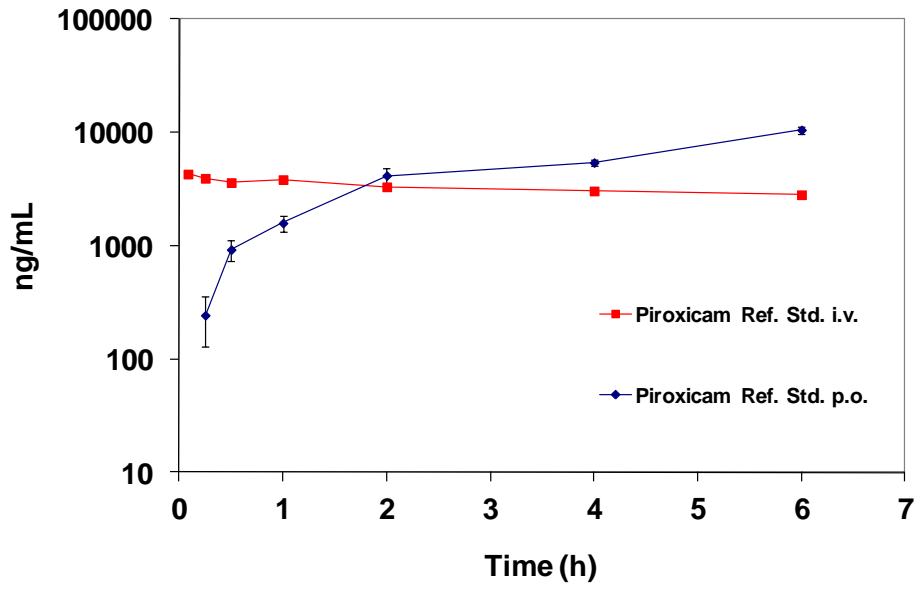


Figure 7.55: Piroxicam six hour plasma levels after intravenous and oral dosing.

Piroxicam Ref. Std.	Rat 1	Rat 2	Rat 3	Mean	stdev	sem
$t_{1/2}$, h				#DIV/0!	#DIV/0!	#DIV/0!
AUC _{0-t} , ng*h/mL	19998	18887	20105	19662	675	389
AUC _{0-∞} , ng*h/mL				#DIV/0!	#DIV/0!	#DIV/0!
Vd, L/kg				#DIV/0!	#DIV/0!	#DIV/0!
CL, mL/min/kg				#DIV/0!	#DIV/0!	#DIV/0!
1 mg/kg i.v.						
Piroxicam Ref. Std.	Rat 1	Rat 2	Rat 3	Mean	stdev	sem
C _{max} , ng/mL	10880	9010	11745	10545	1398	808
t _{max} , h	6.0	6.0	6.0	6.0	0.0	0.0
AUC _{0-t} , ng*h/mL	30384	24684	32659	29242	4108	2375
AUC _{0-∞} , ng*h/mL	ND	ND	ND	ND	-	-
t _{1/2} , h	ND	ND	ND	ND	-	-
Oral Bioavailability %, 6h	31	25	33	30	4	2
5 mg/kg p.o. Capsules						
PBA	Rat 1	Rat 2	Rat 3	Mean	stdev	sem
C _{max} , ng/mL	7029	9408	12032	9490	2502	1447
t _{max} , h	4.0	6.0	6.0	5.3	1.2	0.7
AUC _{0-t} , ng*h/mL	24602	25942	40742	30429	8956	5177
AUC _{0-∞} , ng*h/mL	ND	ND	ND	ND	-	-
t _{1/2} , h	ND	ND	ND	ND	-	-
Oral Bioavailability %, 6h	25	26	41	31	9	5
5 mg/kg p.o. Capsules						
PSA	Rat 1	Rat 2	Rat 3	Mean	stdev	sem
C _{max} , ng/mL	8669	11088	9875	9877	1210	699
t _{max} , h	6.0	6.0	6.0	6.0	0.0	0.0
AUC _{0-t} , ng*h/mL	35080	31911	32508	33166	1684	973
AUC _{0-∞} , ng*h/mL	ND	ND	ND	ND	-	-
t _{1/2} , h	ND	ND	ND	ND	-	-
Oral Bioavailability %, 6h	36	32	33	34	2	1
5 mg/kg p.o. Capsules						

Figure 7.56: Piroxicam and co-crystal six hour calculated pharmacokinetic parameters after intravenous or oral dosing.

PGA		Rat 1	Rat 2	Rat 3	Mean	stdev	sem			
	C_{max} , ng/mL	10488	12000	10545	11011	857	495			
	t_{max} , h	6.0	6.0	4.0	5.3	1.2	0.7			
	AUC _{0-t} , ng*h/mL	30915	45344	54122	43460	11717	6773			
	AUC _{0-∞} , ng*h/mL	ND	ND	ND	ND	-	-			
	$t_{1/2}$, h	ND	ND	ND	ND	-	-			
	Oral Bioavailability %, 6h	31	46	55	44	12	7			
5 mg/kg p.o. Capsules										
P4hBA		Rat 1	Rat 2	Rat 3	Mean	stdev	sem			
	C_{max} , ng/mL	10710	10622	10507	10613	102	59			
	t_{max} , h	4.0	6.0	6.0	5.3	1.2	0.7			
	AUC _{0-t} , ng*h/mL	42074	32763	36451	37096	4689	2710			
	AUC _{0-∞} , ng*h/mL	ND	ND	ND	ND	-	-			
	$t_{1/2}$, h	ND	ND	ND	ND	-	-			
	Oral Bioavailability %, 6h	43	33	37	38	5	3			
5 mg/kg p.o. Capsules										
PSacc		Rat 1	Rat 2	Rat 3	Mean	stdev	sem			
	C_{max} , ng/mL	8722.00	11659	11770	10717	1729	999			
	t_{max} , h	6.0	6.0	6.0	6.0	0.0	0.0			
	AUC _{0-t} , ng*h/mL	25465	56624	46711	42933	15919	9202			
	AUC _{0-∞} , ng*h/mL	ND	ND	ND	ND	-	-			
	$t_{1/2}$, h	ND	ND	ND	ND	-	-			
	Oral Bioavailability %, 6h	26	58	48	44	16	9			
5 mg/kg p.o. Capsules										
PSucA		Rat 1	Rat 2	Rat 3	Rat 4	Rat 5	Rat 6	Mean	stdev	sem
	C_{max} , ng/mL	10853	15080	8947	9483	15434	7585	11230	3292	1349
	t_{max} , h	6.0	6.0	6.0	6.0	6.0	6.0	6.0	0.0	0.0
	AUC _{0-t} , ng*h/mL	36705	60448	41923	36533	45161	17364	39689	14022	5747
	AUC _{0-∞} , ng*h/mL	ND	ND	ND	ND	ND	ND	ND		
	$t_{1/2}$, h	ND	ND	ND	ND	ND	ND	ND		
	Oral Bioavailability %, 6h	37	61	43	37	46	18	40	14	6
5 mg/kg p.o. Capsules										

Figure 7.57: Co-crystal six hour calculated pharmacokinetic parameters after intravenous or oral dosing.

Co-Crystal	AUC (0 - 1h)	
	ng*h/mL	sem
Piroxicam Ref. Std.	2115	707
PGA	2192	550
PSacc	1850	294

Figure 7.58: Piroxicam and co-crystal calculated one hour AUC after oral dosing.